
OPTIMIZED BIOFUELS PRODUCTION BY SYNGAS FERMENTATION

Giacomo Ruggiero

Dottorato in Biotecnologie – XXXIII ciclo

Università degli Studi di Napoli Federico II



Maggio 2021

Dottorato in Biotecnologie – XXXIII ciclo

Università degli Studi di Napoli Federico II



OPTIMIZED BIOFUELS PRODUCTION BY SYNGAS FERMENTATION

Giacomo Ruggiero

Dottorando: Giacomo Ruggiero

Relatore: Prof. Antonio Marzocchella
Prof. Piero Salatino

Coordinatore: Prof. Giovanni Sannia
Prof. Marco Moracci

TABLE OF CONTENTS

RIASSUNTO	1
SUMMARY.....	5
1. INTRODUCTION	8
1.1 Biofuels.....	9
1.2 Syngas fermentation	11
1.2.1 Gasification process	12
1.2.2 Acetogen bacteria	13
1.2.3 Metabolic pathway	14
1.3. <i>Clostridium carboxidivorans</i>	16
1.4 Advantages of syngas fermentation	17
1.4.1 Challenges and open issues	18
1.5 Bioprocess modelling	21
2. AIM OF THE THESIS	24
3. FERMENTATION TESTS	26
3.1 Laboratory set-up.....	26
3.2 Batch Syngas Fermentation by <i>Clostridium carboxidivorans</i> for Production of Acids and Alcohols.....	27
3.3 Gas-fed fermentation of <i>C. carboxidivorans</i>	39
4. MATHEMATICAL MODELLING	44
4.1 Bioreactor modelling for syngas fermentation: Kinetic characterization	44
4.2 Biofilm reactor modelling for Syngas fermentation	65
5. DISCUSSION	86
5.1 Batch fermentation.....	86
5.2 Effect of the continuous gas feeding	87
5.3 Kinetic characterization.....	88
5.4 Effect of the operating conditions	89
5.5 Biofilm bioreactor potential	89
6. CONCLUSIONS AND FUTURE PERSPECTIVES	91
NOMENCLATURE	93
APPENDIX A	94
REFERENCES	98
SCIENTIFIC COMMUNICATION	104

RIASSUNTO

Nel corso degli anni, i problemi di natura ambientale, sociale e politica legati all'utilizzo dei combustibili fossili sono diventati sempre più pressanti. Da un lato, le risorse fossili sono destinate ad esaurirsi nell'arco di qualche decennio, visto il costante aumento dei consumi, dall'altro il loro sfruttamento contribuisce in maniera significativa all'emissione di gas serra, in particolare l'anidride carbonica. I gas serra sono infatti i principali responsabili del surriscaldamento globale, e di conseguenza dei cambiamenti climatici (EIA, 2019). La consapevolezza delle società moderne circa i limiti e pericoli legati allo sfruttamento delle risorse fossili ha forzato la transizione da economia fondata sulle risorse fossili a economia fondata su risorse rinnovabili.

La transizione economica verso l'utilizzo di fonti energetiche alternative e rinnovabili rappresenta una delle maggiori sfide della società moderna. In tal ambito, uno dei fattori chiave per uno sviluppo sostenibile è lo sfruttamento di materie "prime" da riciclo e delle biomasse (materiale biologico di relativa giovane produzione), attraverso lo sviluppo di nuove tecnologie in grado di rendere economicamente sostenibile tale transizione (Halkos & Gkampoura, 2020). Uno strumento che agevola l'economia dei processi eco-sostenibili è il concetto di bioraffineria. Una delle definizioni più accreditate di bioraffineria è: "per bioraffineria si intendono quei processi, sostenibili, di trasformazione delle biomasse in bio-prodotti e bio-energia di valore commerciale". Per quanto riguarda la produzione di energia, sotto forma di calore ed elettricità, esistono già una vasta gamma di tecnologie e processi, quali lo sfruttamento dell'energia eolica, idrica, geotermica e solare. Per quanto riguarda, invece, la produzione di prodotti chimici di interesse, quali ad esempio biocombustibili o bioplastiche, l'unica materia prima a disposizione sono le biomasse. Data la rilevanza universalmente riconosciuta di questi concetti, il numero di studi e di pubblicazioni finalizzati allo sviluppo ed all'ottimizzazione di processi basati sulla bioraffineria è in costante aumento.

I processi di bioraffineria, attualmente, possono contare su una vasta gamma di materie "prime" abbondanti e biomasse. Uno svantaggio tipicamente riscontrato è la caratteristica di processi di produzione non ancora economicamente convenienti, se confrontati ai processi petrolchimici. Questo divario economico è destinato ad essere ribaltato nel tempo per due fattori: da un lato, l'esaurimento delle risorse petrolifere porterà ad un crescente aumento dei prezzi della materia prima; dall'altro lato, l'innovazione tecnologica, legata anche e soprattutto all'utilizzo di piante e microrganismi ingegnerizzati, garantirà un'efficienza più elevata e di conseguenza una maggiore convenienza.

Per quanto riguarda i biocombustibili, quelli che suscitano maggiore interesse sono da un lato il biodiesel, che si ottiene dalla transesterificazione degli acidi grassi, e dall'altro gli alcoli, etanolo e butanolo, con un'attenzione particolare verso quest'ultimo, per via delle sue eccellenti proprietà come combustibile. Etanolo e butanolo vengono prodotti per via fermentativa, tramite l'utilizzo di microrganismi in grado di fermentare gli zuccheri, attraverso un processo noto come fermentazione A-B-E, dove i prodotti finali sono appunto acetone, butanolo ed etanolo (Raganati et al., 2014). Gli zuccheri di fermentazione, in accordo alle tecnologie di produzione di biocombustibili di seconda generazione, sono ottenuti da biomasse non-edibili, quali legna, residui agro-forestali, ma anche materie di scarto di origine antropologica (Lee e Lavoie, 2014). Se da un lato

tali materie prime sono particolarmente economiche da approvvigionare e non competono con le risorse commestibili (umane ed animali), spesso la complessa struttura ligno-cellulosica rappresenta un limite in quanto il pretrattamento necessario ad ottenere degli zuccheri fermentabili è oneroso e rappresenta una alta percentuale del costo complessivo.

Una possibile alternativa alla fermentazione di zuccheri è rappresentata dalla *fermentazione di syngas*, una miscela gassosa i cui componenti principali sono H₂, CO, CO₂, CH₄ e N₂. Alcuni microorganismi, tra cui gli acetogeni, hanno evidenziato la capacità di poter metabolizzare CO e CO₂ come fonte di carbonio e di nuovo CO e H₂ come fonte di elettroni e dunque di energia nei vari processi metabolici (Dürre, 2007). I prodotti principali della fermentazione di syngas sono acido acetico ed etanolo, ma alcuni ceppi sono in grado di produrre nel loro metabolismo anche composti a catena più lunga, quali acido butirrico, acido esanoico, butanolo ed esanolo. Tra questi, quello che ha mostrato le maggiori potenzialità è *Clostridium carboxidivorans*, e che pertanto è stato anche l'oggetto dello studio del presente lavoro di tesi.

La fermentazione di *syngas* è particolarmente promettente perché dà la possibilità di sfruttare una vastissima gamma di prodotti contenenti carbonio da valorizzare, dalle biomasse disponibili in grande quantità, a diversi tipi di rifiuti e sostanze di scarto, da quelli urbani a quelli industriali. Inoltre, vi è la possibilità di sfruttare i reflui di alcune fabbriche, ad es. le acciaierie, che producono grandi correnti gassose ricche di CO e CO₂, il cui sfruttamento rappresenterebbe un vantaggio enorme sotto molteplici punti di vista. I prodotti a base di carbonio possono essere valorizzati per fermentazione previa gasificazione. Tale processo consiste in una reazione di ossidazione parziale ad opera di un agente ossidante, i più comuni sono l'aria, l'ossigeno e il vapore d'acqua. Il risultato dell'ossidazione dei prodotti a base di carbonio è la produzione di una miscela di gas di sintesi, da cui il termine *syngas*. Utilizzando la gasificazione al posto dei pretrattamenti necessari a rendere fermentabili le biomasse, si può sfruttare l'intero contenuto di carbonio, con una tecnologia relativamente semplice e a basso costo. Un limite della strategia di conversione richiamata - gasificazione + fermentazione - è costituito dalla fermentazione del syngas le cui prestazioni sono nettamente inferiori rispetto alle fermentazioni di zuccheri semplici, sia in termini di concentrazioni di metaboliti raggiungibili sia di produttività. Un altro fattore chiave, universalmente identificato come collo di bottiglia del processo, è la capacità di rendere il substrato gassoso facilmente disponibile, ed in quantità adeguate, in fase liquida poiché la solubilità dell'idrogeno e del monossido di carbonio in fase liquida è relativamente bassa. Pertanto, l'obiettivo della ricerca in questo settore consiste anche nel proporre soluzioni all'avanguardia, che consentano di ottimizzare i processi di produzione e renderli economicamente più competitivi. Oggigiorno, una delle società più all'avanguardia in questo settore è la LanzaTech, che dal 2018 ha realizzato un impianto pilota per la fermentazione di syngas ottenuto da gasificazione di biomasse (Ciliberti et al., 2020), attraverso lo sfruttamento di un ceppo batterico geneticamente modificato, sviluppato dalla stessa società.

Il presente lavoro di tesi ha riguardato la produzione di solventi mediante fermentazione di syngas. Ha previsto, in sintesi, di analizzare e comprendere al meglio i meccanismi che regolano il processo di *syngas fermentation* e di fornire validi strumenti di supporto all'ottimizzazione tecnico-economica del processo, sulla base della

valutazione delle principali variabili in gioco. L'attività è stata articolata in diversi aspetti, sia sperimentali che teorici. Uno studio preliminare ha individuato in *Clostridium carboxidivorans* il microorganismo commerciale da investigare ai fini degli approfondimenti di prestazione della fermentazione al variare delle condizioni di esercizio

Un aspetto che ha influenzato l'attività sperimentale è stato la necessità di adeguare i laboratori allo svolgimento di test con il *syngas*. La tossicità e infiammabilità del substrato hanno richiesto l'acquisizione ed installazione di impianti e dispositivi idonei a garantire la conduzione delle prove in sicurezza per gli operatori e per l'ambiente.

La conduzione di test fermentativi con il *syngas* ha richiesto altresì l'approfondimento di protocolli sperimentali. Da un accurato studio della letteratura dedicata all'argomento, è stato scelto, inizialmente, di effettuare test di fermentazione in modalità "batch", ossia fornendo all'inizio della prova tutto il necessario per la crescita del microorganismo: il terreno di coltura, contenente fonti di azoto, vitamine, sali minerali e metalli vari necessari alla crescita (Fernández-Naveira et al., 2017b), l'inoculo, costituito da una coltura precedentemente ottenuta a partire da uno stock conservato in congelatore (a -80°C), e la fonte di carbonio sotto forma di CO. Le prove in batch sono state effettuate all'interno di bottiglie di vetro, del volume totale di circa 280 mL, sigillate ermeticamente con tappo di gomma, all'interno delle quali il gas è stato caricato tramite ago sino alla pressione desiderata, misurata mediante un manometro digitale. La pressione nella bottiglia influenza la concentrazione (linearmente) di substrato solubilizzato (e.g. vedi legge di Henry) che a sua volta influenza la velocità e resa di fermentazione. I test sono stati condotti con *C. carboxidivorans* al variare della concentrazione di substrato fornito all'inizio della prova. I test fermentativi sono stati caratterizzati in termini di concentrazione di substrato, di cellule e di metaboliti sia in fase gas (per le specie presenti) e sia in fase liquida. È stato inoltre osservato come il pH del mezzo di coltura varia nel corso della fermentazione, in base alla quantità di acidi prodotti dal metabolismo cellulare. Sono stati analizzati gli effetti di alcune condizioni di esercizio, quali la pressione parziale iniziale di CO, il rapporto volumetrico gas/liquido all'interno del reattore, e l'effetto di alcuni componenti del terreno, quali l'estratto di lievito e la cisteina, necessaria a mantenere il potenziale redox al di sotto di una soglia necessaria per la crescita del ceppo utilizzato. È stato evidenziato che la cinetica di crescita del suddetto ceppo batterico soffre di inibizione da substrato ed è stata caratterizzata la velocità di crescita per due diversi valori di riempimento delle bottiglie.

È stato messo a punto un impianto per effettuare le fermentazioni in un bioreattore strumentato da banco esercito in continuo rispetto al gas e, se necessario, rispetto al liquido. La campagna preliminare di fermentazione condotta con questo bioreattore ha evidenziato che le prestazioni sono decisamente migliori rispetto a quelle misurate nel corso delle fermentazioni condotte in modalità completamente batch.

Il lavoro sperimentale è stato corredato da un approfondito studio teorico del processo, con la formulazione di un modello matematico finalizzato all'interpretazione dei dati sperimentali. I modelli sono stati basati su bilanci di materia riferiti al substrato, cellule e metaboliti, accoppiati a modelli cinetici per la descrizione dei processi di bioconversione e modelli per lo scambio di materia gas-liquido. La stima dei parametri

cinetici è stata condotta con riferimento a dati fermentativi disponibili in letteratura integrati con quelli dalle prove effettuate. Si è proceduto ad uno studio di sensitività, con l'intento di comprendere la stabilità del modello e la sua attendibilità per quanto riguarda le analisi che sono state fatte successivamente. Lo studio è stato esteso all'effetto di alcuni parametri importanti dal punto di vista del processo in apparecchiature industriali, quali l'agitazione, la portata di alimentazione di gas e/o di liquido e il grado di riempimento del reattore.

Tra le varie possibili soluzioni finalizzate al miglioramento delle prestazioni del processo, è stata posta l'attenzione su un reattore a biofilm, in cui le cellule aderiscono su particelle solide. Il reattore è assimilabile ad un reattore a letto fluidizzato, in cui le particelle di supporto, rivestite da biofilm, fungono da biocatalizzatore e lavorano sinergicamente con le cellule libere in fase liquida. È stato osservato come la presente soluzione reattoristica possa incrementare la produttività e la concentrazione di metaboliti all'interno del brodo di fermentazione. Quest'ultimo aspetto assume un ruolo fondamentale nella riduzione del costo totale della produzione dei solventi, in quanto il costo per il recupero e la purificazione dei bio-prodotti di interesse è fortemente influenzato dalla concentrazione.

SUMMARY

The study carried out during the present Ph.D. program aimed at investigating the fermentation of syngas by *Clostridium carboxidivorans* to produce biofuels, with special attention on butanol. *C. carboxidivorans* is an acetogenic bacteria able to fix C-1 gases into biomass and to produce extracellular metabolites of interest. The work was carried out at the “*Dipartimento di Ingegneria Chimica, dei Materiale e della Produzione Industriale*” of the *Università degli Studi di Napoli ‘Federico II’*. The activities were focused on the study of the kinetic characterization of the selected strain, using as a carbon source a gaseous stream of sole CO, the investigation of the experimental conditions that promote the highest production of cells and metabolites, and the strategies to develop an effective reactor configuration, that allows to optimize the gas exploiting and increase the concentration of butanol and ethanol in the culture medium. The experimental work was coupled with the development of a mathematical model that describes faithfully the behavior of *C. carboxidivorans* in a fermentation process. The model soundness was also assessed. The proposed model was used to simulate a particular reactor system, with biofilm growth on non-porous carrier particles, and to investigate the performance of the bioreactor.

The experimental activity required an accurate design and set-up of the laboratory to operate with syngas. Indeed, syngas is a toxic and inflammable gas. The safe operation for operators and the environment requires to adopt controlled feeding system, sensors to detect any leakage, devices to shut-down the feeding and fermenter system.

Batch cultures

The fermentation of *C. carboxidivorans* was carried out in serum bottles of 280 mL volume. The tests were performed under “batch” conditions, without any supplement during the experiments. The bottles, after the medium load, were sealed with rubber stops and aluminium crimps and boiled to guarantee sterile conditions. The gas was loaded by mean of a needle and a 2-way valve, up to the desired pressure. Tests were carried out at different initial pressure. As the pressure increased the substrate amount increased and the mass transfer rate increased as a consequence of the large driving force. Indeed, the CO concentration in the liquid phase under equilibrium conditions increases with the CO partial pressure, according to Henry’s law. It was assessed, by absorption tests, that the time required to reach equilibrium gas/liquid conditions was much lower than the characteristic fermentation time.

The partial pressure of CO, P_{CO} , ranged between 0.5 and 2.5 bar, to assess its effect on the growth. The process was characterized in terms of CO uptake, estimated by the pressure drop and the gas composition, biomass growth and metabolites production. The decrease of pH from the initial value (5.75) was observed and it was typically associated with acid production.

The test campaign pointed out that the cell growth was substrate inhibited. The best fermentation performance - in terms of solvent production - was measured at initial $P_{CO} = 1.7$ bar. Under these operating conditions, cells reached a concentration of 0.68 g/L, while 400 mg/L of ethanol and 130 of butanol were produced. Batch fermentation didn’t show any reassimilation of acids, even at low pH (around 4.5). As this reaction it is not energetically favourable, the depletion of substrate prohibited this mechanism.

Continuous gas-fed cultures

Fermentation tests were carried out in a mini-bioreactor, 250 mL volume, equipped with device to feed CO continuously, to monitor the pH in the time and the redox potential. The reactor was kept at constant temperature (35 °C) and under constant agitation by rotating impellers (250 rpm), to favour the mass transfer between gas and liquid phase. A first test campaign was carried out at pH set to 5.75. A second campaign was carried out to observe the natural acidification of the medium, and try to push the system to solventogenesis by setting the pH to 5, turning on the control when the medium naturally reached that value.

The continuous system was characterized by fermentation performance - in terms of solvent production - better than those assessed for batch tests. Indeed, the final concentration of ethanol and butanol were double than that measured during the batch tests, 800 mg/L of ethanol and 327 mg/L of butanol. Moreover, during the experiment at variable pH, 784 mg/L of hexanol were detected, after 140 hours of fermentation. The maximum cell concentration didn't vary significantly for bottle and gas-fed fermentation. The pH decrease seemed to affect acid production, allowing the cells to reach a higher concentration. However, a higher number of experiments is required to give more consistency to the results of this section.

Kinetic characterization

The complex metabolism and the growth of *C. carboxidivorans* was described with three lumped reactions. The main reaction is the cell growth characterized by total inhibition (substrate and products). The second reaction is the conversion of acids in alcohols. The third reaction is the direct production of solvents, not associated to cell growth. A mathematical model was based on mass balances referred to species involved in the fermentation, coupled with the kinetics and mass transfer rate between the gas and liquid phases. Model parameters were assessed by regression of data available in the literature - Fernández-Naveira et al. (2016a) and present investigation included) according to the proposed model. A vector of 31 kinetic/yield parameters to describe the fermentation system were assessed.

The model was to catch dynamics phenomena quite well (overall $R^2 = 0.88$). The soundness of the model was assessed by measuring the effect of a perturbation on the parameters, in terms of final concentration of cells and metabolites. Finally, the effect of some operating conditions (gas/liquid ratio, gas flow rate and agitation speed) of industrial interest was addressed. It was pointed out that a high transport rate for gas to liquid – expressed in terms of k_La - has a negative effect on the production. It was speculated that this is due to substrate inhibition on cell growth acts.

Biofilm bioreactor investigation

The proposed mathematical model implemented was extended to assess the potential of a biofilm bioreactor. The biofilm can be described as a layer of aggregated cells adhered on the surface of a carrier. Biofilm thickness may change as a consequence of cell growth, attachment of free-cell from the liquid phase, detachment and mechanical stress.

Promoting the formation of biofilm is one of the most effective strategies for process intensification. The study was carried out by developing a model in MATLAB®

environment. Simulation were carried out to assess the bioreactor performance under steady state and transient conditions. A comparison between the system with and without biofilm was carried out to assess the contribute of the biofilm. The presence of biofilm yielded an enhancement of butanol concentration of 85%, large CO consumption with an increase of about 20 % of the conversion of the CO stream fed to the reactor. The effect of the liquid flow rate and the detachment rate were also investigated.

1. INTRODUCTION

During the last decades, environmental, social and political issues related to the use of fossil resources for production of fuels and chemicals are pressing for switching from a fossil-based economy to a renewables-based economy. Sustainable fuel supply, security, and prices necessitate the implementation of alternative routes to the production of chemicals and fuels with respect to the fossil route.

As a matter of fact, fossil resources use is no longer economically and environmentally sustainable. From 1970 to 2017, the annual global extraction of materials (i.e., fossil resource, metals, non-metal minerals, and biomass) tripled. The extraction continues to grow due to the population's exponential growth, the increasing consumption of energy per capita, the economic and technological development, and the establishment of a new modern way of life (Halkos and Gkampoura, 2020). The European council revised its objectives for reducing greenhouse gas emissions by 80% - 95% from 1990 to 2050, in addition, the European Union has set a new target for the future, by 2030 a rate equal to 27% of energy consumption must come from renewable sources (revised European Directive 2009/28/EC). Current scenarios show the increased fossil resources demand and the relative market price. As a consequence, a negative impact on the environment is expected due to the high amount of greenhouses gases (GHGs) emitted. In particular, the majority of GHGs emissions come from Industry, energy and mobility sectors (Ciliberti et al., 2020).

The shift of society's dependence from fossil-based to renewable biomass-based resources is generally viewed as a key issue for the development of a sustainable industrial society, energy independence and stability, and for the effective management of greenhouse gas emissions (Ragauskas et al., 2006). However, the economic success of the bio-based production of commodities and energy vectors typically asks for the exploitation of the biomass by valorisation of all high-value components according to the biorefinery concept combined with the circular economy strategy. Several definitions of biorefinery were proposed in the recent years, but the most exhaustive still remains that proposed by the IEA Bioenergy Task 42 "Biorefineries": "Biorefining is the sustainable processing of biomass into a spectrum of marketable bio-products and bio-energy" (Cherubini, 2010). It should be stressed that energy and heat can be produced using different types of renewable resources - e.g. solar, wind, hydropower, and geothermal energy – bio-products can be produced just processing biomass.

The ever-growing need to switch from linear to circular economy and industrial processes requires innovative technologies able to reduce carbon dioxide and GHG emissions. Global demand for liquid fuels (including biofuels) in 2018 amounted to 99.3 million barrels per day and it is projected to increase to 101.8 million barrels per day in 2020. When compared to the daily oil demand of 93.3 million barrels in 2014, the increasing demand trajectory is clear, as shown in Figure 1.1 (EIA, 2019). Several studies have been focused on the development and optimization of technologies for obtaining fuels based on biomass such as ethanol, butanol, biogas, and biodiesel as environmentally friendly energy vectors in substitution of fossil fuels. Ethanol and butanol can be obtained via fermentation of sugars or starch feedstocks, biogas can be produced via anaerobic fermentation of organic matter, and biodiesel can be produced

via transesterification reaction between alcohol and vegetable oils (e.g., soybean, sunflower, coconut oils) (Fernández-Naveira et al., 2017b; Kennes et al., 2013).

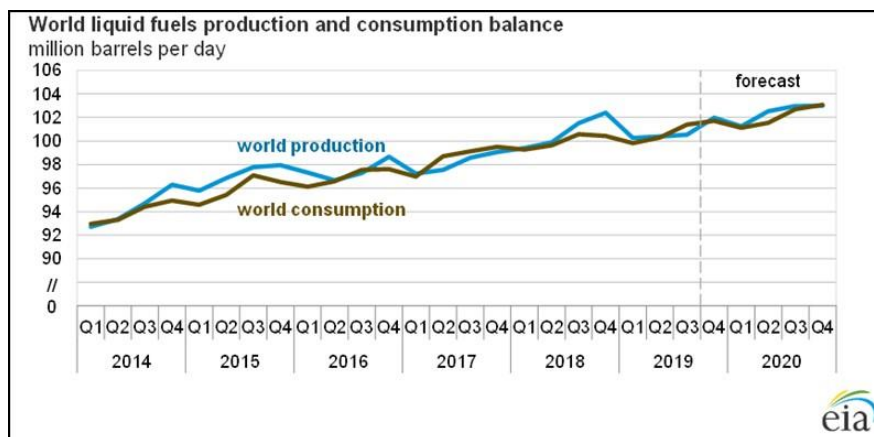


Figure 1.1: EIA, Short-Term Energy Outlook, October 2019.

1.1 Biofuels

Biofuels can be defined as fuels produced starting from biological material. The carbon balance of biofuels is close to neutral because the amount of CO₂ produced by combustion of these fuels is almost the same that the vegetable source captured from atmosphere during its growth. For this reason, bio-based fuels are a more environmentally friendly option when compared to fossil-based fuels (Lee and Lavoie, 2014). Biofuels are directly generated from plants and microorganisms. A synoptic diagram of renewable resources, conversion paths and products is reported in Figure 1.2.

The fuels produced from biomass are identified mainly as first- and second-generation biofuels.

First-generation biofuels are produced from sugar, starch, vegetable oil or animal fats. Seeds and grains such as wheat, corn and rapeseed are the main basic feedstocks. The most common first-generation biofuels are bioethanol, biodiesel and starch-derived biogas. The high sugar or oil content of the raw materials is the main advantage of first-generation biofuels, favouring their easy conversion into biofuel. The main drawback of first-generation biofuels is the feedstock competition with food and feed industries for the use of water and agricultural land. Because of this competition, these biofuels give rise to ethical, political and environmental concerns. To overcome these issues, production of second-generation biofuels gained an increasing worldwide interest as a possible “greener” alternative to fossil fuels and conventional biofuels (Cherubini, 2010). To overcome these issues, second-generation biofuels were developed.

Second-generation biofuels are defined as fuels produced from a wide spectrum of feedstock not in competition with food and/or feed industries. The typical feedstock used to produce these fuels are not-edible lignocellulosic biomass. These biomasses are usually separated in three categories: homogeneous (e.g. wood chips); quasi-homogeneous (e.g. agricultural and forest residues); and non-homogeneous (e.g. municipal solid wastes) (Lee and Lavoie, 2014). Contrarily to first-generation, second

generation biofuels have several advantages: price for this biomass is significantly less than the price for vegetable oil, corn, and sugarcane; not only seeds and grains, but the whole plant can be used for bioenergy purposes; high land-use efficiency and environmental performance; different bioproducts can be generated starting from the same feedstock (Cherubini, 2010; Lee and Lavoie, 2014). The main drawback of second-generation biofuels is the more complex structure of lignocellulosic feedstock that causes an increase of the conversion process cost. Indeed, the only pretreatment area may represent between 30% and 50% of the total equipment cost for an industrial scale plant (Valdivia et al., 2016).

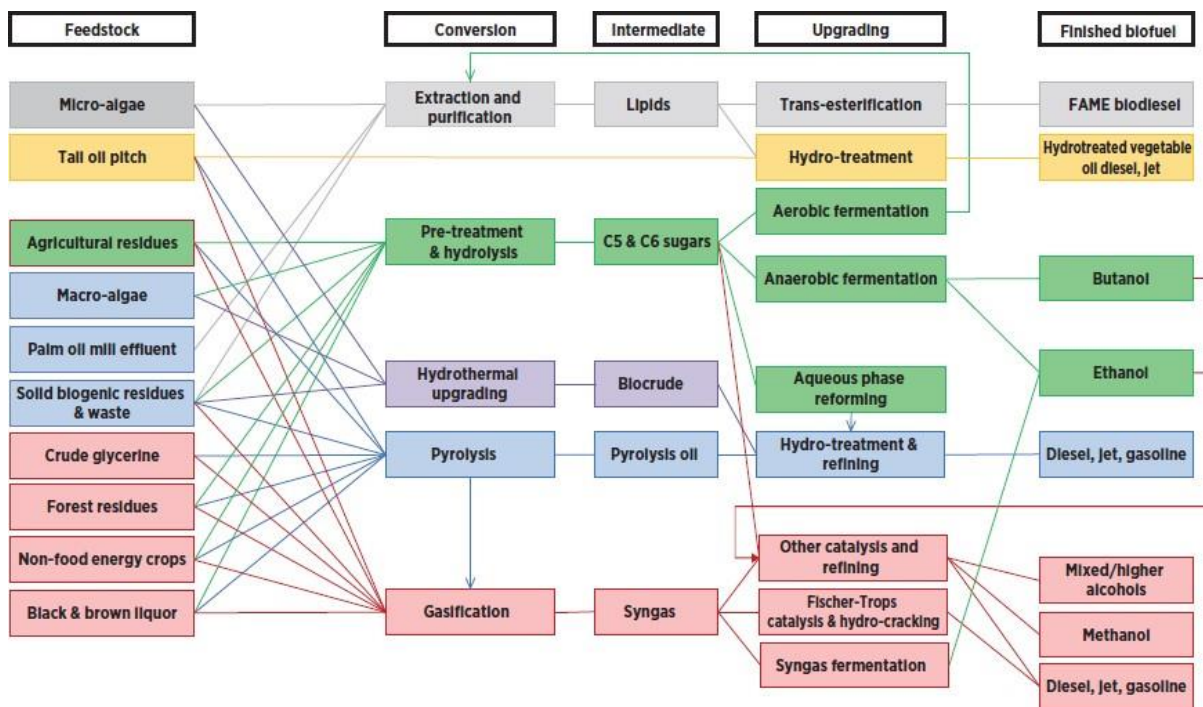


Figure 1.2: Biofuels production processes outlook, including feedstocks, technologies and final product (IRENA Innovation Outlook, Advanced Liquid Biofuels, 2016).

Biofuels include butanol. Butanol is a simple four-carbon alcohol considered a superior biofuel candidate with respect to ethanol (Lu et al., 2012). Indeed, butanol has interesting features compared to ethanol: higher energy content, lower vapor pressure and a similar air-to-fuel ratio to gasoline (Lu et al., 2012; Jin et al., 2011). A comparison of physical/chemical properties of butanol, ethanol and gasoline is reported in Table 1.1.

The most interesting property of butanol is its energy density very similar to gasoline's. For this reason, butanol may be used in the internal combustion engines currently ongoing.

Syngas fermentation is one of most promising technologies for the future sustainable biobased economies due to its potential as an intermediate step in the conversion of waste carbon to biofuels and other chemicals. It may constitute an efficient and competitive route for the valorisation of various waste materials, especially

if supported by systems engineering principles are employed targeting process optimization.

Table 1.1. Properties of some alcohols and conventional fossil fuels (Wagner et al., 2017).

Property	Gasoline	Diesel	Ethanol	n-Butanol
Density (g/L) at 20 °C	0.72 - 0.78	0.82 - 0.86	0.790	0.808
Octane number	80 - 99	20 - 30	108	96
Lower Heating value (MJ/kg)	42.7	42.5	26.8	33.1
Oxygen content (%w)	-	-	34.8	21.6
Autoignition temperature (°C)	300	210	434	385
Energy density	32	35.86	19.6	29.2

As shown in Figure 1.2, a large variety of feedstock is suitable for the gasification-syngas fermentation route. Moreover, some industrial processes (e.g., oil refining, steelmaking, production of carbon black, methanol and coke, gasification, and pyrolysis) release a huge amount of waste gases, where sometimes CO and H₂ are present in a significant amount. These waste gases can be used as raw materials for biological conversion into biofuel/biochemical, through fermentation.

1.2 Syngas fermentation

Syngas fermentation from C-based feedstock is a hybrid thermal-biological route to produce liquid biofuels. It includes the gasification of biomass and carbonaceous solid wastes to syngas, and the fermentative conversion of C1 gases (CO and CO₂) into alcohols. Lignocellulosic gasification is a valid thermochemical approach for the conversion of C-based feedstock - organic solid matter included - into a gaseous mixture made of H₂, CO, CO₂, and CH₄, named synthetic gas or syngas. Although about 55% of syngas is still produced from coal, biomass utilization - mainly from lignocellulose origins - is constantly growing (Ciliberti et al., 2020). The syngas fermentation is an innovative and promising strategy because it has the potential to successfully overcome the main flaws and weaknesses of the traditional catalytic conversion and biological processes.

Syngas can be supplied by a very wide range of possible feedstocks, including agricultural wastes, dedicated energy crops, forest residues, and municipal organic wastes, or even glycerol and feathers (Mohammadi et al., 2011; Dudynksy et al., 2012). Furthermore, some industries such as steel manufacturing, oil refining and chemical production generate large volume of CO and/or CO₂ rich gas streams as wastes. Tapping into these sources using microbial fermentation process essentially converts existing toxic waste gas streams into valuable commodities such as biofuels. Another application regards CO₂ captured from power plants, that can be blended with H₂ from renewable electricity generated via electrolysis (Liew et al., 2016).

Autotrophic acetogenic, carboxydophilic, and methanotrophic bacteria are able to capture carbon as C1 gases (CO, CO₂, or CH₄), and to convert the carbon in products that replace the fossil-derived counterparts. As a consequence, gas fermentation is a versatile industrial platform for the sustainable production of commodity-chemicals and fuels from gaseous resources derived from industrial processes, coal, biomass, municipal solid waste (MSW), and extracted natural gas.

The overall process of gas fermentation is shown in Figure 1.3. It is possible to

point out again the versatility of gas fermentation with the wide spectrum of possible raw materials.

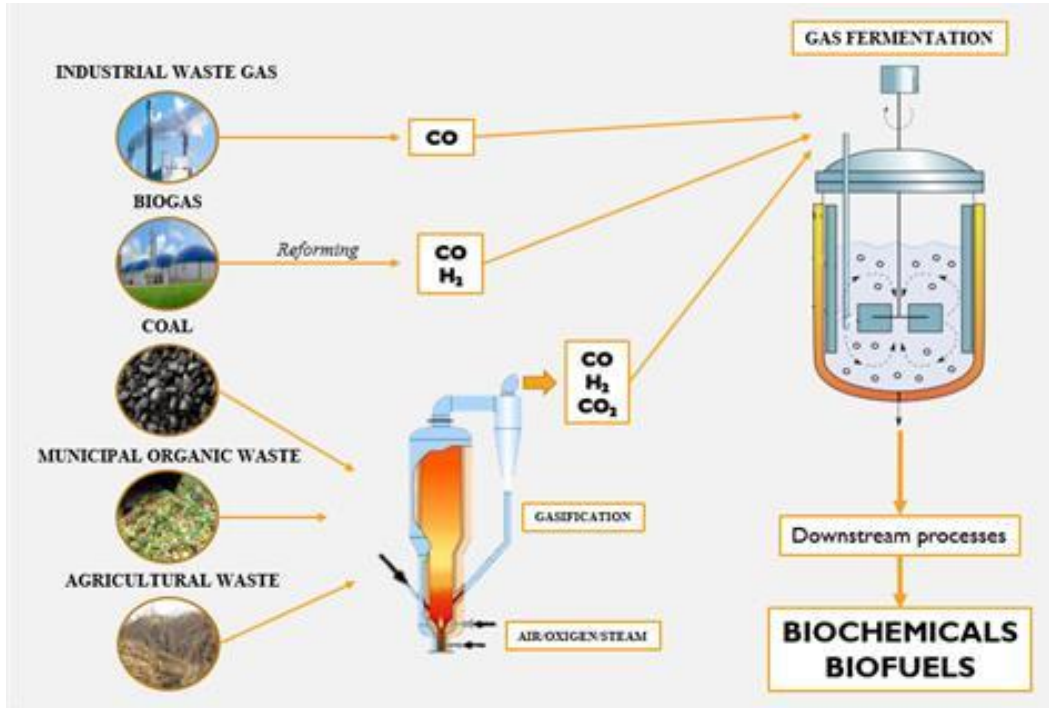


Figure 1.3: Syngas fermentation process (Shen et al., 2015).

Many microorganisms can metabolize syngas as carbon and energy source (Oelgeschläger and Rother, 2008), but only a few are able to convert it into biofuels. Among them, *Butyribacterium methylotrophicum* (Henstra et al., 2007), *C. ragsdalei* (Babu et al., 2010) were reported to be able to produce butanol from syngas, as well as *C. carboxidivorans* (Liou et al., 2005) which can produce both butanol and hexanol (Fernández-Naveira et al., 2016b; Phillips et al., 2015).

1.2.1 Gasification process

Gasification is a thermo-chemical conversion of carbonaceous feedstock to gaseous products through a partial oxidation process. It takes place inside a reactor, defined “gasifier”, at elevated temperatures (800 - 1500 °C).

In biomass gasification the lignocellulosic structure of biomass is thermally cracked into a gas mixture made of carbon monoxide (CO), hydrogen (H₂) and carbon dioxide (CO₂) and a small amount of methane (CH₄). Depending on the biomass type and composition, the raw syngas also contains small amounts of sulphur compounds (H₂S), nitrogen compounds (NH₃, NO_x), tars (i.e. condensable hydrocarbons), alkali metals, and chlorine. The composition of syngas is also affected by gasifying agent, type of gasifier and operating conditions (Abubackar et al., 2011). The feedstock is subjected to partial oxidation due to a lower concentration of oxygen than the stoichiometric requirement. Oxygen is supplied by a gasifying agent or carrier, such as air, pure oxygen, water steam, or their mixture. Although CO₂ can also be used as a gasifying agent, its use is less frequent. Moreover, the use of supercritical water is an

innovative technology, without the need for pre-treatment, which achieves a high H₂ yield and reduces tar and char production. According to the IEA Bioenergy Task 33, there are 114 working biomass gasification projects worldwide, 15 plants idle or on hold, and 13 are under construction or in planning. (Ciliberti et al., 2020).

One main limitation of gasification technology is represented by the formation of tars. Tars are classified into primary, secondary, and tertiary tars. Primary tars consist of both oxygenated compounds (alcohols, carboxylic acids, ketones, aldehydes, etc.) and substituted phenols (cresol, xylenol, etc.). Secondary tars are alkylated aromatics, such as toluene, ethylbenzene, xylenes, styrene, and hetero-aromatics, such as pyridine, furan, dioxin, and thiophene. Finally, tertiary tars consist of aromatics and polycyclic aromatic hydrocarbons (PAH), such as benzene, naphthalene, phenanthrene, pyrene, and benzopyrene. While primary tars are produced directly from the pyrolysis of cellulose, hemicellulose, and lignin, secondary and tertiary tars are the result of several complex reactions that have not been fully clarified yet. At the end of the entire process, two main product mixtures are present: a solid mixture and a gaseous mixture. The solid mixture contains the unreacted organic fraction and inert materials, such as tars and ashes. The gaseous mixture contains syngas and a small amount of impurities, such as light hydrocarbons (ethane, ethylene, acetylene), hydrogen sulfide (H₂S), sulfur dioxide (SO₂), hydrogen chloride (HCl), nitrogen oxides (NO_x), nitrogen (N₂), and ammonia (NH₃). The syngas's final composition and characteristics are related to the type of biomass, gasifying agent, gasifier type, and reactor's operational conditions, such as temperature, pressure, equivalence ratio (ER), residence time, and catalyst used. For these reasons, in the last few decades, gasification has been intensively studied to investigate the effects of these factors, and thus, to identify the optimal conditions for the process (Liakakou et al., 2021).

The final composition of the syngas depends on the feedstock, the applied technology and the type of reducing agent. For what concerns the feedstock, the most commonly used is wood, and secondary agro-industrial residues. The technologies involved to produce syngas are essentially fixed bed and fluidized bed reactors, with the latter favoured for the higher performance. The reducing agent can affect very strongly the final concentration, in particular air-gasification results in a very high content of N₂ in the final mixture, while O₂ or steam lead to a syngas rich in CO and H₂, with a much high calorific value. Although data on the negative effect of CH₄ have not been reported, this component is not used by microorganisms during syngas fermentation. Therefore, the CH₄ concentration in the syngas should be as low as possible. All the aforementioned impurities produced during the process can reduce the fermentability of syngas due to their negative effects on microorganisms. Therefore, one of the major challenges in biomass gasification is producing syngas with a low or absent impurities content. Biomass gasification needs further investigation studies to achieve an ideal syngas composition, thereby making the syngas fermentation process as efficient as possible (Ramachandriya et al., 2016).

1.2.2 Acetogenic bacteria

Acetogenic bacteria are a specialized group of bacteria with the peculiar ability to capture carbon as C1 gases and fix it into biomass, acetate and other metabolic products via the "Wood-Ljungdahl" pathway. Homoacetogenic bacteria, also called

acetogens, are obligate anaerobic bacteria able to grow chemolithotrophically on various substrates including C1 compounds such as carbon monoxide, carbon dioxide plus hydrogen, formate and methanol. Homoacetogenic bacteria fermentation produce volatile fatty acids and alcohols such as acetate, butyrate and ethanol, but mainly acetate, under ambient temperature and pressure (Mohammadi et al., 2011).

Acetogens are present in 23 different bacterial genera, which highlights that acetogenesis is not a phylogenetic trait. Most acetogens are found in one phylum, the Firmicutes (which are Gram-positive bacteria with low GC content). Several genera such as *Clostridium* contain acetogenic as well as non-acetogenic species, whereas other genera such as *Acetobacterium* or *Sporomusa* only contain acetogens. Most known acetogens belong to the genera *Clostridium* and *Acetobacterium* (Munasinghe and Khanal, 2011; Mohammadi et al., 2011).

1.2.3 Metabolic pathway

The metabolic pathway that allows acetogenic bacteria to grow and synthesize end-products that can be used as liquid fuels is known as Wood-Ljungdahl pathway (Figure 1.4). The acetyl-CoA pathway consists of two separate branches: the eastern branch (methyl branch) and the western branch (carbonyl branch). CO can directly enter in the pathway through the Western branch, while another molecule of CO can be oxidised to CO₂ by a monofunctional CO dehydrogenase (CODH) according to the biological water gas shift reaction. The energy surplus of the CO oxidization is captured as reduced ferredoxin. A fraction of the produced CO₂ enters the Eastern branch of the reductive acetyl-CoA pathway. The fraction depends on if CO serves as both carbon and energy source, or if an additional energy source such hydrogen is present which can be utilized in a hydrogenase (HYA) reaction. It should be noted that electron production is thermodynamically more favourable from CO than from H₂, and hydrogenases are reversibly inhibited by CO. Thus, at high CO concentration, no or only little hydrogen uptake will occur, but it will increase once CO is utilised, and the concentration drops.

In the first step of the Eastern (or methyl) branch, the thermodynamically unfavourable conversion of CO₂ is catalyzed by formate dehydrogenase (FDH). Then the formate undergoes through several reaction with mostly metallo- or vitamin-dependent enzymes, in order to supply the methyl group for the last reaction in which acetyl-CoA is formed. In the other branch (Western or carbonyl), CO can either be used directly, or generated from CO₂, and serves as the carbonyl group for acetyl-CoA synthesis. The unique multi-subunit bifunctional metalloenzyme CO dehydrogenase (CODH)/Acetyl-CoA synthase (ACS) is a characteristic and name-giving feature of the pathway. This key enzyme is capable of reducing CO₂ to CO in the Western branch and accepting the methyl group of the corrinoid-Fe/S-protein of the Eastern branch and condensing both the methyl and the carbonyl moiety with a CoA group to produce a molecule of acetyl-CoA (Ragsdale and Pierce, 2008; Daniell et al., 2012).

Enzyme activities in the Wood-Ljungdahl pathway are subjected to the availability of chemical nutrients like metals or cofactors provided in the medium. For example, the B vitamin pantothenate is a component of coenzyme A and can limit the rate of carbon fixation during syngas fermentation (Gaddy et al., 2007; Phillips et al.,

2015). For this reason, providing the proper amount of these micronutrients along the fermentation is strictly required.

The produced acetyl-CoA molecule can subsequently be used for the formation of a whole range of products, including long chain alcohols (butanol and hexanol).

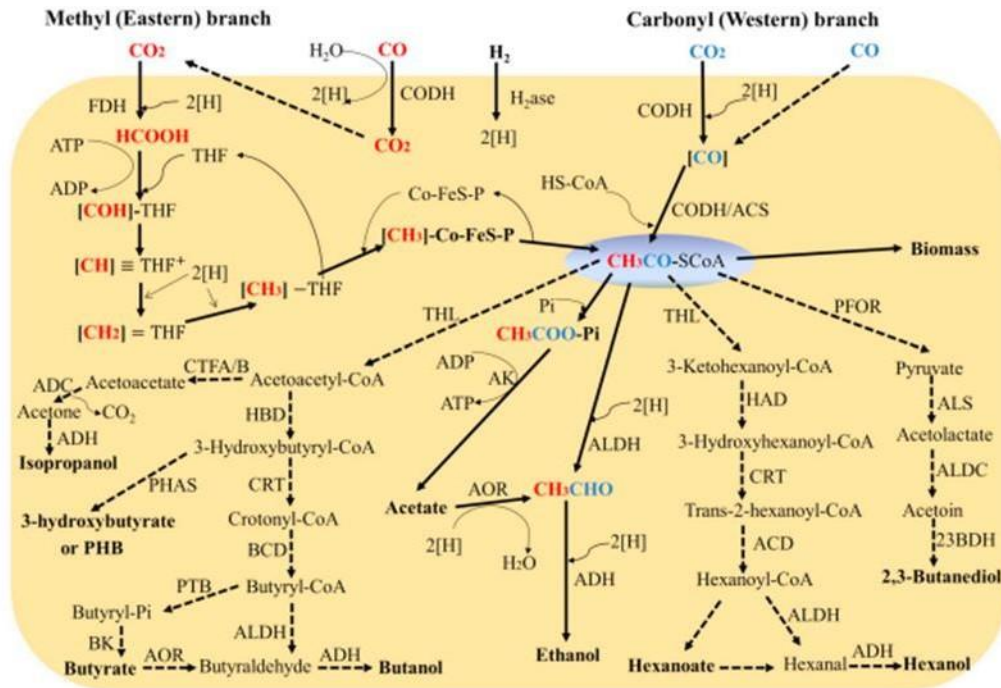


Figure 1.4: Metabolisms flow diagram for CO, H₂ and CO₂ in acetogenic bacteria via Wood-Ljungdahl pathway and its variations. Red color shows carbon flow in methyl branch. Blue color shows carbon flow in carbonyl branch. Dashed arrows represent pathways for synthesis of medium-carbon chain metabolites or biopolymer. Major enzymes involved in the pathway include: Acetate/ethanol production: FDH, formate dehydrogenase; CODH, carbon monoxide dehydrogenase; H₂ase, hydrogenase; ACS, acetyl-CoA synthase; AK, acetate kinase; AOR, aldehyde ferredoxin oxidoreductase; ALDH, aldehyde dehydrogenase; and ADH, alcohol dehydrogenase, butyrate/butanol production: THL, thiolase; HBD, 3-hydroxybutyryl-CoA dehydrogenase; BCD, butyryl-CoA dehydrogenase; PTB, phosphotransbutyrylase; and BK, butyrate kinase, hexanoate/hexanol production: HAD: 3-hydroxyacyl-CoA dehydrogenase; ACD: acyl-CoA dehydrogenase, 2,3-butanediol production: PFOR, pyruvate ferredoxin oxidoreductase; ALS, acetolactate synthase; ALDC, acetolactate decarboxylase; 23BDH, 2,3-butanediol dehydrogenase, acetone/isopropanol production: CTFA/B, acetoacetyl-CoA:acetate/butyrate-CoA-transferase; ADC, acetone decarboxylase, PHB production: PHBS, poly-3-hydroxybutyrate synthase. (Suna et al., 2019)

On one hand, acetyl-CoA could be converted to both acetate and ethanol. On the other hand, in the case of butanol production, acetyl-CoA is first enzymatically transformed into butyryl-CoA, which could also directly be converted to butyric acid and butanol as end products. Acids, i.e. acetate or butyrate, formed from acetyl-CoA or butyryl-CoA, can also further be converted to the corresponding alcohols (Fernández-Naveira et al., 2017b). Exponential biomass growth and acidogenesis (with production of acids and acidification of the medium) are two related processes and take place

simultaneously. Based on the few results published so far, acetic acid appears first and is produced at somewhat higher concentrations than butyric and hexanoic acid in *C. carboxidivorans* (Fernández-Naveira et al., 2017a).

The conversion of the different acyl-CoA to alcohols is known as solventogenesis. This phase in clostridia has been considered to start when the conditions are not favourable anymore for growth, i.e. low pH, low ATP levels, accumulation of high concentrations of organic acids, sporulation, low level of availability of reducing energy. In case of acetate, the acid yields acetaldehyde in a reaction catalyzed by ferredoxin: aldehydeoxydoreductase (AOR). Then, ethanol is produced through the reduction of acetaldehyde. Similar enzymes are used for the conversion of butyric acid (and hexanoic acid) into butyraldehyde (and hexaldehyde) first and subsequently into butanol (and hexanol).

Besides the indirect conversion, that occurs through the re-assimilation of the acids, an alternative route has been reported in several studies. In fact, each acyl-CoA could be directly converted in the aldehyde form due to the action of a dehydrogenase enzyme (AAD). Subsequently, the reaction catalyzed by the alcohols dehydrogenase (ADH) leads to the production of ethanol, butanol and hexanol. However, it is not certain which one is predominant. Several researchers reported that consumption of acids is associated with alcohols production (Younesi et al., 2005; Maddipati et al., 2011). They mentioned that during the solventogenic phase the acids concentration declined together with an increase of pH and alcohols. Various experiments have proven that alcohols formation also occurred during exponential growth (Kundiyana et al., 2010). Probably, this would mean that alcohols production is mixed growth associated.

Regarding solvents, the highest product concentration has always been found for ethanol followed by butanol and finally hexanol. Those alcohols are produced in different chronological order during CO or syngas fermentation, with short chain alcohols appearing first while longer chain ones appear later. Therefore, whether alcohols are the desired end products, it is necessary to identify the optimum medium composition and conditions for an efficient conversion of accumulated organic acids with the concomitant production of solvents (Fernández-Naveira et al., 2017b).

1.3. *Clostridium carboxidivorans*

A few number of acetogenic strains is able to produce not only ethanol, but also long chain alcohols, like butanol and hexanol, at significant concentrations. *C. carboxidivorans* is the most promising strain for butanol production on large scale.

C. carboxidivorans (Figure 1.5) is a Gram positive, mesophilic, and obligate anaerobic carboxidotroph, originally isolated from an agricultural settling lagoon in Oklahoma, USA. Its cells are mobile, with rod-shape (0.5×3 µm) and can present sporulated forms, which appear like a terminal or subterminal protuberance (Fernández-Naveira et al., 2017a; Liou et al., 2005).

C. carboxidivorans can perform a chemoautotrophic growth on syngas, using CO or H₂/CO₂, or a chemoorganotrophic one using several sugars such as glucose, xylose, fructose, cellobiose and arabinose. It can ferment these carbon sources to produce acids, mainly acetic acid, butyric acid, and hexanoic acid, and alcohols, i.e. ethanol, butanol and hexanol (Liou et al., 2005; Phillips et al. 2015).

C. carboxidivorans metabolizes CO as single substrate and uses it both as carbon and energy source. CO₂ can be used only as carbon source when hydrogen is present as energy source. The acetogens depend on the Wood-Ljungdahl pathway, also known as the acetyl-CoA pathway, to convert inorganic carbon into biomass and products. The WLP uses CO, CO₂ and H₂ as a source of energy and carbon leading to the acetyl-CoA production. During fermentation of syngas, electrons are obtained from the oxidation of hydrogen, catalyzed by hydrogenase, or from the oxidation of CO to CO₂, catalyzed by CO dehydrogenase (CODH) (Schuchmann and Müller, 2014). Subsequently, the acetyl-CoA is then either integrated in cellular biomass or converted to metabolic products according to the Hexanol-Butanol-Ethanol (HBE) fermentation pathway.

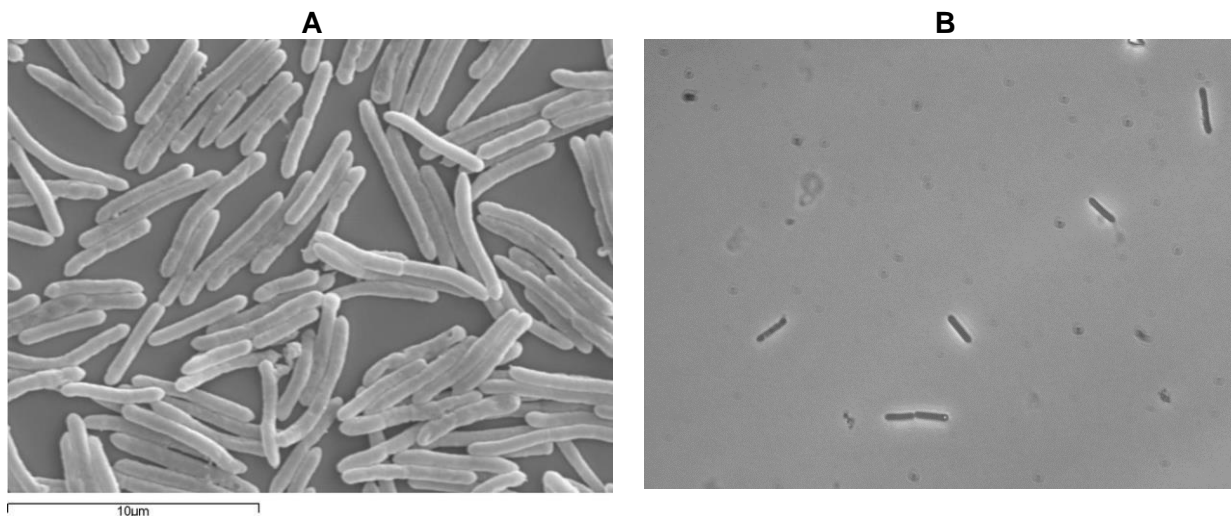


Figure 1.5: SEM of *C. carboxidivorans* grown on CO: **A** pic was published by Fernández-Naveira et al., (2017a); **B** pic was taken during the experimental campaign of the present work.

1.4 Advantages of syngas fermentation

Use of bacteria as biocatalyst has successfully offset several weaknesses of the traditional catalytic conversion process. Biocatalysts operate at moderate temperature and pressure (30 – 37 °C and near atmospheric pressure) than catalytic chemical reactions (200 – 350 °C and 10 – 200 atm) and it results in substantial energy saving. Moreover, several issues promote the biotechnological routes instead of the catalytic route. One of the strongest points of gas fermentation, compared to traditional fermentation processes, is in the biomass pre-treatment step. The hydrolytic route to treat raw biomass is not always sustainable—from an economic, energetic, and environmental point of view— especially if the lignin fraction is too high, and even though the overall Carbon-fraction of the biomass is promising (Fernández-Naveira et al., 2017a). The thermochemical route, on the other side, might include the gasification/pyrolysis technology under high temperatures, to convert the lignocellulosic structure of biomass to intermediate gas (syngas) or liquid products. Therefore, the thermochemical route is capable to exploit the whole carbon-fraction of the biomass. The mixture of carbon monoxide (CO), hydrogen (H₂), carbon dioxide (CO₂), methane (CH₄), and trace gases—can be further processed in a biological step.

Biofuels from syngas may be produced through the Fischer–Tropsch (FT) route and the syngas fermentation route. The FT process uses metal catalysts to convert syngas into liquid hydrocarbons, but a clean-up unit is required to remove impurities (for example sulphur containing compounds). Moreover, the catalyst requires specific syngas composition in order to work correctly (Pendyala et al, 2009). Although conversion of syngas to fuels using metal-based catalysts is a reliable technology, the catalytic route is restricted by some barriers. Drawbacks such as low catalyst selectivity, intensive operation cost due to the utilization of high temperatures and pressurized reactors wide product distribution requiring a specific ratio of gas components to yield a desired product - and catalyst poisoning by trace of sulphur gases in the syngas contribute to the high cost of synthesis fuels (Daniell et al., 2012).

Other important considerations about the benefits of gas fermentation are:

- High reaction specificity is achieved in biological conversion in comparison to catalytic process due to the high enzymatic specificity. As a result of the high specificity, product yield is improved, the recovery of product is simplified and less toxic by-products are evolved during the process (Latif et al, 2014).
- Biocatalysts are less sensitive to the syngas composition in terms of CO/CO₂/H₂ ratios, whereas traditional catalysts need a specific ratio of gas components to yield a desired product.
- Even organic feedstocks, that may be toxic or recalcitrant to enzymatic process, can be fermented after gasification, including also coal and wastes as chemical difference between feedstocks is almost insignificant in the gasification process (Daniell et al, 2012).
- Most biocatalysts can tolerate small amounts of contaminants such as sulphur and chlorine, unlike metal-based catalysts.

1.4.1 Challenges and open issues

To commercialize biofuels produced by syngas fermentation, it is necessary to increase the maximum productivity, yield and concentration of the products. Studies should focus on the optimization of the reactor system and its operating conditions. Other issues of interest to increase process economics are minimizing gas pre-processing, media/water reuse, and lowering product separation costs.

A review of the products from the most known microorganisms able to grow using CO as gaseous substrate is presented in Table 1.1.

The formation of products from gas fermentation is affected by several factors and typically key products are produced under non-optimal growth conditions. Therefore, high concentration of key products may not be produced in a single processing step. Multiple processing stages could broaden the portfolio of products obtained from syngas fermentation together with high end-product concentrations. A review of the productivity of the main products of syngas fermentation is presented in the Table 1.2.

One of the major challenging issues related to syngas fermentation is the gas-liquid mass transport. The liquid phase of a bioreactor usually is a viscous broth, therefore guaranteeing an effective distribution of the gas molecules inside is not trivial and requires an adequate study and optimization.

Table 1.2. Main microorganisms able to produce alcohols by syngas fermentation, and their max doubling time (Köpke et al., 2011).

Organism	Products	Min. doubling time on CO
<i>Butyribacterium methylotrophicum</i>	Acetate, ethanol, Butyrate, butanol	13.9 hours
<i>C. autoethanogenum</i>	Acetate, ethanol	4.0 hours
<i>C. carboxidivorans</i>	Acetate, ethanol, butyrate, butanol	4.3 hours
<i>C. drakei</i>	Acetate, ethanol, butyrate	5.8 hours
<i>C. ljungdahlii</i>	Acetate, ethanol	3.8 hours
<i>C. ragsdalei</i>	Acetate, ethanol	4.0 hours
<i>C. scatologenes</i>	Acetate, ethanol, butyrate	7.7 hours
<i>Oxobacter pfenngii</i>	Acetate, butyrate	13.9 hours

Table 1.3. Examples of volumetric productivity, titer, and yield of some gas fermentation target products (Redl et al., 2017).

	Volumetric productivity, mmol/L/day	Titer	Yield, mol/mol CO	Microbial strain
Ethanol	193	450	0.14	<i>C. ljungdahlii</i>
	0.25	5.5		
Butanol	n.a.	25.6	n.a.	<i>C. autoethanogenum</i>
	3.5	6	0.074	Co-culture
	2.7	8	0.0080	<i>C. carboxydivorans</i> P7
Hexanol	2	4	0.05	Co-culture
	2.1	5	0.0038	<i>C. carboxydivorans</i> P7

The parameter via which the mass transfer capacity can be assessed is the gas–liquid volumetric transfer coefficients (k_La). There are few studies regarding this issue. It is supposed that limited characterization can be due to the difficult in the accurate measurement of the dissolved CO concentration (Köpke et al., 2011). The value of k_La is affected by several operating variables, the most important are the geometry and size of the reactor system, the agitation speed, the shape of the impellers, the bubblers, the flow rate and so on.

Several solutions have been proposed to improve the mass transport rate and to increase the solubility of the gas in the fermentation media. A review of the most accredited is shown in Figure 1.6. Particularly worth of interest is the monolithic biofilm reactor (1.6e), as the possibility to form biofilm by *C. carboxidivorans* will be deeply discussed later.

Solutions typically aim to enhance the gas to liquid flow rates, the specific gas–liquid interfacial areas and to increase the pressure. Moreover, different reactor configurations, innovative impeller designs, microbubble disperser and many different technological solutions, can provide huge benefits. However, many of these proposed solutions increase significantly the energy cost of the overall process, and they are not economically attractive for commercial syngas fermentation (Drzyzga et al., 2015).

Another important point to consider, when it comes to design a bioreactor, is the

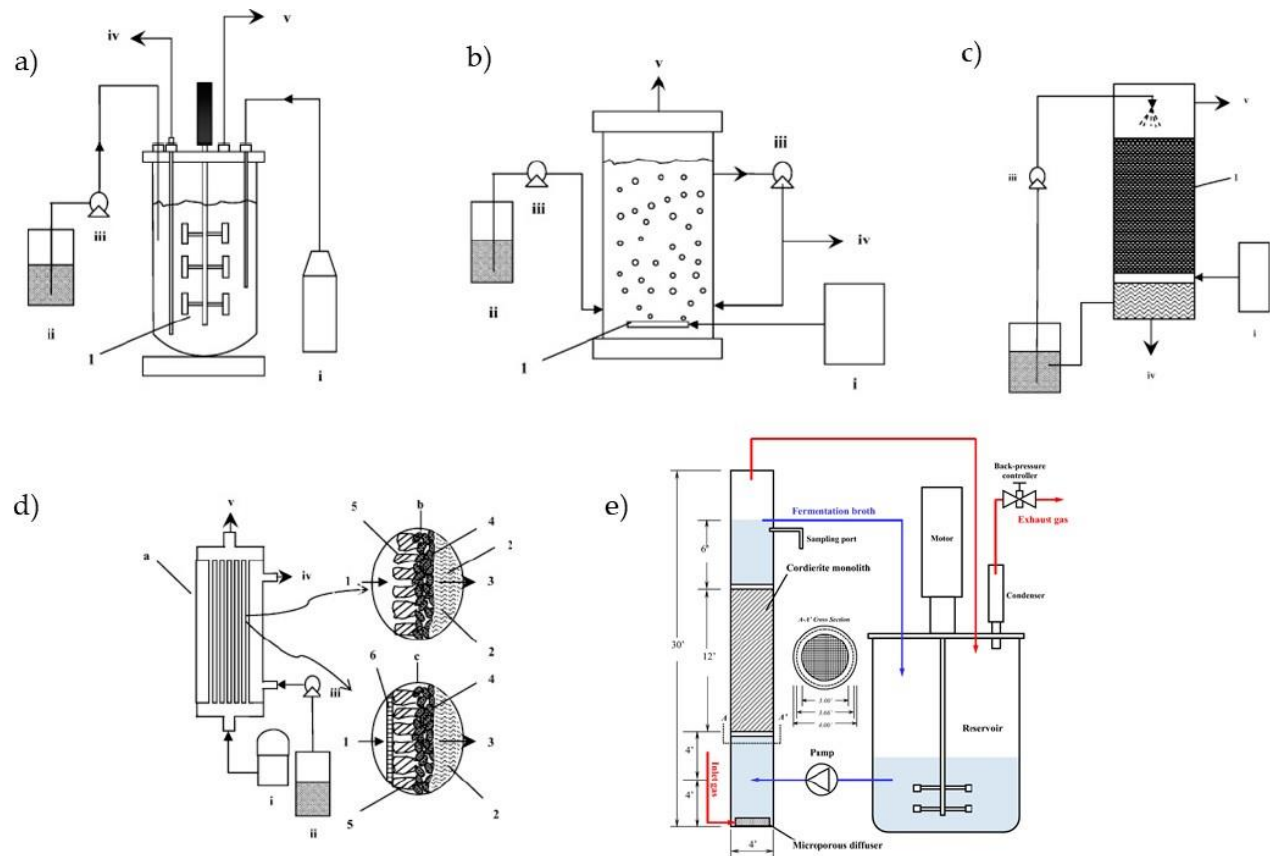


Figure 1.6: Schematic illustrations of common bioreactors for syngas fermentation: (a) mechanical continuous stirred tank reactor (CSTR), (b) bubble column reactor (BCR), (c) trickle-bed reactor (TBR), (d) hollow-fiber membrane bioreactor (HFMBR) (Abubackar et al., 2011); , and (e) MBR (Shen et al., 2014).

possibility to retain the microbial cells inside of the reactor: in this way a higher concentration of microorganism can be achieved, leading to a higher productivity of the desired products.

One of the most common strategies used to achieve this goal is favoring the formation of cellular aggregates (biofilm) that can adhere to a solid support. The ability of forming biofilm is something related to the specific strain, therefore a specific study about this potential should be carried out case by case. However, *Clostridia* have shown a good propensity to attach on a solid support (Raganati et al., 2016).

Biofilm processes may display significant advantages over conventional cell suspension or containment systems: larger biomass loading, larger permissible dilution rates without biomass washout, easy cell–liquid separation, and protection against toxic or inhibitory compounds (Gòdia et al., 1995; Schügerl et al., 1997; Nicoletta et al., 2000; Qureshi et al., 2005).

Models to describe syngas fermentation are still scarce in the literature, and only a few authors have attempted to adjust kinetic expressions to experimental data. Younesi et al. (2005) and Mohammadi et al. (2014) adjusted logistic curves to the growth of *C. ljungdahlii* on artificial syngas using experimental data from batch fermentation essays in serum bottles. Mohammadi et al. (2014) were also able to fit

Gompertz equations to their experimental profiles of product formation, and uptake rate equations for CO, presenting estimations of kinetic parameters that were later adopted by Chen et al. (Chen et al., 2015) in their dynamic Flux Balance Analysis (FBA) model of a syngas fermentation bubble column. In the present study, a dynamic model was constructed for gas fermentation of *C. carboxidivorans*, with ethanol and butanol production, in a continuous stirred tank reactor (CSTR). The unknown model parameters were estimated with a multi-response minimization framework using experimental culture data from the literature and the significance of parameters was assessed with statistical analysis.

Promoting the formation of microbial aggregates/biofilms is an effective strategy for achieving enhanced productivity in bioprocesses. Formation of aggregates makes it possible to obtain cultures characterized by cell densities (biomass per unit volume) much larger than those commonly harvested in liquid broths (Nicoletta et al., 2000; Qureshi et al., 2005). The possibility of achieving large cell densities is an attractive feature that can be exploited in a number of applications of fermentation to improve process intensification. Currently, immobilization of cells and membrane reactor technology (Figure 1.6) are the two common pathways to achieve high-density confined cell cultures in either discontinuous or flow reactors. Immobilization of cells by adhesion on natural, typically inexpensive, supports is the first step for the production of biofilm. Figure 1.7 shows a SEM image of a monolith biofilm reactor. Proper choice of granular supports, together with careful selection of the microbial strain, are the keys to a successful design of multiphase biofilm reactors. The establishment of solid-supported biomass loading in continuous biofilm reactors results from the competition between cells adhesion/growth on the granular carrier and detachment of biofilm fragments from the granules (Russo et al., 2008).

1.5 Bioprocess modelling

Syngas fermentation may be carried out in three-phase reactors: the syngas stream is the gaseous phase, the culture medium is the liquid phase, the suspended/immobilized cells are the solid phase. Some key issues characterize the syngas fermentation process: i) mass transfer from the gas phase to the liquid phase to deliver substrates (CO/CO₂/H₂) into the culture broth; ii) cell growth characterized by substrate inhibition; iii) low product yields, typical of C1 substrate fermentation. All these issues must be addressed to optimize the overall syngas conversion and to maximize the biofuel productivity. Recently, the number of papers regarding the modeling and simulation of syngas fermentation are increasing (de Medeiros et al., 2019, Safarian et al., 2020).

Fermentation is a complex process, which involves numerous reactions, metabolic products, genes, enzymes, metabolic switching mechanisms with interconnections between them and dependence on environmental/operating conditions. Experimental analysis is the first step to obtain information of a new or poorly understood biosystem and to achieve more knowledge about the behaviour of the system. Downside of this approach might be the fact that fermentation processes are typically time consuming due to slow kinetics, which results in a high operating cost

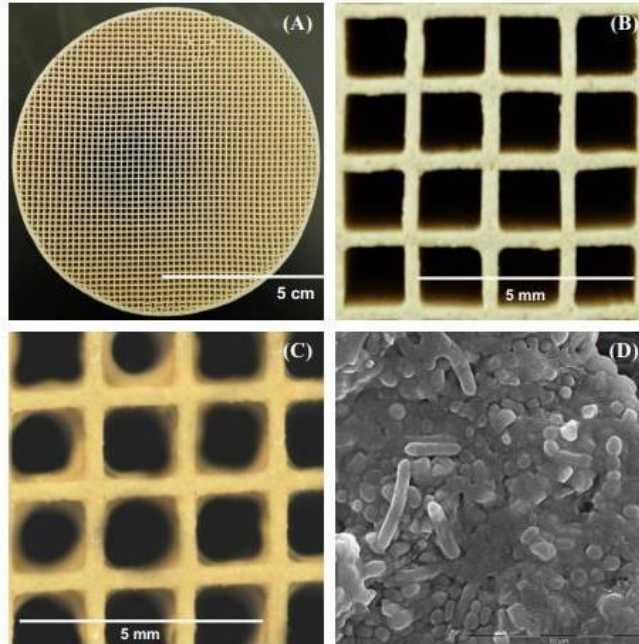


Figure 1.7: (A) Top view of monolith; (B) top view of monolith (enlarged); (C) formed biofilm of *C. carboxidivorans* P7 at the end of batch syngas fermentation; (D) SEM imaging of *C. carboxidivorans* biofilm attached on monolithic microchannel wall (Shen et al., 2015).

together with the cost of the consumables. In addition, fermentation performance is often affected by operating conditions such as temperature, pH, substrate concentration and presence of inhibitors. Therefore, the selection of the optimal operating conditions would require a great number of experiments with different combinations of those (Birgen, 2019).

To assess optimal operating conditions by carrying out a limited number of lab experiments, the development of kinetic models describing the cell growth, product formation, and substrate consumption is necessary (Gunes, 2021). Mathematical models, able to describe process features, as realistically as possible, could be a concrete opportunity for process optimization. Furthermore, it could provide insight into the main characteristics of the fermentation processes as well as the influence of different operating conditions and their interlinking.

Models based on fermentation equations and other stoichiometric models based on metabolic flux analysis are essentially steady- state models. Therefore, these models do not provide any time variant or temporal information on formation of different metabolites. Thus, applicability of these models for design and optimization of bioreactors is rather limited. This shortcoming is overcome by kinetic simulation models: they reveal dynamic behaviour of all metabolites and give information on the dominant metabolic pathways that have maximum influence on production of main products (Mayank et al., 2013).

In the classical approach of developing bioprocess dynamic models, mathematical relations are employed for describing the relevant mechanisms. Two main systems must be analyzed: the bioreactor system and the biological cell system. Considering

some assumption such as batch configuration, perfect mixing (i.e. liquid and gas phase is assumed to be homogeneous) and constant temperature, the following general equation (1.1) could describe the variation of each components inside a bioreactor:

$$\frac{dC_i}{dt} = R_i + N_i \quad (1.1)$$

where C_i is the i^{th} component concentration, R_i the reaction kinetics and N_i the mass transfer rate (González-Figueroa et al., 2018).

Bioreactor models include mass transfer issues and flow patterns in both gas and liquid phases. For example, in several bioprocesses one of the most frequently cause of limitation to cell growth is the amount of dissolved oxygen (and inorganic carbon) for aerobic bacteria (and autotrophs), and the case of gas fermentation is similar to aerobic fermentation, from this point of view. Generally, gaseous substrates have a very low solubility in fermentation media. The mass transfer capacity between gas and liquid phases could be a bottleneck in some bioprocesses. The mathematical description of the mass transfer rate from the gas phase to the liquid phase is based on general concepts of mass transfer theory. The mass transport rate may express by the expression (1.2):

$$N = k_L a (C^* - C_L) \quad (1.2)$$

where k_L ($m^{-1} s^{-1}$) is the mass transfer coefficient, and a (m) the specific exchange area. It is very difficult to measure both k_L and a separately in a fermentation, therefore the two parameters are combined in the term $k_L a$, the volumetric mass transfer coefficient. The parameter illustrates the agitation capacity, it depends on the design and operating conditions. The concentration gradient is considered as the driving force of the mass transfer. C_L is the dissolved gas concentration and C^* represents the saturation concentration of a component at the gas/liquid phase, assumed to be in equilibrium with his gas phase as expressed by Henry's Law (Garcia-Ochoa and Gomez, 2009)

Cell models include the kinetics on the individual cell level and on the whole cell population level. The reaction term R is the result of an extremely complex metabolic reactions network. Mathematic descriptions of microorganism kinetics are often simplifications of the reality. In general, cell models can be classified in structured/unstructured and segregated/non-segregated. Cell models considering the existence of intracellular components are called structured, otherwise they are termed unstructured. They may also assume the existence of a morphological structure, being then termed segregated models, or may assume that all cells are identical (only one morphological form) being then termed non-segregated models.

For bioprocess optimization, control and supervision, unstructured and non-segregated models are the only ones of practical interest. In developing such models, principles of macroscopic stoichiometry and empirical kinetic correlations are employed. Unstructured kinetic models represent the metabolic behaviour of the biomass cell production describing the process in terms of the growth of microorganisms, the utilization of substrates and the formation of products. From simple experimental data, it is possible to obtain information to represent cellular growth with unstructured kinetic models.

2. AIM OF THE THESIS

Syngas fermentation could become a promising alternative compared to the currently chemical production processes as well as to the traditional bioprocesses. One of the great benefits is that waste/low-cost materials could be transformed into energy rich biofuels and chemicals, contributing to the capture of industrial waste gases that would require a specific treatment. For this reasons, bioconversion of syngas into products with added value can also provide a solution for the increasing energy demand and be an aid in reducing greenhouse gas emissions. Although this technology seems a suitable alternative to the consolidate production routes, in order to scale it up and to make this biotechnological route economically feasible, significant efforts have to be made.

The overall objective of this Ph.D. thesis has been to understand the mechanisms and the phenomena that affect the performance of a syngas fermentation process, with a particular attention given to butanol production. The activities have been carried out at the Dipartimento di Ingegneria Chimica, dei Materiale e della Produzione Industriale of the Università degli Studi di Napoli *Federico II*.

The aims of the activities carried out during the PhD research period have been:

- a) review of the reports, patents and/ papers focused on the production processes and technologies for biofuel productions by syngas fermentation. The focus has regarded the processes, the strains, and the apparatus/devices typically used. The key issue for the strain selection has been the ability to produce long-chain alcohols. *Clostridium carboxidivorans* has been selected “model strain” to carry out fermentation experiments;
- b) Development of a reactor system suitable for the characterization of the growth rate of the selected microorganism and the production rate of metabolites, under safe conditions provided. Indeed, the fermentations present the risks related to work with toxic and flammable gas mixtures;
- c) Kinetic characterization of the selected microorganism in terms of growth rate and of solvent production rate under different operating conditions;
- d) Simulation of the conversion processes in potential bioreactors to be used in industrial production. Models have been proposed to describe the dynamics of the selected strain taking into account lumped conversion mechanisms and principles of chemical engineering regarding ideal reactors and transport phenomena

A six-month research period has been carried out at University of Western Ontario, in London (ON), Canada. During this period, different techniques were studied, to improve the quality and the effectiveness of fermentation tests and analysis method. An experimental campaign has been scheduled to assess the effect of the ratio of CO:H₂:CO₂ on *C. carboxidivorans* growth. Unfortunately, due to several technical issues regarding the equipment, and storage/reactivation of strains, the fermentation tests have not been successful, and it has not been possible to collect useful experimental data.

The scheduled activities have included a six-month research period at the Solaris Biotechnology s.r.l.. The activities have been organized for the period February-July 2020. However, the COVID-19 pandemic scenario has not allowed the stage at the industry. The activity would have been focused on the set-up and development of an

effective reactor system for syngas fermentation. In agreement with the director of the Solaris Biotechnology s.r.l., the activity has been remodeled. In particular, the activity has been carried out under remote conditions and it has regarded the simulation of a continuous fermenter. It is expected that in a near future it will be possible to compare the simulation results with the operation of a real industrial fermenter.

Apparatus set-up

The activity has regarded the preparation of the laboratory to operate with substrate toxic and inflammable. As a matter of fact, carbon monoxide is a very dangerous gas, not only for its toxicity (LD50 is 5000 ppm), but being odorless and colorless.

In particular, the operation of the fermentation runs has asked to design, select, set-up and test a dedicated safety system. The system has included a box to house pressurized vessels of syngas, a fume hood, devices to measure the concentration of CO, H₂ and O₂ in the laboratory close to the fermentation area, a control unit.

C. carboxidivorans fermentation

Fermentation tests have been carried out to characterize the growth kinetics of *C. carboxidivorans* and the stoichiometry of the CO conversion. Two typologies of fermentation campaign have been carried out. The first campaign has regarded batch tests in closed vessels. The second campaign has regarded a fermenter operated under continuous conditions with respect to the gas phase and under batch conditions with respect to the liquid phase.

Tests of the campaign in the closed vessel have been carried out in sealed serum bottles to minimize the amount of the medium/substrate. Test have been addressed to assess the effect of some key parameters, e.g. pH, redox potential, and CO partial pressure.

Tests carried out in a controlled fermenter have been focused to assess the effects of a series of operating conditions. The pH has been kept constant at pre-set value. The CO concentration in the liquid phase has been tuned by changing the gas stream flow rate and the gas-liquid mixing.

Syngas fermentation modelling

A model has been proposed to describe the fermentation dynamics, to address industrial development of the process and to support the optimization/scale-up of the process.

The complex metabolism has been schematized with a set of overall reactions that enclose the cell growth, the metabolites production growth associated and non-growth associated. The model parameters have been assessed by regression of experimental data according to the proposed model. A vector of 31 kinetic and yield parameters has been estimated.

The developed model has been applied to simulate a biofilm reactor system. The beneficial effects of the biofilm formation has been assessed by a series of simulations carried out with MATLAB software.

3. FERMENTATION TESTS

This section focused on the fermentation tests. The first section reports the activity regarding the set-up of the lab dedicated to operate with syngas, a toxic and flammable gas. The second section (§ 3.2) reports on the fermentation tests carried out in closed fermenters under batch conditions with respect to both the gas and the liquid phases. The study was aimed at characterizing the effect of the operating conditions of fermentation. The third section (§ 3.3) focused on fermentation tests carried out in a mechanically agitated fermenter operated under batch conditions with respect to the liquid phase and continuous conditions with respect to the gas phase. The study was aimed at the assessment of the performances, in terms of alcohols production, exploiting the continuous supply of substrate, tuning the flux of gas to operate the system as a differential reactor. The high availability of CO and the strong agitation system are expected to provide better results when compared with the batch tests. The effect of pH on the fermentation was also investigated.

Every fermentation test was carried out in the same culture medium (Phillips et al., 2015), because the formulation is established and widely used as a standard for *C. carboxidivorans*. The effects related to medium composition were not investigated in the present thesis.

3.1 Laboratory set-up

During the first year of the PhD program the activity has regarded the preparation of the laboratory to operate with substrate toxic and inflammable. As a matter of fact, carbon monoxide is a very dangerous gas, not only for its toxicity (LD50 is 5000 ppm) but being odorless and colorless. Specific instrumentations are required to detect CO and H₂, a highly explosive gas.

A system of fume hood has been realized to guarantee an adequate aspiration to prevent that the gases could reach dangerous concentrations in case of leakage. The hoods have been designed taking into account the maximum syngas flow rate expected to be delivered to the fermenter,

The syngas cylinders have been housed in a box outside the laboratory. A dedicated distribution line has been realized to deliver the gases to the reactor at the set low pressure ($\Delta P = 0.5 - 1$ bar). The maximum concentration of CO allowed in the environment was set to 40 ppm, monitored 24/7 by a detector installed near the gas inlet. In case of anomaly or gas leakage, the system has been programmed to immediately shut down the gas flow by means of a solenoid valve connected to the cylinder. Manual reset of the syngas supplying prevents any no programmed deliver.

The design, authorization and set-up of the storage and delivering system of the syngas has required to harmonize the plant requirements, the current safety regulation and the public work regulations. The harmonization asked about one year.

The operation of the fermenter in the prepared laboratory has asked the drafting of a safety document and the scheduling of check activity.

3.2 Batch Syngas Fermentation by *Clostridium carboxidivorans* for Production of Acids and Alcohols¹

F. Lanzillo^a, G. Ruggiero^a, F. Raganati^a, M.E. Russo^b, A. Marzocchella^a

^a Department of Chemical, Materials and Production Engineering—University of Naples Federico II,

^b Institute of Science and Technology for Energy and Sustainable Mobility (STEMS) - CNR

Abstract: Syngas (CO, CO₂, and H₂) has attracted special attention due to the double benefit of syngas fermentation for carbon sequestration (pollution reduction), while generating energy. Syngas can be either produced by gasification of biomasses or as a by-product of industrial processes. Only few microorganisms, mainly clostridia, were identified as capable of using syngas as a substrate to produce medium chain acids, or alcohols (such as butyric acid, butanol, hexanoic acid, and hexanol). Since CO plays a critical role in the availability of reducing equivalents and carbon conversion, this work assessed the effects of constant CO partial pressure (P_{CO}), ranging from 0.5 to 2.5 bar, on cell growth, acid production, and solvent production, using *Clostridium carboxidivorans*. Moreover, this work focused on the effect of the liquid to gas volume ratio (V_L/V_G) on fermentation performances; in particular, two V_L/V_G were considered (0.28 and 0.92). The main results included—(a) P_{CO} affected the growth kinetics of the microorganism; indeed, *C. carboxidivorans* growth rate was characterized by CO inhibition within the investigated range of CO concentration, and the optimal P_{CO} was 1.1 bar (corresponding to a dissolved CO concentration of about 25 mg/L) for both V_L/V_G used; (b) growth differences were observed when the gas-to-liquid volume ratio changed; mass transport phenomena did not control the CO uptake for $V_L/V_G = 0.28$; on the contrary, the experimental CO depletion rate was about equal to the transport rate in the case of $V_L/V_G = 0.92$.

Keywords: *Clostridium carboxidivorans*; syngas; ethanol; butanol; growth kinetics.

Introduction

The continuous increase in the demand for energy and materials throughout the world—as a consequence of the rapid increase of the world population and of the growing industrialization of the developing countries—increased environmental pollution and the pressure on fossil resources. Apart from environmental fallout, exploitation of fossil resources strongly affects the economic and social worldwide scenario—resource country independence, natural resource cost, etc. A potential solution to these issues is offered by the exploitation of renewable sources processed under sustainable conditions (Gowen and Fong, 2011; (Abdehagh et al., 2014). Ethanol and higher chain alcohols (e.g., butanol) are potential substitutes of fossil fuels as well as of chemical building blocks (Fernández-Naveira et al., 2016a). Alcohols can be produced by processing renewable resources via thermochemical or biotechnological routes. The first generation processes were based on renewable resources in competition with food

¹ Paper published: Processes, 2020, Vol. 8: 1075. <https://doi.org/10.3390/pr8091075>

resources (e.g., starch, sugar, vegetable oils). Although production of first generation biofuels in United States and in Brazil continues as a commercially mature technology, increasing criticism regarding ethical sustainability issues, addressed the European Community to promote attention towards second-generation biofuels (Mohammadi et al., 2011).

Second-generation biofuels are produced by processing resources not in competition with food (e.g., lignocellulosic biomass). The bio-chemical route includes the conversion of cellulose and hemicellulose fraction of biomass feedstock to a mixture of fermentable reducing sugars, using enzymes or acid hydrolysis. The hydrolytic route is not sustainable—from an economic, energetic, and environmental point of view—when the lignin fraction is too high, even though the overall Carbon-fraction of the biomass is promising (Fernández-Naveira et al., 2017a). The thermochemical route might include the gasification/pyrolysis technology under high temperatures, to convert the lignocellulosic structure of biomass to intermediate gas (syngas) or liquid products. As a consequence, the thermochemical route is able to exploit all Carbon-fraction of the biomass. The gasification produces syngas—a mixture of carbon monoxide (CO), hydrogen (H₂), carbon dioxide (CO₂), methane (CH₄), and trace gases—that can be further processed. The millions of tons of waste, e.g., stalk, food waste, waste gas etc., produced by anthropic activities, are a potential feedstock to produce bioenergy, along with solving environmental problems.

Some industrial processes (e.g., oil refining, steelmaking, production of carbon black, methanol and coke, gasification, and pyrolysis) release a huge amount of waste gases, where CO and H₂ (syngas) are the main components. These waste gases can be used as raw materials for biological conversion into biofuel/biochemical, through fermentation. The syngas fermentation exploits microorganisms, such as acetogens, that are able to use a mixture of H₂, CO, and CO₂, to produce fuels and chemicals, such as ethanol, butanol, hexanol, acetic acid, butyric acid, and methane. *C. carboxidivorans* is one of such microorganisms that is able to grow on synthesis gas, to produce liquid biofuels (ethanol and butanol) using a variation of the classical Wood–Ljungdahl pathway (Fernández-Naveira et al., 2017b). The industrial utilization of syngas can accelerate the recovery of carbon resources and decrease the dependence on fossil fuels.

Syngas fermentation processes might also meet the strategic needs of the low-carbon development path. Therefore, studies on syngas fermentation are particularly necessary (Stoll et al., 2018) to achieve industrial development of this process.

Fermentation process should overcome some issues. One of the challenges is related to the low water solubility of CO and other compounds (e.g., H₂), which limits the mass transport rate of the substrate to the liquid phase in suspended-growth bioreactors or to the biofilm in attached-growth bioreactors, limiting the production yield of (bio)fuels or platform chemicals of interest, at the same time. Some previous and on-going studies focus on minimizing such drawback. Among others, the use of membrane systems, as well as attached-growth bioreactors, seem to allow a more efficient mass transfer of poorly soluble compounds (Jin et al., 2009); the use of micro-bubble spargers in suspended-growth bioreactors has the same effect (Bredwell et al., 1998). Another drawback to be taken into account, and already previously observed in conventional acetone–butanol–ethanol (ABE) fermentation from carbohydrates, is solvent toxicity

(Raganati et al., 2014). This is an important factor to take into account in butanol fermentation, as acetogenic bacterial cells rarely tolerate more than 2% butanol (Procentese et al., 2015). This study reports recent results regarding the conversion of CO into acids/alcohols, carried out by *C. carboxidivorans*, a Gram positive, mesophilic, and obligate anaerobic carboxydrotroph. *C. carboxidivorans* is known to grow autotrophically with syngas and chemoorganotrophically with a great variety of sugars. It is able to ferment these carbon sources to produce acids and alcohols (Liou et al., 2005; Phillips et al., 2015).

The bacterium was grown under batch conditions, with no pH control, and by using CO as the sole carbon source. The objective was to develop and optimize culture conditions to increase the production of acid/alcohols through anaerobic CO fermentation. In particular, this study aimed to assess the effects of the CO partial pressure on the microorganism growth kinetics and on fermentation performances.

Materials and methods

Microorganism and Culture Media

C. carboxidivorans DSM 15243 was supplied by Deutsche Sammlung von Mikroorganismen und Zellkulturen (DSMZ) in the form of dried pellets. Stock cultures were reactivated according to the DSMZ procedure. A synthetic rich medium (Wilkins Chalgren Anaerobic Broth Base, WCAB) was used to rehydrate and reactivate the microorganism, and glycerol was used as the cryo-protective agent. Reactivated cultures were stored at -80 °C. The thawed cells were inoculated into 12 mL of WCAB in 15 mL Hungate tubes (pre-cultures). Cells were grown under anaerobic conditions for 24 h at 35 °C, they were then transferred into fermentation bottles. Tests were carried out in triplicates (biological replicates) to support reproducibility. The reported results are the mean values.

The composition of the standard fermentation medium was (Phillips et al., 2015) 1 g/L yeast extract; 25mL/L mineral solution (a source of sodium, ammonium, potassium, phosphate, magnesium, sulfate, and calcium); 10 mL/L trace metal solution; 10 mL/L vitamin solution; 1 mL/L resazurin; and 0.60 g/L cysteine-HCl. The mineral stock solution contained (per liter distilled water) 80 g NaCl, 100 g NH₄Cl, 10 g KCl, 10 g KH₂PO₄, 20 g MgSO₄, and 4 g CaCl₂. The vitamin stock solution contained (per liter distilled water) 10 mg pyridoxine, 5 mg each of thiamine, riboflavin, calcium pantothenate, thioctic acid, para-amino benzoic acid, nicotinic acid, and vitamin B12, and 2 mg each of D-biotin, folic acid, and 2-mercaptoethane-sulfonic acid. The trace metal stock solution contained (per liter distilled water) 2 g nitrilotriacetic acid, 1 g manganese sulfate, 0.80 g ferrous ammonium sulfate, 0.20 g cobalt chloride, 0.20 g zinc sulfate, and 20 mg each of cupric chloride, nickel chloride, sodium molybdate, sodium selenate, and sodium tungstate (Phillips et al., 2015). All chemicals were from Sigma Aldrich (Milan, Italy).

Batch Tests

Fermentation tests were carried out in 250 mL serum bottles (DWK Life Sciences-Wheaton, Millville, NJ, USA). A pre-set volume of medium was loaded in bottles and boiled. The N₂ stream was sparged into the bottles during the cooling down of the medium. As the temperature of the medium reached 40 °C, 0.06 g/L cysteine-HCl was supplemented as the reducing agent, the pH was adjusted to 5.75 with 2 M NaOH, and N₂ was continuously flushed. The bottles were sealed with Viton stoppers, capped with aluminium crimps, and autoclaved for 20 min at 121 °C. The bottles were maintained under anaerobic conditions, they were pressurized with 100% CO and inoculated. Bottles were kept under agitation at 130 rpm on an orbital shaker, housed in an incubation chamber at 35 °C. The initial culture medium was set at 55 mL and 120 mL. Therefore, the liquid-to-gas volume ratio (V_L/V_G) was 0.28 and 0.92, respectively. The CO pressure in the headspace was set between 0.5 and 2.5 bar. Tests carried out at 0.5 and 1.0 bar CO partial pressure were performed in mixture with N₂ (Total pressure = 1.5 and 2.0 bar, respectively). In all other tests, the reported initial CO pressures were the total pressures.

Analytical Methods

pH was measured offline in 1.5 mL samples by a pH-meter (Hanna Instruments, Woonsocket, RI, USA). One milliliter of culture was daily sampled from fermentation bottles. Each culture was characterized in terms of cell concentration and soluble products. The samples were centrifuged (13,000 rpm, 10 min) by using a centrifuge (Centrifuge MiniSpin®, Eppendorf Italia, Milan, Italy), before analysing the concentration of water-soluble products by HPLC (HP1100, Agilent Co., Santa Clara, CA, USA). The optical density (OD₆₀₀) was measured at 600 nm by using a UV–visible spectrophotometer (SPECORD 50 UV-VIS, Analytik Jena, Jena, Germany). The biomass concentration (gDM/L) was assessed by processing the measured absorbance, according to a previously generated calibration curve (1 OD = 0.4 gDM/L). The concentrations of water-soluble products—acetic acid, butyric acid, hexanoic acid, ethanol, and butanol—were measured by using an HPLC (HP1100, Agilent Co., Santa Clara, CA, USA), equipped with Rezex . ROA-Organic Acid H+ column (8%), 150x7.8 mm, and a UV detector at a wavelength of 284 nm, at room temperature. The mobile phase was 7 mM H₂SO₄ solution fed at 0.8 mL/min flow rate.

Gas samples of 3 mL were periodically taken from batch bottles to monitor the CO and CO₂ concentrations. Gas-phase CO/CO₂ concentrations were measured using a gas chromatograph (GC, HP6890, Agilent Co., Santa Clara, CA, USA) equipped with a thermal conductivity detector (TCD).

The GC was fitted with a 15-mHP-PLOT Molecular Sieve 5A column (Internal Diameter, 0.53 mm; film thickness, 50 µm) (Sigma Aldrich, Milan, Italy). The pressure in the fermentation bottles was measured using a pressure manometer (Keller), before and after each gas sampling. Liquid and gas measurements were processed to assess the parameters reported hereinafter:

- CO conversion (ξ_{CO}), the ratio between the CO converted and the CO fed at the beginning of the test;

- CO-to-product “i” yield coefficient ($Y_{i/CO}$), the ratio between the produced mass of product “i” (cells or acid/solvent), and the decrease of the CO mass during the same time interval;
- The specific cell growth rate (μ). It was estimated at the beginning of the exponential phase as the slope of the biomass concentration (X) vs. time curve, on a log scale.

Results and discussion

CO Fermentation

The aim of this work was to assess the effects of the CO partial pressure in the headspace of the fermenter on the microorganism growth kinetics and on the fermentation performances. Tests to characterize cell growth and acids/solvents production under different CO pressure were carried out using batch fermenters. The CO pressure in the headspace was set between 0.5 and 2.5 bar. Tables 3.1 and 3.2 report relevant data of fermentation tests carried out by setting the liquid/gas volumetric ratio at 0.28 and 0.92, respectively. Results were reported in terms of—maximum concentration of cells (X), ethanol (E), butanol (B), acetic acid (AA), butyric acid (BA), and hexanoic acid (HA). CO to ethanol yield ($Y_{E/CO}$), CO conversion degree (ξ_{CO}), and specific cell growth rate (μ) are also reported. No data were reported on hexanol because the corresponding production rate was negligible. Each test was carried out in triplicates (biological replicates). Data reported in tables and figures are the mean values between them. The standard error was always lower than 2%.

Table 3.1. Data from the fermentation tests carried out by setting the liquid volume at 55 mL ($V_L/V_G = 0.28$).

P_{CO} bar	X g_{DM}/L	AA mg/L	BA mg/L	HA mg/L	E mg/L	B mg/L	$Y_{E/CO}$ g/g	ξ_{CO} %	μ h^{-1}
0.5	0.67	1280	325	145	130	70	0.063	97.9	0.088
1.0	0.61	1740	320	140	220	110	0.049	94.2	0.10
1.5	0.68	1550	345	250	315	120	0.097	49.5	0.094
1.7	0.68	1620	380	210	400	130	0.094	57.0	0.092
2.0	0.68	1200	390	285	380	100	0.11	39.0	0.099
2.2	0.73	1600	405	230	230	105	0.061	44.1	0.086
2.3	0.53	970	390	250	180	110	0.047	29.3	0.086
2.5	0.62	950	380	290	150	105	0.043	31.7	0.089

Figure 3.1 reports time resolved data of pH, cell (X), and metabolite (B, E, AA, BA, HA) concentration, measured during batch fermentation tests carried out in batch bottles, setting the liquid/gas volume ratio at 0.28 and the initial CO pressure at 1.7 bar. *C. carboxidivorans* started to grow since the inoculation, and the lag phase was negligible. Maximum biomass concentration (0.68 g_{DM}/L) was at about 46 h (Figure 3.1A), and maximum concentration of AA, BA, and HA (about 1600, 370, and 205 mg/L, respectively) were measured later, at about 60 h (Figure 3.1B). Acids were detected since 24 h and increased continuously with time, approaching a constant value after about 70 h. The initial pH of the medium was set at 5.6 in this test.

Table 3.2. Data from fermentation tests carried out setting the liquid volume at 120 mL ($V_L/V_G = 0.92$).

P_{CO} bar	X g_{DM}/L	AA mg/L	BA mg/L	HA mg/L	E mg/L	B mg/L	$Y_{E/CO}$ g/g	ξ_{CO} %	μ h^{-1}
0.5	0.38	715	85	70	120	25	0.17	100	0.072
1.0	0.34	800	100	60	115	25	0.076	99.9	0.081
1.5	0.40	800	110	80	120	35	0.059	98.4	0.075
1.7	0.35	1110	124	80	130	45	0.056	97.2	0.072
2.0	0.42	1580	176	85	225	70	0.067	94.2	0.086
2.2	0.47	1870	230	90	190	75	0.062	100	0.062
2.3	0.39	1500	130	80	90	60	0.031	92.6	0.065
2.5	0.38	1520	100	60	90	80	0.030	86.8	0.060

During the acetogenic phase, medium acidification was observed because no pH control was used during the fermentation tests. The pH decreased gradually with time and approached the minimum of about 4.6, at the end of the test. Ethanol and butanol concentration departed from zero after about 24 h, and increased with time up to about 395 and 130 mg/L, respectively, after about 70 h (Figure 3.1B). Solvent production was not coupled with acid consumption—solvent concentration (ethanol and butanol) increased with time without any reduction of acid concentration.

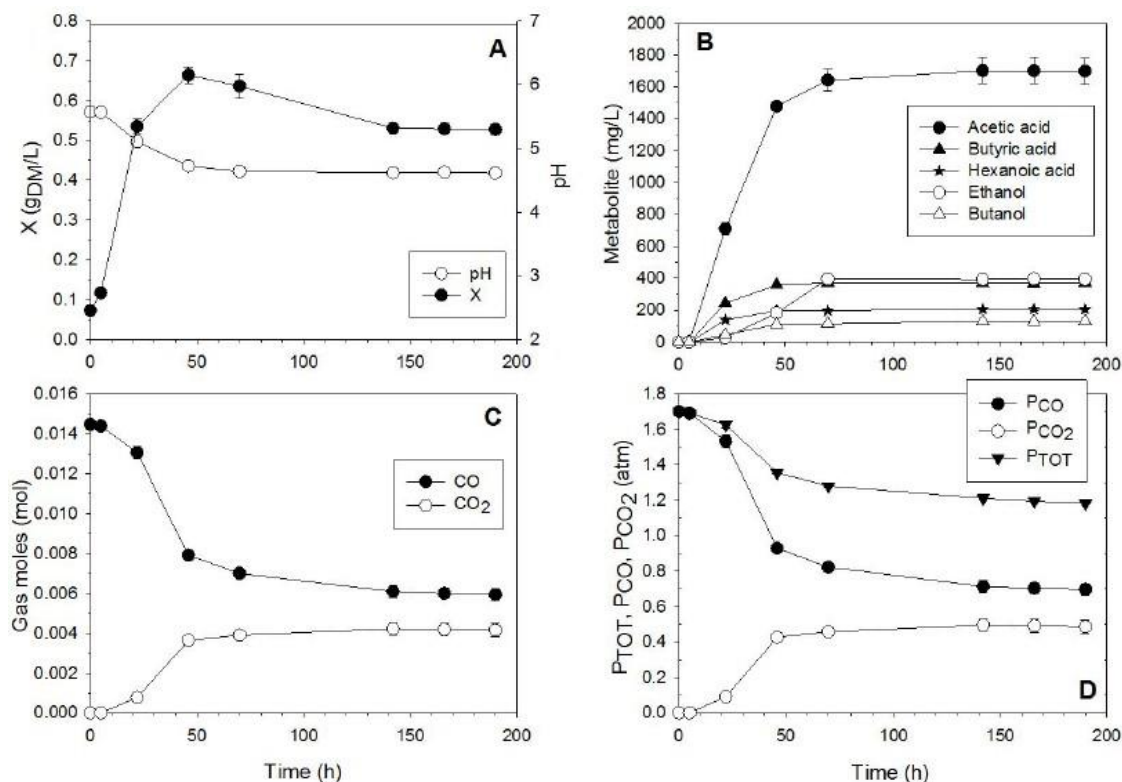


Figure 3.1. Data vs. time measured during a batch fermentation—initial $P_{CO} = 1.7$ bar; $V_L/V_G = 0.28$. (A) Cell concentration and pH; (B) metabolite concentration; (C) CO/CO₂ moles temporal profiles in the headspace of bottles; and (D) total and partial CO/CO₂ pressure in the headspace of bottles.

The observed path to produce solvents was not in agreement with previous results reported by Abubackar et al. (2015) for CO fermentation by *C. autoethanogenum* and the expected path for clostridia known for the ABE fermentation from carbohydrates. In particular, Abubackar et al. (2015) pointed out that CO was converted into acetic acid and ethanol was produced by conversion of the accumulated acetic acid. Therefore, two possible scenarios might be inferred—(i) alcohols were formed directly from the conversion of CO; and (ii) alcohols were produced by acid conversion. In both cases it resulted in a direct production of ethanol and butanol, without any switch from acetogenic to solventogenic phase.

CO consumption was assessed during the fermentation test. Figure 3.1C reports the moles of CO and CO₂ in the bottles headspace; Figure 3.1D reports total pressure and partial pressure of CO and CO₂ measured in the headspace. The analysis of Figure 3.1 points out that bacterial growth and metabolites production were coupled with CO consumption and CO₂ production. After 200 h, about 57% of the initial CO was consumed. From the analysis of Figure 3.1C,D, it was also evident that the rate of CO consumption increased as the cell concentration increased at the beginning of the fermentation, to slow down as acid concentration increased.

Effect of the CO pressure

The effect of CO partial pressure on growth kinetics and metabolite production was assessed by setting the initial P_{CO} between 0.5 and 2.5 bar (Tables 3.1 and 3.2) (tests at 0.5 and 1.0 bar CO pressure were carried out in mixture with N₂, total pressure = 1.5 and 2.0 bar; in all other tests, the reported initial pressures were total pressures). From the analysis of data reported in Tables 3.1 and 3.2, the results showed that:

- P_{CO} affected maximum cell concentration measured during fermentation tests. Maximum cell concentration was about 0.7 g_{DM}/L for initial P_{CO} between 0.5 and 2.2 bar, and decreased at higher initial P_{CO} . Substrate inhibition might be responsible for the decrease of cell growth with P_{CO} .
- CO conversion measured during fermentation tests carried out at $V_L/V_G = 0.28$, decreased with initial P_{CO} . CO conversion was almost total at low initial P_{CO} (0.5 and 1 bar), and it significantly decreased as initial P_{CO} was higher than 1 bar.
- The best performance in terms of ethanol/butanol production was obtained with $V_L/V_G = 0.28$ at initial $P_{CO} = 1.7$ bar.

Figure 3.2 reports the measured specific cell growth rate as a function of CO concentration in the liquid phase. It was assumed that at the beginning of the fermentation the CO in the liquid phase (CO_L) was under equilibrium conditions with the gas phase. Specific growth rate was calculated for each initial CO concentration by plotting $\ln(X)$ vs. time. The experimental data would suggest that: i) the specific cell growth rate is affected by the CO concentration according to substrate inhibition behaviour; ii) the specific cell growth rate is affected by the amount of CO available for unit of volume of liquid.

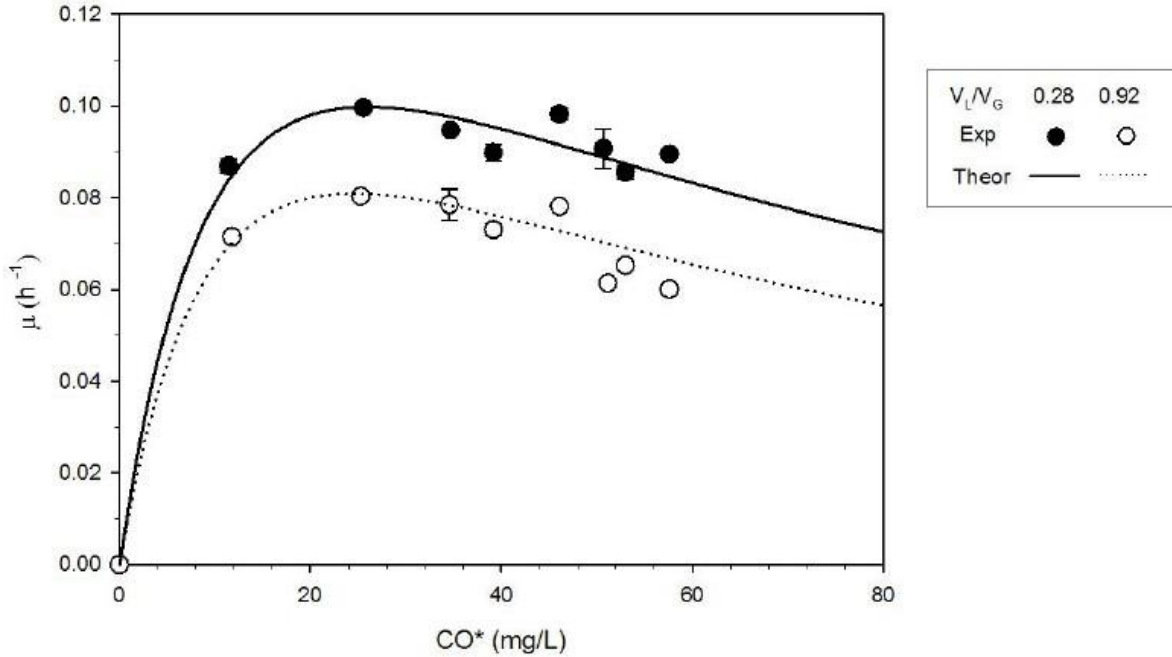


Figure 3.2: Specific cell growth rate of *C. carboxidivorans* as a function of initial CO pressure in the headspace of the fermenter. Lines are the plot of Eq. 3.1 (parameters in Table 3.3).

Kinetic data were processed according to an unsegregated–unstructured model—the Haldane model (Equation (3.1)) characterized by substrate inhibition was used (μ_{max} , K_{CO} and K_I parameters of the model).

$$\mu = \mu_{max} \cdot \left(\frac{CO_L}{CO_L + K_{CO} + CO_L^2/K_I} \right) \quad (3.1)$$

Data regression according to Equation (3.1) provided the kinetic parameters reported in Table 3.3. The plot of the expected values of μ , assessed according to Equation (3.1), is reported in Figure 3.2. The good agreement between experimental data and expected values ($R^2 = 0.88$) supported that *C. carboxidivorans* growth rate was characterized by CO inhibition within the investigated range of CO concentration. In particular, the optimal P_{CO} was 1.1 bar (corresponding to a dissolved CO concentration of about 25 mg/L), for both the V_L/V_G used. Substrate inhibition occurred during the initial oxidation of the electron donor substrates, and reduced or stopped the oxidation of the electron donor, through either competitive or non-competitive inhibition, resulting in slow substrate consumption rates (Rittman et al., 2005). In particular, CO was a substrate that showed a substrate inhibitory effect above a critical concentration because CO inhibits metalloenzymes by forming stable complexes, resulting in reduced enzymatic activity. Notably, most enzymes in the acetyl-CoA pathway possess redox activities due to their metallic centers (Ragsdale et al., 2004). Yasin et al. (2015) reported the observed behavior of the specific growth rate vs. CO concentration (CO inhibition) for different microorganisms. High pressure fermentation could be detrimental

when the dissolved CO concentration was greater than the kinetic requirements of the microbes; therefore, identifying the optimum dissolved CO concentration was necessary to design and control large-scale fermenters.

Table 3.3. Kinetic parameters assessed by the regression of experimental data according to the proposed model (Eq. 1).

V_L/V_G , -	μ_{\max} , h^{-1}	K_{CO} , mg/L	K_i , mg/L
0.28	0.22	15	45
0.92	0.18	15	40

Hurst and Lewis (2010) assessed the effects of constant CO partial pressure, ranging from 0.35 to 2.0 bar, on cell growth, acetic acid production, and ethanol production, using *C. carboxidivorans*. They did not experience substrate inhibition on cell growth rate. A possible explanation of this different behavior with respect to the one reported in this work could be related to the different gas composition used. Indeed, Hurst and Lewis (2010) used a mixture of CO and CO₂. Therefore, it was not possible to distinguish between the effect of CO and CO₂ (double substrate) on the growth rate. Moreover, Fernández-Naveira et al. (2017b) pointed out that product inhibition had a significant effect on cell growth and acid/solvent production. However, the inhibitory effect of the acids and solvents was not taken into account in this study because the specific growth rate was estimated at the beginning of the exponential phase—the metabolite concentrations were more than 10-fold lower than the inhibitory concentrations reported in the literature (Fernández-Naveira 2016b). Other studies reported in the literature used CO as the sole carbon/electron source. Nevertheless, to the authors' knowledge, models/kinetics to describe *C. Carboxidivorans* fermentation are still scarce in the literature, and only a few authors have attempted to adjust kinetic expressions to experimental data, even though, identifying the microorganism growth kinetics (and thus, the optimum dissolved CO concentration) is necessary to design and control large-scale fermenters. Younesi et al. (2005) and Mohammadi et al. (2014) adjusted the logistic curves to the growth of *C. ljungdahlii* on artificial syngas, using experimental data from batch fermentation essays in serum bottles. Mohammadi et al. (2014) were also able to fit Gompertz equations to their experimental profiles of product formation, and uptake rate equations for CO, presenting estimations of kinetic parameters.

A possible strategy to obtain kinetics information on *C. Carboxidivorans* would be to fit the model parameters with literature data. However, this procedure turned out to be a challenge due to several reasons. First, the number of experimental papers on syngas fermentation is relatively small, compared to other types of fermentation; moreover, an even smaller number provides data with coproduction of higher alcohols such as butanol. Among these, some provide exploratory data of very long cultures in which several accidents or interventions occur, and others fail to provide clear information about the process conditions (e.g., often the gas flow rates are omitted from the text, probably because they were not fixed during the experiment). Therefore, the authors thought that a systematic study dealing with both data acquisition and their elaboration for kinetics assessment was necessary before moving to other topics, such as bioreactor design.

Effect of the Gas-to-Liquid Volume Ratio

Tests carried out under different liquid-to-gas volume ratio (V_L/V_G) pointed out that cell growth was affected by this operating condition. Cultures carried out at $V_L/V_G = 0.28$ were characterized by a growth rate higher than that measured for cultures carried out at $V_L/V_G = 0.92$ (Tables 3.1 and 3.2). Time resolved data of CO in the gas phase of bottles are reported in Figure 3.3, for the cultures carried out at $V_L/V_G = 0.28$ and $V_L/V_G = 0.92$ and initial $P_{CO} = 2$ bar. As expected, CO in the bottle headspace decreased with time. Tests carried out at $V_L/V_G = 0.92$ were characterized by higher CO uptake rates with respect to tests carried out at $V_L/V_G = 0.28$. Moreover, CO depletion was recorded for the tests carried out at $V_L/V_G = 0.92$.

The increase of μ as V_L/V_G decreased was interpreted by taking into account the mass of CO available for cells and the gas-to-liquid transport rate. In particular, the competition between CO uptake and CO transport between the gas and liquid phases was addressed. Data of CO moles and cell density (Tables 3.1 and 3.2) measured during tests carried out at the same initial P_{CO} were processed to assess the amount of CO available for the unit of cell mass, as a function of fermentation time. Figure 3.4 reports the moles of CO per gram of bacterial mass for the tests carried out at $P_{CO} = 2$ bar. As expected, the CO per gram of bacterial mass was larger for the $V_L/V_G = 0.28$ cultures, throughout the fermentation tests. For both V_L/V_G used, the CO per gram of bacteria decreased with time and approached a constant value. In particular, CO depletion was recorded for the test carried out at $V_L/V_G = 0.92$, as the fermentation time was larger than 74 h.

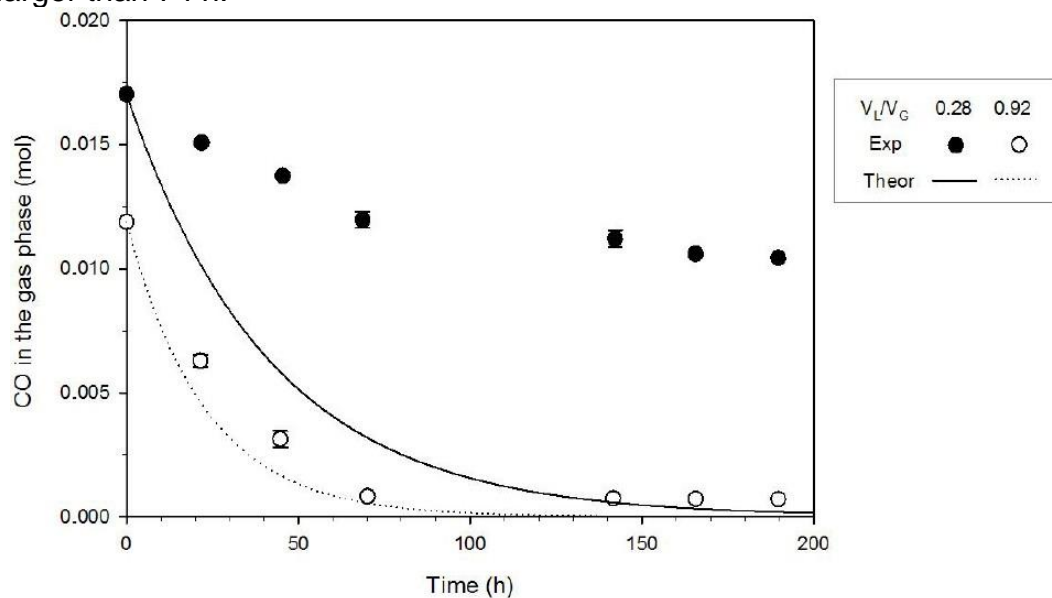


Figure 3.3: CO in the headspace vs. fermentation time. Initial $P_{CO} = 2$ bar. Experimental data and plots of Equation (3.4).

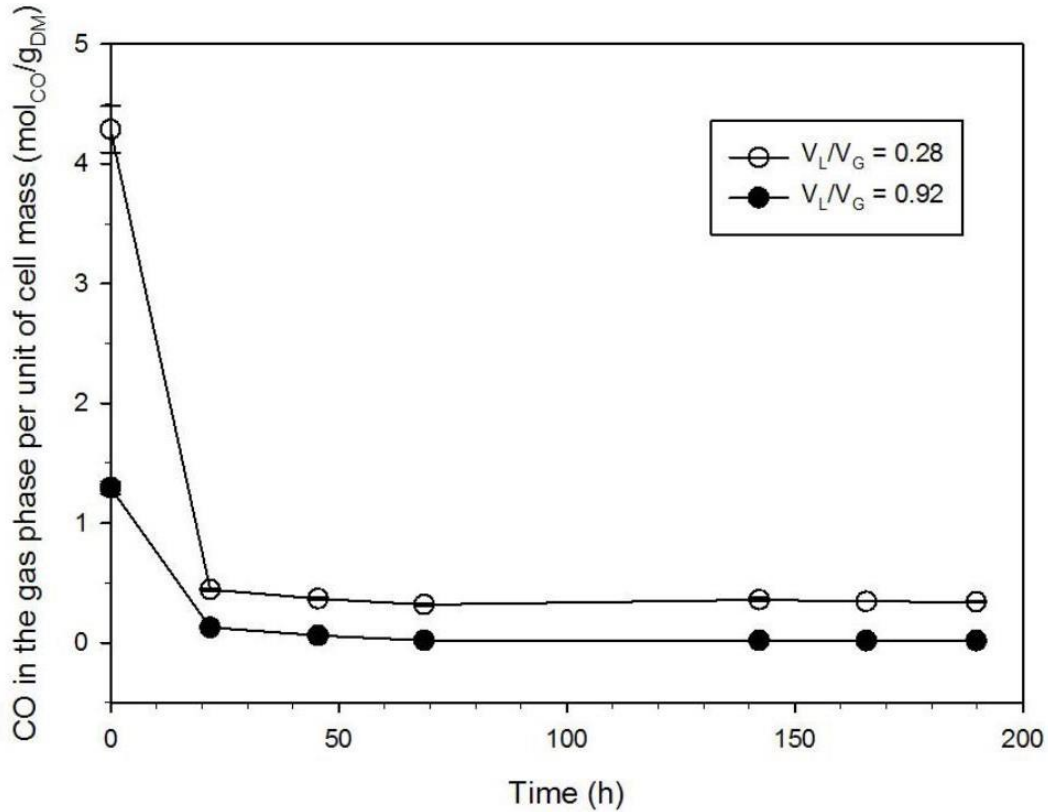


Figure 3.4. CO in the bottle headspace per unit of cell mass. Initial $P_{CO} = 2$ bar.

CO transport rate from the gas-to-liquid phase was assessed to verify if the specific cell growth rate was controlled by mass transport phenomena. The mass transport coefficient (k_{La}) for CO was 4.69 h^{-1} and 2.64 h^{-1} for the bottles operated at $V_L/V_G = 0.28$ and 0.92 , respectively (Frankman, 2009). The mass balance referred to CO and extended to the bottle headspace yields:

$$\frac{dn_{CO}}{dt} = -V_L k_{LaCO} (CO^* - CO_L) \quad (3.2)$$

where n_{CO} is the CO mole number, CO_L is the concentration of CO in the liquid phase, k_{LaCO} is the mass transport coefficient for CO referred to the liquid volume, CO^* is the liquid concentration under equilibrium conditions with the gas phase. Under conditions characterized by very fast CO conversion in liquid phase, the process overall rate was mass-transport controlled. The CO mass-transport rate was maximum because CO in the liquid phase was 0, CO was promptly converted as it flowed into the culture, and Equation (3.2) yielded:

$$\frac{dn_{CO}}{dt} = -V_L k_{LaCO} (CO^* - CO_L) = -V_L k_{LaCO} \frac{P_{CO}}{H_{CO}} = -V_L k_{LaCO} \frac{n_{CO} \cdot RT}{H_{CO} \cdot V_G} \quad (3.3)$$

where H_{CO} is the Henry constant referred to CO, T is the temperature, and R is the universal gas constant. Integration of Equation (3.3), with respect to time yields:

$$n_{CO} = n_{CO}^0 \cdot \exp\left(-V_L k_{L,CO} a_{CO} \frac{P_{CO}}{H_{CO} \cdot V_G}\right) t \quad (3.4)$$

Under mass-transport control conditions, CO in bottle headspace changed with time, according to Equation (3.4). Figure 3.3 reports the plot of Equation (3.4) for both values of V_L/V_G . The comparison between experimental data and expected CO depletion in the headspace pointed out that the mass transport phenomena did not control CO uptake for $V_L/V_G = 0.28$ —transport phenomena were able to pump CO into the culture at sufficient rate. On the contrary, expected CO depletion in the headspace for tests carried out at $V_L/V_G = 0.92$, was close to that measured—the experimental CO depletion rate was about the transport rate. These results were in accordance with the ones reported by Frankman (2009). As a consequence of the reported analysis on the effects of the V_L/V_G ratio, the characterization of kinetics and fermentation stoichiometry carried out at $V_L/V_G = 0.28$ was more reliable than those carried out at $V_L/V_G = 0.92$.

Conclusions

The present study aimed at assessing the effects of CO pressure on growth kinetics and on fermentation performances of *C. carboxidivorans*. The results showed that:

- P_{CO} affected microorganism growth kinetics; indeed, *C. carboxidivorans* growth rate was characterized by CO inhibition within the investigated range of CO concentration, and the optimal P_{CO} was 1.1 bar (corresponding to a dissolved CO concentration of about 25 mg/L) for both the V_L/V_G used.

- Growth differences were observed when the gas-to-liquid volume ratio was changed; the mass-transport phenomena did not control CO uptake for $V_L/V_G = 0.28$; on the contrary, the experimental CO depletion rate was about equal to the transport rate in the case of $V_L/V_G = 0.92$. Therefore, the characterization of kinetics and fermentation stoichiometry carried out at $V_L/V_G = 0.28$ was more reliable than those carried out at $V_L/V_G=0.92$.

3.3 Gas-fed fermentation of *C. carboxidivorans*

The present work aimed to carry out the fermentation of *C. carboxidivorans* in a continuous gas-fed reactor system, to assess the potential of the proposed configuration. The effect of pH has been investigated by the comparison of two studied cases: the first at constant pH, the second with natural acidification for 6 hours, then constant pH.

Materials and methods

C. carboxidivorans DSM 15243 was supplied by Deutsche Sammlung von Mikroorganismen und Zellkulturen (DSMZ) in the form of dried pellets. Stock cultures were reactivated according to the DSMZ procedure. A synthetic rich medium (Wilkins Chalgren Anaerobic Broth Base, WCAB) was used to rehydrate and reactivate the microorganism, and glycerol has been used as the cryo-protective agent. Reactivated cultures were stored at -80 °C. Once unfrozen, cells were inoculated into 12 mL of WCAB in 15 mL Hungate tubes (pre-cultures). Cells have grown under anaerobic conditions for 24 h at 35 °C, they were then transferred into fermentation bottles.

The composition of the standard fermentation medium has been (Phillips et al., 2015)—1 g/L yeast extract; 25 mL/L mineral solution (a source of sodium, ammonium, potassium, phosphate, magnesium, sulfate, and calcium); 10 mL/L trace metal solution; 10 mL/L vitamin solution; 1 mL/L resazurin; and 0.60 g/L cysteine-HCl. The mineral stock solution contained (per liter distilled water) 80 g NaCl, 100 g NH₄Cl, 10 g KCl, 10 g KH₂PO₄, 20 g MgSO₄, and 4 g CaCl₂. The vitamin stock solution contained (per liter distilled water) 10 mg pyridoxine, 5 mg each of thiamine, riboflavin, calcium pantothenate, thioctic acid, para-amino benzoic acid, nicotinic acid, and vitamin B12, and 2 mg each of D-biotin, folic acid, and 2-mercaptoethane-sulfonic acid. The trace metal stock solution contained (per liter distilled water) 2 g nitrilotriacetic acid, 1 g manganese sulfate, 0.80 g ferrous ammonium sulfate, 0.20 g cobalt chloride, 0.20 g zinc sulfate, and 20 mg each of cupric chloride, nickel chloride, sodium molybdate, sodium selenate, and sodium tungstate (Phillips et al., 2015). All chemicals were provided from Sigma Aldrich (Milan, Italy).

Apparatus

Figure 3.5 shows a sketch of the apparatus adopted for the continuous syngas fermentation. It has included 250 mL MiniBio reactor (Applikon technologies), a control unit, peristaltic pumps, a heating apparatus, probes for pH and dO₂ control, a mass flow controller, a gas leakage sensor and a safety box for cylinders.

The bioreactor was fed with a continuous flux of CO, regulated by a mass flow controller equipped to the control unit. The gas feeding was used during the start-up operations to achieve anaerobic conditions in the reactor, and to saturate the culture medium before the inoculum. The control unit monitored the parameters of the process: temperature, pH, oxygen, gas flow and agitation speed. By mean of a PID controller, the control unit regulated the peristaltic pump (P) and the heater (H) to maintain the desired conditions. The exhaust gas leaving the reactor was captured by the fume hoods and diluted with N₂ to a concentration suitable for disposal, under the limits of toxicity and flammability.

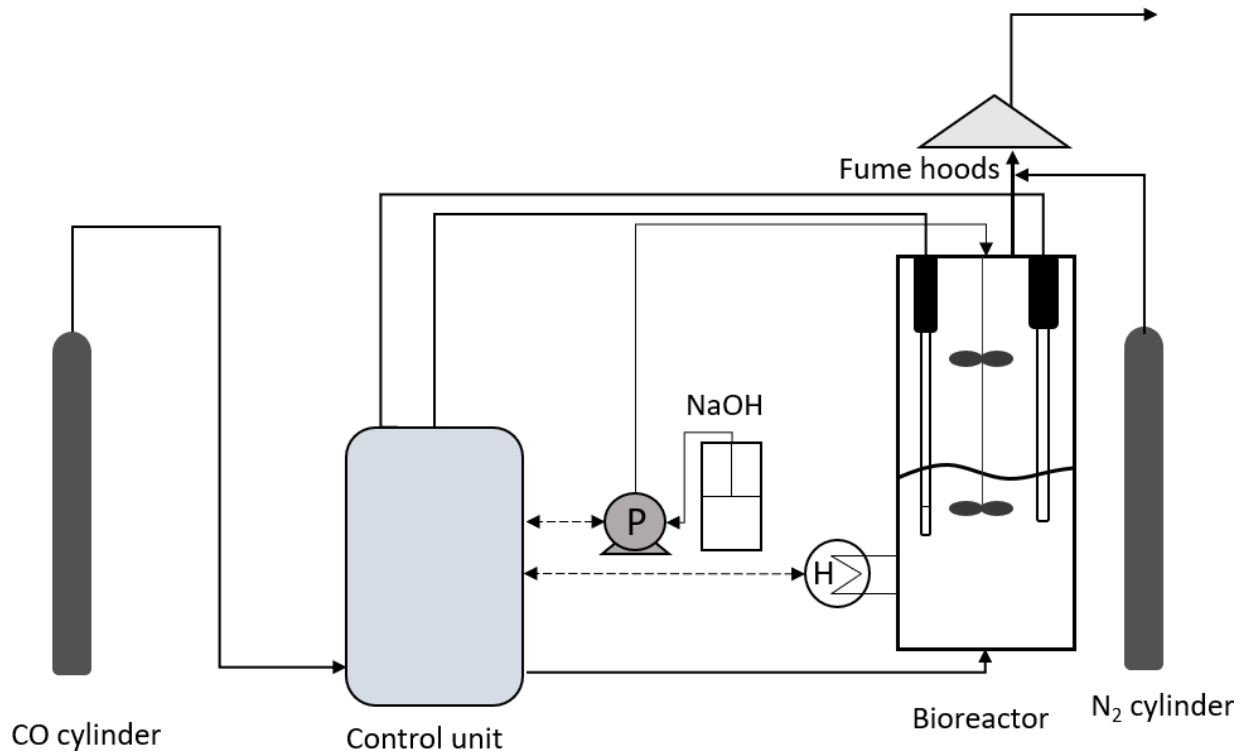


Figure 3.5: Sketch of the fermenter apparatus. H) electrical heater. P) peristaltic pump.

Procedure

Fermentation tests experiments have been carried out in the apparatus described in the previous section. All the components of the culture medium have been loaded in the reactor vessel, with the exception of vitamins and reducing agent, and boiled. After the sterilization cycle, the system has been purged with pure CO gas, to remove the air and to saturate the medium. As the medium was oxygen-free, vitamin solution and cysteine-HCl have been supplemented to the set concentration and the pH has been adjusted to the pre-set value 5.75 by supplementing 2M NaOH. Then, the medium has been inoculated. The agitation has been provided by means of impellers, set to 250 rpm. The culture was fed with 10 mL/min of CO pure gas. The initial volume of culture has been 120 mL.

The pH of the medium has been controlled by of 2M NaOH and 2M HCl solutions, fed by means of peristaltic pumps. Two test types have been carried out. The test type one was characterize by keeping the pH at 5.75 throughout the fermentation. The test type two was characterized by no pH control to observe the natural acidification of the medium until pH was as low as 5, then the pH control system has been activated to keep pH constant. The aim of the test type two has been to observe how the bacteria would adapt to a different condition, supposed to promote the reassimilation of the acids and a solventogenic phase.

Analytical Methods

pH has been measured offline in 1.5 mL samples by a pH-meter (Hanna Instruments, Woonsocket, RI, USA). One milliliter of culture was sampled from the reactor twice per day. Each culture was characterized in terms of cell concentration and soluble products. The samples were centrifuged (13,000 rpm, 10 min) by using a centrifuge (Centrifuge MiniSpin®, Eppendorf Italia, Milan, Italy), before analysing the concentration of water-soluble products by HPLC (HP1100, Agilent Co., Santa Clara, CA, USA). The optical density (OD_{λ}) was measured at 600 nm by using a UV–visible spectrophotometer (SPECORD 50 UV-VIS, Analytik Jena, Jena, Germany). The biomass concentration (g_{DM}/L) was assessed by processing the measured absorbance, according to a previously generated calibration curve (1 OD = 0.4 g_{DM}/L). The concentrations of water-soluble products—acetic acid, butyric acid, hexanoic acid, ethanol, and butanol—were measured by using an HPLC (HP1100, Agilent Co., Santa Clara, CA, USA), equipped with Rezex . ROA-Organic Acid H+ column (8%), 150x7.8 mm, and a UV detector at a wavelength of 284 nm, at room temperature. The mobile phase was 7 mM H_2SO_4 solution fed at 0.8 mL/min flow rate. The oxygen concentration was monitored overtime, by mean of a dissolved oxygen probe equipped to the reactor (AppliSens DO₂-sensor), to guarantee the anaerobic conditions into the system. The gas phase was not analysed because the system was assumed to work as a differential reactor for the CO (this means that the amount of CO consumed, compared with the amount of CO supplied, is negligible).

Results and discussion

Figures 3.6 and 3.7 report the cell concentration and the metabolite concentration measured during two *C. carboxidivorans* fermentation tests. Common operating conditions were: temperature 35°C; gas flow rate of the CO stream 0.600 L/h; stirring rate 250 rpm; Figures 3.6A and 3.7A and B refer to a test carried out setting the pH at 5.75. Figures 3.6B and 3.7 C and D refer to a tests carried out without pH control until time 6 h, then the pH was set at 5.

Both tests were characterized by absence of lag phase. The fermentation dynamic is very close to that carried out in serum bottle.

The cell concentration vs. time measured during the test carried out at pH constant=5.7 has been characterized by a maximum (about 0.56 g/L) at time about 45-50. Acid concentration vs. time have been characterized by a maximum - 760, 210 and 130 mg/L respectively for acetic, butyric and hexanoic acids - at about time about 26 h. Figure 3.7A shows clearly how the fermentation may be divided in two phases: acidogenesis, during the first 20 - 30 hours of the process, and solventogenesis, that took place in the following 30 - 40 hours. No significative variation has been observed thereafter. Alcohols have started to accumulate after 10-15 h of fermentation and their concentration have approached a maximum value after 70 h: 800 mg/L of ethanol and 327 mg/L of butanol. The reassimilation of the acids, evident in Figure 3.7A, took place even if the pH level was maintained at the same level, suggesting that a lower pH is not a necessary condition to promote the production of alcohols, but anyway preferable.

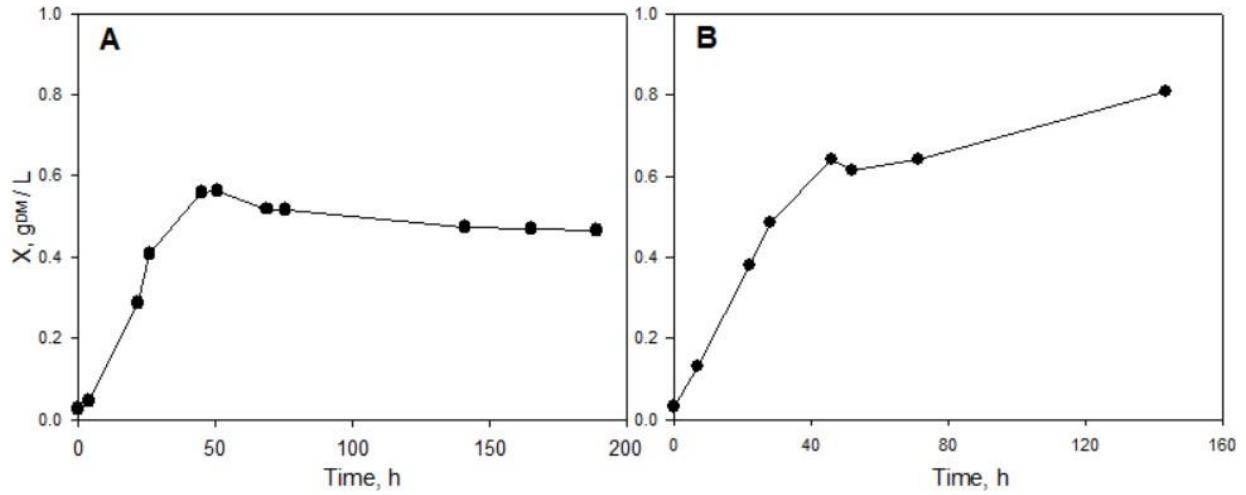


Figure 3.6: Time-resolved profile of cell concentration in the gas-fed reactor for the two experimental setup proposed: A) pH constant at 5.75; B) pH free for 6 hours, then constant at 5.00.

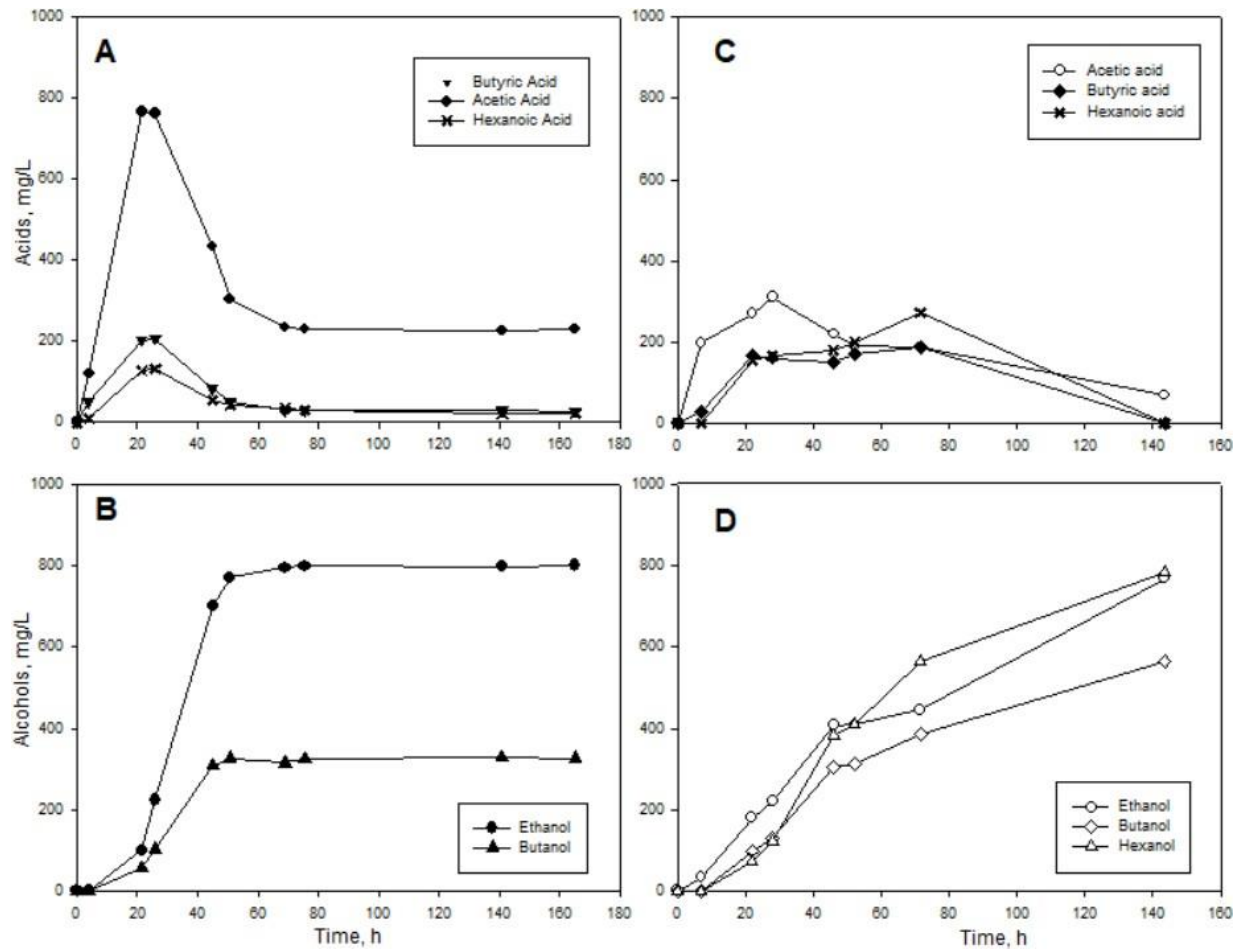


Figure 3.7: Time-resolved profile of metabolites in the gas-fed reactor measured during the tests reported in Figure 3.6. A) and B) refer to the test carried out pH constant at 5.75; C) and D) refer to the test carried out at pH free for 6 hours, then constant at 5.00.

A possible explanation is that a low pH slows down the formation of acids, preventing the manifestation of a peak of acid concentration. On one side, this allows the growth to keep going for a longer time. On the other side, it seems to promote the production of long chain alcohols, butanol and hexanol, that reach a concentration very close to the ethanol's.

As the system has been operated under differential conditions with respect to the gas phase species, it has not possible to estimate the conversion rate and the yield on CO. It has been possible to compare the yields of acids and alcohols per gram of biomass (Table 3.4). The data have been assessed as the ratio between the metabolite concentration and the cell concentration, calculated at the moment of maximum for the *i* specie.

Table 3.4. Experimental yields of metabolites on biomass.

Yield on X, g/g _x	Exp. 1	Exp. 2
Acetic acid	1.865	0.639
Butyric acid	0.505	0.439
Hexanoic acid	0.323	0.344
Ethanol	1.704	0.954
Butanol	0.696	0.699
Hexanol	n.d.	0.972

From the analysis of the data reported in Table 3.4, the following considerations may be done.

- The yield in acetic acid was almost triple under pH=5 constant. The yield in ethanol was also high;
- the yields of butyric acid and butanol were similar in both typology tests;
- the yields of hexanoic acid was high in the typology with pH controlled at 5.

Main remarks

A reactor system to carry out continuous gas-fed fermentation tests of *C. carboxidivorans* has been designed, set-up and operated. The continuous gas feeding had a positive effect on the fermentation, highlighting the ability of the bacteria to convert the acids into alcohols. It may be inferred that the supply of CO provided the energy needed for the bioconversion. In both the experiments, the final concentration of butanol and ethanol was much higher than the batch tests, furthermore a significant amount of hexanol was detected.

Operating with different values of pH seems to affect the kind of metabolites produced, in particular a lower level of pH promotes the formation of organic compounds with longer carbon chain.

Further experiments are required to get an overall view of the phenomena.

4. MATHEMATICAL MODELLING

The experimental activity has been accompanied by a deep theoretical study aimed to develop a mathematical model able to predict the dynamic evolution of a gas fermentation process by *C. carboxidivorans*.

In the first section, data collected were used to fit the model and estimate a vector of 31 parameters that describes the proposed reaction network. The goodness of the model was evaluated by the statistical indicator R^2 and by a sensitivity analysis aimed to assess the soundness of the model.

In the second section, the model was used as a predictive tool, to explore the potentiality of a biofilm reactor system, a promising solution to overcome the main limitations of gas fermentation: low productivity and low concentrations of the products of interest.

4.1 Bioreactor modelling for syngas fermentation: Kinetic characterization²

G. Ruggiero^a, F. Raganati ^a, M.E. Russo^b, P. Salatino^a, A. Marzocchella^a

^a Department of Chemical, Materials and Production Engineering–University of Naples Federico II,

^b Institute of Science and Technology for Energy and Sustainable Mobility (STEMS) - CNR

Abstract

Syngas fermentation is one of most promising technologies for the future sustainable biobased economy. The interest is driven by the syngas fermentation potential as an intermediate step in the conversion of waste carbon to biofuel/chemicals. It may be an efficient and competitive route for the valorisation of various C-based waste materials. In this study, a dynamic model is presented for syngas fermentation with acetogenic bacteria in a continuous stirred tank reactor. The model takes into account gas–liquid mass transfer rate, substrate (CO) uptake rate and three conversion paths: biomass growth associated with acid and alcohol production, alcohol production by acid conversion, and direct production of alcohols non growth-associated. The unknown kinetic parameters and yields were estimated from literature data using the maximum likelihood principle and the model soundness was verified by statistical index analysis. The sensitivity of kinetic parameters was assessed to assess the stability of the obtained results. It was observed a high overall accuracy in the prediction, with a mean r^2 of 0.88. The sensitivity study pointed out that the biomass growth reaction is the conversion step characterized by the highest impact on the system performance. The effect of some key operating conditions was also investigated. It is worth to note the unexpected result that the decrease of the mass transfer rate increases the production of cells and metabolites of interest.

Keywords: Modelling; Syngas; *Clostridium carboxidivorans*; Optimization; Biofuels.

² Submitted

Introduction

The rapid increase of the world population and of the industrialization of the developing countries are increasing the environmental pollution and the pressure on fossil resources. Apart from environmental fallout, exploitation of fossil resources strongly affects the economic and social worldwide scenario as regards resource country independence, natural resource cost, etc. A potential solution to these issues is offered by the exploitation of renewable resources processed under sustainable conditions (Gowen et al., 2011).

Ethanol and higher chain alcohols (e.g., butanol) are potential substitutes of fossil fuels as well as of chemical building blocks (Abdehagh et al., 2014). Alcohols can be produced by processing renewable resources via thermochemical or biotechnological routes. Cost, matter and energy required to produce alcohols strongly depend on the renewable resources selected. The production processes of the first-generation biofuels were based on renewable resources are quite economical. However, the resources are in contrast with ethical rules because they are in competition with food resources (e.g., starch, sugar, vegetable oils) and addressed the European Community to promote attention towards second-generation biofuels (Mohammadi et al., 2011). Second-generation biofuels are produced by processing resources not in competition with food (e.g., lignocellulosic biomass). The bio-chemical routes include the conversion of cellulose and hemicellulose fraction of biomass feedstock to a mixture of fermentable reducing sugars, using enzymes or acid hydrolysis. The hydrolytic route may not be sustainable — from an economic, energetic, and environmental point of view — when the lignin fraction is too high, even though the overall Carbon-fraction of the biomass is promising (Fernández-Naveira et al., 2017b). The thermochemical route may include the gasification/pyrolysis technology, to convert biomasses – lignocellulose fraction included – and any C-based matter to intermediate gas (syngas) or liquid products. The gasification produces syngas — a mixture of carbon monoxide (CO), hydrogen (H₂), carbon dioxide (CO₂), methane (CH₄), and trace gases — that can be further processed.

It should be noted that the produced syngas may be associated with the huge amount of waste gases - CO and H₂ may be present at a significant concentration – is released by some industrial processes (e.g., oil refining, steelmaking, production of carbon black, methanol and coke, power plants). The waste gases, as the syngas, can be used as raw materials for biological conversion into biofuel/biochemical via biotechnological route.

Gas fermentation exploits microorganisms, such as acetogens, that may use a mixture of H₂, CO, and CO₂, to growth and to produce metabolites including fuel-like solvents and chemicals. *Clostridium carboxidivorans* is a microorganism that may grow on gaseous substrate to produce liquid biofuels according to the classical Wood–Ljungdahl pathway (Dürre and Eikmanns, 2015). The strain gained an increasing attention because of its ability to produce long-chain alcohols (butanol and hexanol), as well as ethanol. This kind of fermentation is known as H-B-E fermentation (Fernández-Naveira et al., 2017a).

The industrial exploitation of syngas can accelerate the recovery of carbon resources and decrease the dependence on fossil fuels according to the circular economy strategies. Syngas fermentation processes might also meet the strategic

needs of the low-carbon development path. Therefore, development of consolidated processes based on syngas fermentation are particularly necessary (Stoll et al., 2018) to promote the industrial development of this process. Issues to be addressed include the low water solubility of CO and other compounds (e.g., H₂), the low syngas specific conversion rate, and the metabolites toxicity towards cells. The low water solubility of the syngas components limits the mass transport rate of the substrate to the liquid phase in suspended-growth bioreactors and/or to the biofilm in attached-growth bioreactors. As a result, the production yield of (bio)fuels or platform chemicals of interest are limited too. Some previous and on-going studies focus on minimizing such drawbacks. The use of membrane systems coupled with attached-growth cell bioreactors as well as the use of micro-bubble spargers in suspended-growth bioreactors (Bredwell and Worden, 1998) have been proved to be characterized by a good efficient mass transfer of poorly soluble compounds. The solvent toxicity (Raganati et al., 2014) is also a stressing issue because acetogenic bacterial cells rarely tolerate more than 2% butanol (Procentese et al., 2015).

Models to support the syngas fermentation available in the literature are still a few and only some authors have attempted to propose kinetic expressions to fit experimental data. Younesi et al. (2005) and Mohammadi et al. (Mohammadi et al., 2014) fitted logistic curves to the growth of *C. ljungdahlii* on artificial syngas by regression of experimental data from batch fermentation tests carried out in serum bottles. Mohammadi et al. (2014) fitted Gompertz equations with respect to experimental data of product formation and uptake rate equations for CO. They reported the estimations of kinetic parameters that were used by Chen et al. (2015) in their dynamic Flux Balance Analysis (FBA) model of a syngas fermentation bubble column. A modelling study aimed at the estimation of the growth parameters of *C. ljungdahlii* in a continuous gas-fed reactor has been carried out by de Medeiros et al. (2019). A sensitivity analysis has been also carried out.

A dynamic model for gas fermentation of *C. carboxidivorans* has been proposed. The model has been applied to the production of ethanol and butanol in a continuous stirred tank reactor (CSTR). The model parameters have been estimated according to the multi-response minimization framework by processing experimental culture data from the literature. The significance of parameters has been assessed by statistical analysis.

Theoretical framework/Model development

The dynamic model developed in the present study describes a two-phase gas-liquid stirred tank bioreactor operated under continuous conditions with respect to the gas (syngas) phase and under batch or continuous conditions with respect to the liquid phase. Chemical species are: carbon monoxide (CO), carbon dioxide (CO₂), acetic (AA) and butyric acid (AB), ethanol (E), butanol (B) and biomass (X). Gaseous species were considered in both gas and liquid phases, acids and alcohols were only in the liquid phase. The reactor is assumed to have a height/diameter ratio of 2 and an impeller diameter equal to 40% of the reactor diameter, a standard value for most bioreactors.

Data sources

The assessing of the model parameters by the regression of data from the literature data is a challenge task for several reasons. First, the number of papers on syngas fermentation of *C. carboxidivorans* is quite small compared with other types of fermentation. Second, the limited number of data set regards tests carried out under operating conditions often not suitable for parameters regression, e.g. medium pH and gas composition not constant throughout the tests. Third, some papers provide exploratory data of very long cultures during which operating conditions change without control. Fourth, clear information about the operating conditions (e.g., the gas flow rate) are not reported.

The present work assumes as reference test a fermentation: i) carried out at known constant operating conditions for the first 250 hours; ii) characterized in terms of concentration of cells, substrate, acetic and butyric acid, ethanol and butanol (Fernández-Naveira et al., 2016a). The substrate consumption was reported as CO fraction of the gas-out flow and it was processed to obtain the time-resolved profile of the amount of CO in the out stream of the reactor (mol/h).

Assumptions

The Figure 4.1 reports the basic sketch of the fermentation system modelled in the present paper. The main assumptions made to assess the model parameters are reported hereinafter.

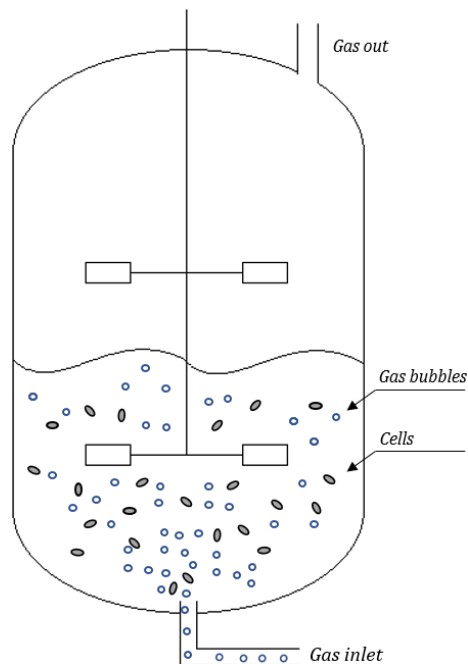


Figure 4.1: Sketch of the modelled fermenter.

- The system is considered isothermal (33°C) and at constant pH (5.75), in accordance with the experimental conditions of the reference test (Fernández-Naveira et al., 2016a).
- Two (ideal) gaseous species were considered: CO and CO₂.
- The gas stream delivered to the reactor was pure CO. The gas flow was assumed $Q_G = 0.600$ L/h, in accordance with the experimental conditions (Fernández-Naveira et al., 2016a).
- The gas phase was well mixed.
- Liquid phase was assumed to be well mixed. The cells are uniformly distributed.
- Metabolites and water are absent in the gas phase. Their volatilities were neglected.
- The gas solubility in the liquid has been modelled according to the Henry's Law.
- Physical-chemical properties of the culture medium was approximated as pure water.

Stoichiometry and kinetics

The complex metabolism, involving gas fixation, cell growth and production of metabolites, has been schematized assuming that: CO is the key nutrient; all other substrates are supplied at sufficient rate in the culture medium. A graphic schematization of the proposed mechanism for CO fermentation of *C. carboxidivorans* is reported in Figure 4.2. A kinetic unstructured/unsegregated model has been used (Younesi et al., 2005).

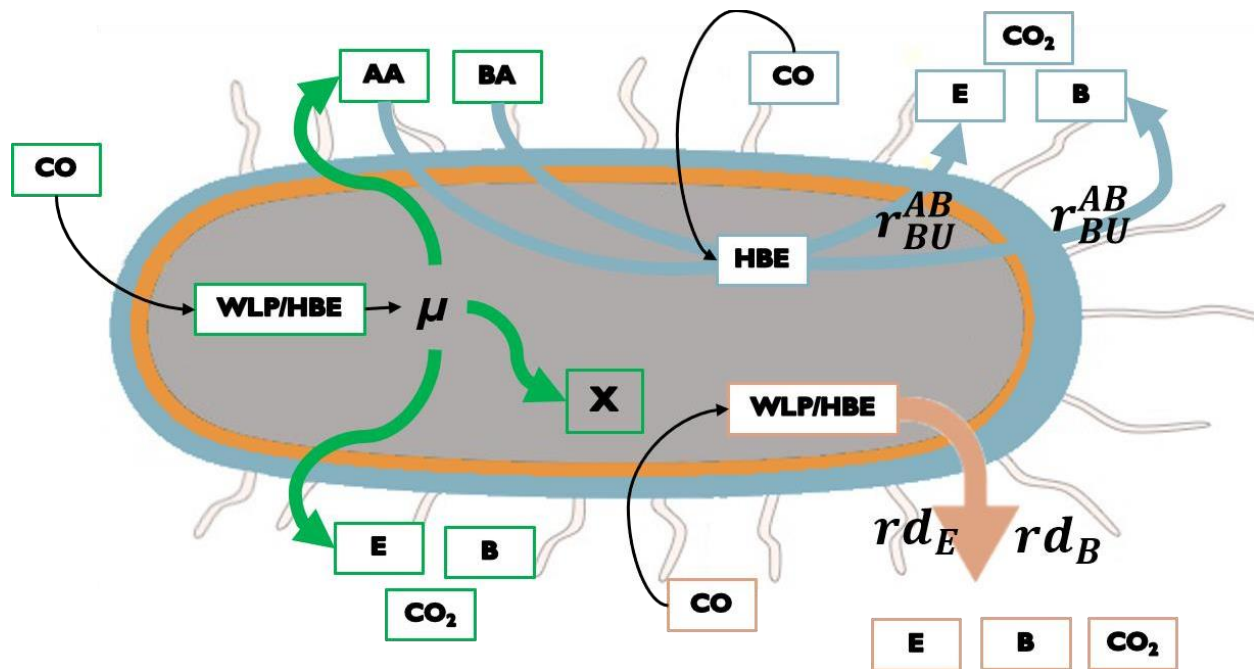


Figure 4.2: Sketch of the CO fixation and production of metabolites.

Table 4.1 reports the reactions considered in the present model. The first column of the table reports the reaction rate associated to the row reaction. Three overall biochemical reactions were considered (green arrow in Figure 4.2): biomass growth associated with metabolite (acid and alcohol) production (s1), carboxylic acid

conversion into alcohols (s2, s3) and production of alcohols non-growth associated (s4, s5). The kinetic models of the reactions are reported in Table 4.1 and 4.2.

The kinetics of the cell growth (k1) was described by the Haldane kinetic model with respect to the dissolved CO (Mohammadi et al., 2014). The inhibition effect of acids and alcohols on the cell growth was also taken into account. Acids and solvents production have been associated to the cell's growth, according to reaction s1.

The reaction rate equations k2 and k3 refer to the uptake of acetate and butyrate. They are a double-substrate Monod kinetic, with K_{ET} , K_{BU} , K_{AA} , K_{BA} as the model constant. According to the reported models, the reactions s2 and s3 are deactivated as AA and BA are not present in the medium.

The reaction rate equations k4 and k5 refers to the direct production of ethanol and butanol from CO. They are zero-order kinetics with respect to CO and products. Reactions s4 and s5 describe a non-growth associated route to produce solvent, not connected to the conversion of acetate/butyrate.

Table 4.1. Stoichiometry of the assumed bioconversion and reaction rates.

Associated reaction rate	Reaction
$\mu = \left[\frac{1}{h} \right]$	$\frac{1}{Y_X^{CO}} CO + \dots \xrightarrow{\mu} X + Y_{AA}^X AA + Y_{BA}^X BA + Y_{E/X}^E E + Y_{B/X}^B B + Y_{CO_2/X}^{CO_2} CO_2 + \dots \quad (s1)$
$r_{ET}^{AA} = \left[\frac{g_E}{g_X h} \right]$	$Y_{CO/E}^{CO} CO + Y_{AA/E}^{AA} AA + \dots \xrightarrow{r_{ET}^{AA}} E + Y_{CO_2/E}^{CO_2} CO_2 + \dots \quad (s2)$
$r_{BU}^{AB} = \left[\frac{g_B}{g_X h} \right]$	$Y_{CO/B}^{CO} CO + Y_{BA/B}^{BA} BA + \dots \xrightarrow{r_{BU}^{AB}} B + Y_{CO_2/B}^{CO_2} CO_2 + \dots \quad (s3)$
$rd_E = \left[\frac{g_E}{g_X h} \right]$	$Y_{CO/E}^{\beta} CO + \dots \xrightarrow{rd_E} E + Y_{CO_2/E}^{\beta} CO_2 + \dots \quad (s4)$
$rd_B = \left[\frac{g_B}{g_X h} \right]$	$Y_{CO/B}^{\beta} CO + \dots \xrightarrow{rd_B} B + Y_{CO_2/B}^{\beta} CO_2 + \dots \quad (s5)$

Mass transfer rate

The overall mass transfer coefficient ($k_L a$) was estimated by the correlation (4.1). The eq. (4.1) takes into account the agitator-power-per-volume ratio (P_g/V_L) and the superficial gas velocity (u_g). To estimate the power consumption and the superficial velocity, it's necessary to know the geometrical shape of the reactor, therefore it is assumed to have a height/diameter ratio of 2 and an impeller diameter equal to the 40%

of the reactor diameter, a standard value for most bioreactors, and similar to the system exploited in the experimental work.

Table 4.2. Kinetic models of the reaction rates.

Reaction rate expression	
$\mu = \frac{\mu_M CO_L}{(CO_L + K_{CO} + \frac{CO_L^2}{K_I})} \cdot \left(1 - \frac{A_{TOT}}{A_{MAX}}\right)^\alpha \left(1 - \frac{S_{TOT}}{S_{MAX}}\right)^\alpha$	(k1)
$r_{ET}^{AA} = \frac{-r_{MAX}^E \cdot CO_L}{(CO_L + K_{ET})} \cdot \frac{AA}{AA + K_{AA}}$	(k2)
$r_{BU}^{AB} = \frac{-r_{MAX}^B \cdot CO_L}{(CO_L + K_{BU})} \cdot \frac{AB}{AB + K_{AB}}$	(k3)
$rd_E = \beta_{E/X}$	(k4)
$rd_B = \beta_{B/X}$	(k5)

The k_{La} was estimated for air in water at 20°C and temperature corrected according to the eq. (4.2) (de Medeiros et al, 2019). The k_{La_j} was calculated for each species “i” according to the eq. (4.3) with respect to the reference air-water k_{La} by applying the penetration theory (Talbot et al., 1991), Df_j being the mass diffusivity of species j in water.

$$k_{La} = 3600 \left(\frac{P_g}{V_L}\right)^\nu \cdot (u_g)^c \quad (4.1)$$

$$\frac{k_{La}^{(20)}}{k_{La}^{(T)}} = 1.024^{(20-T)} \quad (4.2)$$

$$k_{L_j} a_j = k_{L_{air}} a_{air} \cdot \left(\frac{Df_j}{Df_{air}}\right)^{1/2} \quad (4.3)$$

Mass balance equations

The model is based on the mass balance referred to CO, cells and metabolites. The mass balances extended to the volume of the homogenous liquid phase (V_L) included accumulation terms, conversion/production terms and gas-liquid mass transfer rates. The mass balances extended to the gas phase included accumulation terms, and gas-liquid mass transfer rates.

A mass balance referred to the gaseous species (CO and CO₂) was also reported to model the gas flow – in terms of composition and flow rate - in and out the reactor. Under constant pressure in the bioreactor the volumetric gas flow rate Q_{out} (L/h) from the reactor was calculated according to the mass balance - expressed in terms of moles – extended to the gas phase. Equation 4.4 reports the molar flow rate from the reactor taking into account the gas feeding and the mass transfer rate of CO from gas-to-liquid and of CO₂ from liquid-to-gas.

$$N_{Gout} = Q_G CO_{Gin} - \frac{V_L(k_{LaCO} \cdot (CO^* - CO_L))}{MM_{CO}} + \frac{V_L(k_{LaCO_2} \cdot (CO_{2L} - CO_2^*))}{MM_{CO_2}} \quad (4.4)$$

$$Q_{out} = \frac{N_{Gout} RT}{P} \quad (4.5)$$

where CO* and CO₂* are the liquid phase concentration of CO and CO₂ expressed in g/L, under equilibrium conditions, according to the Henry's law, calculated by equations 4.6 and 4.7.

$$CO^* = CO_G \cdot R \cdot T \cdot H_{CO} \quad (4.6)$$

$$CO_2^* = CO_{2G} \cdot R \cdot T \cdot H_{CO_2} \quad (4.7)$$

Equations (4.6) and (4.7) report the overall conversion rate of CO and production rate of CO₂, r_{CO} and r_{CO_2} respectively. Equations have been proposed taking into account the rate and the yield reported in Table 4.1 and 4.2:

$$r_{CO} = \left(\frac{\mu}{Y_{X/CO}} + Y_{CO/E} r_{ET}^{AA} + Y_{CO/B} r_{BU}^{AB} \right) X \quad (4.8)$$

$$r_{CO_2} = + (Y_{CO_2/X} \mu + Y_{CO_2/E} r_{ET}^{AA} + Y_{CO_2/B} r_{BU}^{AB} + Y'_{CO_2/E} r'_E + Y'_{CO_2/B} r'_B) X \quad (4.9)$$

The mass balance referred to the substrate, cells and metabolites are now on order.

Gas phase:

$$V_G \frac{dCO_G}{dt} = \frac{Q_{in} \cdot P}{T \cdot R} - Q_{out} CO_G - V_L k_{LaCO} (CO^* - CO_L) \quad (m1)$$

$$V_G \frac{dCO_{2G}}{dt} = -Q_{out} CO_{2G} + k_{LaCO_2} V_L (CO_{2L} - CO_2^*) \quad (m2)$$

Liquid phase:

$$\frac{dCO_L}{dt} = k_{LaCO} (CO^* - CO_L) - r_{CO} \quad (m3)$$

$$\frac{dCO_{2L}}{dt} = -k_{LaCO_2} (CO_{2L} - CO_2^*) + r_{CO_2} \quad (m4)$$

$$\frac{dX}{dt} = \mu \cdot X \quad (m5)$$

$$\frac{dAA}{dt} = (Y_{AA/X} \cdot \mu - Y_{AA/E} \cdot r_{ET}^{AA}) \cdot X \quad (m6)$$

$$\frac{dBA}{dt} = (Y_{BA/X} \cdot \mu - Y_{BA/B} \cdot r_{BU}^{AB}) \cdot X \quad (m7)$$

$$\frac{dE}{dt} = (Y_{E/X} \cdot \mu + r_{ET}^{AA} + rd_E) \cdot X \quad (m8)$$

$$\frac{dB}{dt} = (Y_{B/X} \cdot \mu + r_{BU}^{AB} + rd_B) \cdot X \quad (m9)$$

The model parameters and yields to be estimated are listed in Table 4.3. The Table also reports for each parameter the value set as first calculation attempt and the interval of the numerical investigation. The value set of the first attempt for the fitting has been assessed by processing the experimental data from Fernández-Naveira et al. (2016a). The first attempt kinetic parameters have been assessed by linearization of the experimental data.

Table 4.3. Parameters of the kinetic model. The value set as first calculation attempt and the interval of investigation are reported for each parameter.

Parameter	First attempt	Range	Unit	Parameter	First attempt	Range	Unit
μ_{max}	0.22	0-5	1/h	$\beta_{E/X}$	0.012	0-1	gEt/(gxh)
K_{CO}	0.015	0-5	gCO/L	$\beta_{B/X}$	0.018	0-1	gB/(gxh)
K_I	0.045	0-5	gCO/L	α'	1	0-5	-
$Y_{AA/X}$	11	0-20	gAA/gX	$Y_{X/CO}$	0.1	0-10	gx/gCO
$Y_{BA/X}$	2.4	0-20	gBA/gX	S_{MAX}	5	0-30	gSolvent/L
$Y_{E/X}$	1.6	0-20	gE/gX	α''	1	0-5	-
$Y_{B/X}$	0.3	0-20	gB/gX	$Y_{CO/E}$	3	0-30	gCO/gEt
r_{MAX}^E	0.078	0-1	gEt/(gxh)	$Y_{CO/B}$	7	0-30	gCO/gB
K_{AA}	3	0-10	gAA/L	$Y_{CO2/X}$	0.15	0-30	gCO2/gX
K_{ET}	0.000005	0-5	gCO/L	$Y_{CO/E} \beta$	0.6	0-30	gCO/gEt
r_{MAX}^B	0.05	0-5	gB/(gxh)	$Y_{CO/B} \beta$	0.75	0-30	gCO/gB
K_{AB}	2	0-10	gBA/L	$Y_{CO2/E}$	5	0-100	gCO2/gEt
K_{BU}	0.000002	0-5	gCO/L	$Y_{CO2/B}$	5	0-100	gCO2/gB
$Y_{AA/E}$	1	0-50	gAA/gE	$Y_{CO2/E} \beta$	1	0-100	gCO2/gEt
$Y_{BA/B}$	1	0-50	gBA/gB	$Y_{CO2/B} \beta$	1	0-100	gCO2/gB
A_{MAX}	8	0-50	gAcid/L				

The first attempt yield parameters have been set equal to the experimental yields. Fernández-Naveira et al. (2016a) have not report any data regarding CO₂ production. Therefore, the first attempt values for parameters related to CO₂ production have been assessed by processing the data reported in §3.1.

The extension of the investigation interval was set to include potential results available in literature and to keep the calculation time within reasonable value.

Sensitivity analysis

Sensitivity analysis was carried out to assess the soundness of the proposed model. The assessment regarded the final concentration of cells, ethanol and butanol, as a function of the increase/decrease of the kinetic parameters and yields of 20%. The sensitivity function defined for cell, ethanol and butanol concentration are reported hereinafter. The suffix "END" is the concentration calculated at 240 h fermentation time.

$$\Omega_X = \frac{X_{END}^{\pm 20\%} - X_{END}}{X_{END}} \cdot 100 \quad (4.10)$$

$$\Omega_E = \frac{E_{END}^{\pm 20\%} - E_{END}}{E_{END}} \cdot 100 \quad (4.11)$$

$$\Omega_B = \frac{B_{END}^{\pm 20\%} - B_{END}}{B_{END}} \cdot 100 \quad (4.12)$$

Results and discussion

The results of the kinetic assessment and the sensitivity study are reported hereinafter.

Parametric regression

The solution of the dynamic fermentation model described by the system of ODEs equations (m1-m9) - along with the equations used to estimate Q_{out} and k_{La} - provides the estimation of the model parameters reported in in Table 4.4. Parameters were estimated using a trust-region reflective algorithm method from MATLAB library.

The analysis of data reported in Table 4.4 and the comparison with data reported in the literature are reported hereinafter.

- Value of μ_{MAX} and K_I . The estimated value of μ_{MAX} (0.373 h⁻¹) and K_I (0.003 gCO/L) were in agreement with data reported in the literature (Doll et al., 2018).
- Substrate inhibition. The inhibition effect of the substrate without product inhibition provides the CO_L concentration that maximizes the first term of the growth kinetic rate eq. k1. It was $CO_L^{Opt} = \sqrt{K_{CO} \cdot K_I}$ equals to 0.0057 g/L. The CO_L^{Opt} assessed is lower than the solubility of the CO in water at 33°C (0.023 g/L), the temperature considered in the experiment and in the simulation. Therefore, the fermentation process is expected to be enhanced - in terms of cell growth rate - by reducing the concentration of CO in the gas stream fed to the reactor.

Parameter	Value	Unit	Parameter	Value	Unit
μ_{max}	0.373	1/h	$\beta_{E/X}$	0.002	$g_{Et}/(g_{Xh})$
K_{CO}	0.011	g_{CO}/L	$\beta_{B/X}$	0.016	$g_B/(g_{Xh})$
K_i	0.003	g_{CO}/L	α'	0.759	-
$Y_{AA/X}$	11.92	g_{AA}/g_X	$Y_{X/CO}$	0.020	g_X/g_{CO}
$Y_{BA/X}$	2.417	g_{BA}/g_X	S_{MAX}	5.184	$g_{Solvent}/L$
$Y_{E/X}$	0.970	g_E/g_X	α''	2.544	-
$Y_{B/X}$	0.163	g_B/g_X	$Y_{CO/E}$	1.627	g_{CO}/g_{Et}
r_{MAX}^E	0.310	$g_E/(g_{Xh})$	$Y_{CO/B}$	5.466	g_{CO}/g_B
K_{AA}	3.305	g_{AA}/L	$Y_{CO2/X}$	1.209	g_{CO2}/g_X
K_{ET}	0.013	g_{CO}/L	$Y_{CO/E} \beta$	1.7645	g_{CO}/g_{Et}
r_{MAX}^B	0.168	$g_B/(g_{Xh})$	$Y_{CO/B} \beta$	0.186	g_{CO}/g_B
K_{BA}	2.395	g_{BA}/L	$Y_{CO2/E}$	5.271	g_{CO2}/g_{Et}
K_{BU}	0.011	g_{CO}/L	$Y_{CO2/B}$	4.474	g_{CO2}/g_B
$Y_{AA/E}$	1.255	g_{AA}/g_E	$Y_{CO2/E} \beta$	1.588	g_{CO2}/g_{Et}
$Y_{BA/B}$	1.059	g_{BA}/g_B	$Y_{CO2/B} \beta$	1.886	g_{CO2}/g_B
A_{MAX}	9.192	g_{Acid}/L			

- Product inhibition. The estimated critical concentration of acids and alcohols (S_{MAX} and A_{MAX}) - concentration at which no cell growth occurs anymore - were about 5.2 and 9.2 g/L, respectively. At this acid concentrations the pH of the medium is so low to promote the shift from acidogenesis to solventogenesis phase (non-growth phase) (Fernández et al., 2017b). As regard solvent toxicity, an inhibition was found to take place during the bioconversion of C1 gases by clostridia, (Fernández-Naveira et al., 2016b), even if a systematic study, but to quantify this effect properly, a systematic study should be performed.
- Solvent production. The solvent (ethanol/butanol) production through acid uptake, kinetics k_2 and k_3 . On one hand, the maximum ethanol specific production rate (0.310 g_{Et}/g_{Xh}) was about two-fold the maximum butanol specific production rate (0.168 g_B/g_{Xh}). On the other hand, the saturation constants for CO (K_{ET} and K_{BU}) and for acids (K_{AA} and K_{BA}) in eq. k_2 and k_3 were close each other. Therefore, the ethanol production rate was almost twice the butanol production rate during all the fermentation tests.
- Non-growth associated direct alcohol (ethanol/butanol) production, kinetics k_4 and k_5 . The estimated specific production rates (0.002 and 0.016 $g_{solvent}/g_{Xh}$) were definitively several orders of magnitude lower than the indirect solvent production rates (0.310 and 0.168 $g_{solvent}/g_{Xh}$). Therefore, the solvent production via the non-growth associated route was found to be negligible with respect to other possible routes (growth-associated direct production, indirect production via acid uptake), under the operating conditions tested. It should be pointed out that the indirect alcohol production path was the main active path throughout the fermentation tests because it is only function of cells and CO concentration and it does not suffer any

inhibition. It is expected that at high alcohol concentration the inhibition phenomena dominate. To author knowledge, such high value were never reached in any fermentation test reported in literature.

- Yields coefficients. The assessed yields coefficients (Table 4.4) for ethanol and butanol were lower than the maximum theoretical values (stoichiometric values). It is reminded that stoichiometric values were assumed as first attempt in the regression. The assessed yields for acetic and butyric acids were consistent with the stoichiometric values. The deviation observed for ethanol and butanol is probably explained by the multiple mechanism that lead to their formation, contrary to what happens for acids.
- Specific production of metabolites. The system was characterized by high production of metabolites per cells: high value of $Y_{AA/X} = 11.92 \text{ g}_{AA}/\text{g}_X$ and $Y_{BA/X} = 2.417 \text{ g}_{BA}/\text{g}_X$. As expected, the yield of CO in X was very low (0.02 grams of biomass per gram of CO): the large fraction of the CO was converted into acids, alcohols, CO₂.

The correlation coefficient R^2 - the statistic indicator used to mark the quality of the model fitting - was calculated. The R^2 assessed for each model variable and the average of all of them are reported in Table 4.5. The R^2 data are encouraging for all the analysed variables: the correlation coefficient assessed for the metabolites were particularly high. The promising result was based on the regression of a relatively small set of experimental data, and it may be further improved when more experimental data are available. The quite high R^2 values assessed for each variable encouraged further analysis of the present study.

Table 4.5. Average squared correlation coefficient (R^2) between predicted values and experimental data.

X	CO	AA	ET	AB	BU	Average
0.7594	0.7376	0.9629	0.9911	0.8769	0.9798	0.8834

The fidelity of the model in describing the growth of *C. carboxidivorans* has been confirmed. The inhibition mechanism considered influences remarkably the cells growth, as it forecasts the total inhibition.

A different kinetic growth model has been proposed (de Medeiros et al., 2019), which differs from the present model for the following features:

- it accounts only acetate and ethanol as fermentation products;
- it considers H₂ and CO₂ contributes to the growth;
- partial inhibition of CO, ethanol and acetate;

As the two models differs in many key aspects, a comparison to assess the accordance is not trivial. However, it is possible to compare the results obtained for *C. carboxidivorans* and *C. ljungdahlii* (de Medeiros et al., 2019) in terms of specific growth rate and yield of CO in biomass.

- The estimated specific growth rate μ in the present work ranges between 0.0699 in optimal conditions to 0.365 h⁻¹ in CO-saturated medium conditions and absence of products. The estimated yield $Y_{X/CO}$ in the present work is 0.02 g_X/g_{CO}.

- The specific growth rate from CO estimated for *C. ljungdahlii* is 0.035 h^{-1} . The estimated yield is $Y_{X/\text{CO}} = 0.027 \text{ gX/gCO}$.

Both the strains follow the Wood-Ljungdahl pathway. Therefore, the closeness of the results is expected. This comparison gives a further confirm of the reliability of the proposed model, especially in the part related to the growth and conversion of CO.

For what concerns the production, a similar comparison would be inappropriate, as the different inhibition kinetics lead to very different results in terms of productivity and final concentrations.

The figure 4.3 reports the plot of the time-resolved profiles of the simulated variables and the experimental data used for the parameter assessment. The final cell concentration was slightly over-estimated, as expected when the cells R^2 is analysed.

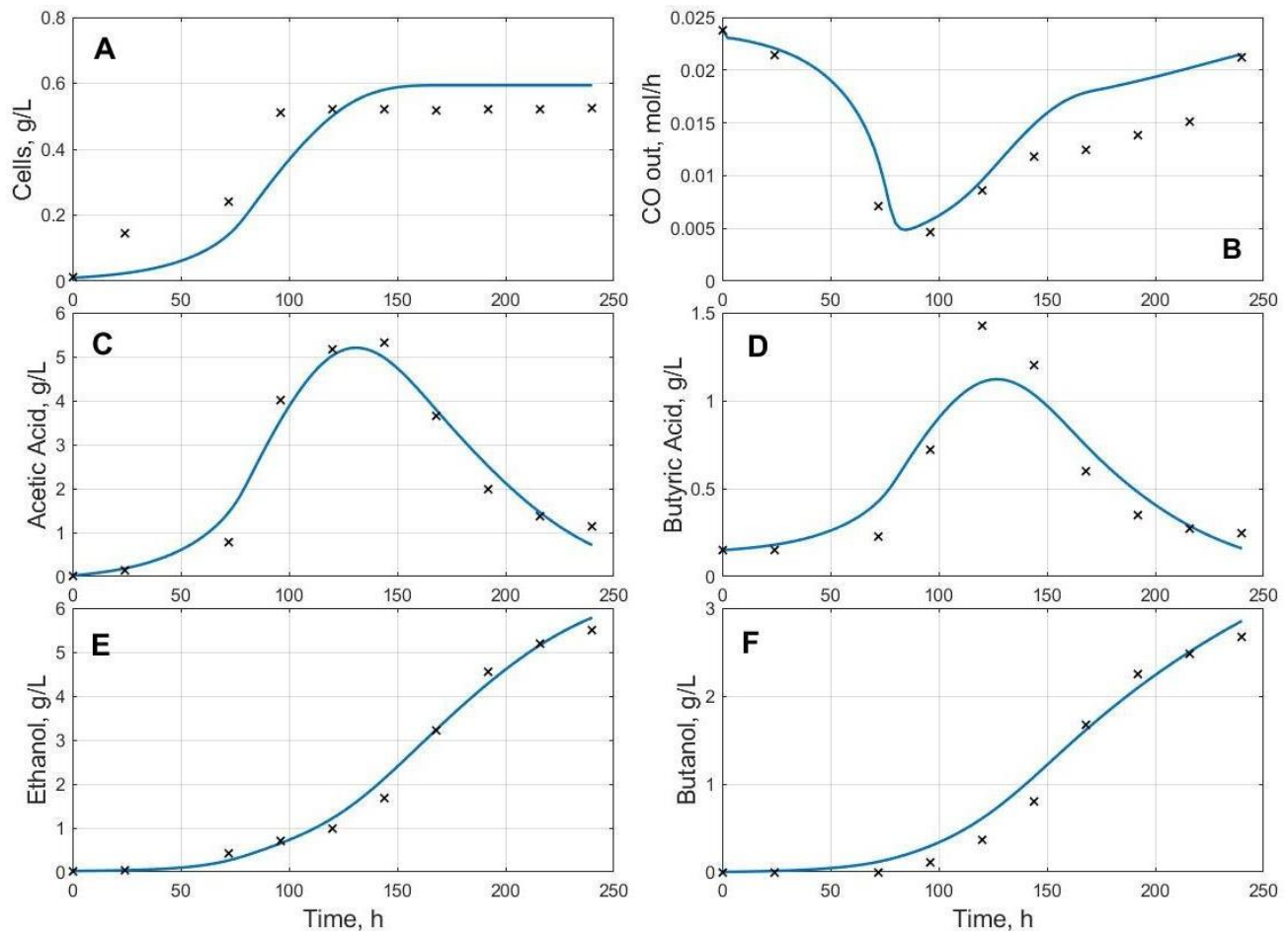


Figure 4.3: Syngas fermentation: solid line) simulation results of the fermentation model by setting the model parameter at value reported in Table 4.4; symbols) experimental data (Fernández-Naveira et al., 2016a). Time-resolved profiles of: A) cells concentration, B) substrate consumption; C) acetic acid concentration; D) ethanol concentration; E), butyric acid concentration; F) butanol concentration.

Sensitivity analysis

The sensitivity of the model variable (cell, ethanol and butanol final concentrations) was assessed in agreement with eq.s (4.10) through (4.12): the $\Omega_{END}^{\pm 20\%}$ was the value of Ω calculated at the 240 h fermentation time by setting the model parameter at $\pm 20\%$ the value reported in Table 4.4. The Table 4.6 reports the results of the sensitivity analysis. The Table 4.6 does not report sensitivity results for sensitivity smaller than 0.1%.

The final concentration of the investigated variables was mainly affected by the value set for the model parameters μ_{MAX} , K_I , A_{MAX} , and S_{MAX} . These model parameters characterize the cell growth kinetic (s_1 , k_1): it could be expected that this step affected strongly the conversion process as it changes the amount of the playing actor-cells. It is worth to note that μ_{MAX} is the only parameter that may affect the variation of the model variable at an extent larger than the imposed perturbation: up to about 23% of the ethanol/butanol concentration vs a perturbation of 20% of the parameter.

As expected, the yield factors $Y_{AA/X}$ and $Y_{AB/X}$ affected mainly the quantities of acids produced for unit mass of cells: the production eq.s k2 and k3. As $Y_{AA/X}$ increases, the maximum value of the cell concentration drops remarkably because the fermentation medium saturated with inhibitors more quickly.

It is worth to note the effect of the parameters peculiar of the inhibition behaviour: K_I as representative of the substrate inhibition, and A_{MAX} and S_{MAX} representative of the product inhibition. The sensitivity of about 8-15% points out that the performance of *C. carboxidivorans* as regards the solvent production may be strongly affected by improving the resistance to the inhibition phenomena.

Altogether, the sensitivity analysis points out the soundness of the model and the reliability of the assessed parameters.

Table 4.6. Effect of a simulated perturbation of parameters value on the calculated value of cells, ethanol and butanol concentration after 240 h of fermentation.

	$\Delta\%$	μ_{max}	K_{CO}	K_I	$Y_{AA/X}$	$Y_{BA/X}$	$Y_{E/X}$	$Y_{B/X}$	r_{MAX}^E	K_{AA}	K_{ET}	r_{MAX}^B	K_{BA}
	Unit:	1/h	gco/L	gco/L	gAA/gX	gBA/gX	gE/gX	gB/gX	gE/(gxh)	gAA/L	gco/L	gB/(gxh)	gBA/L
Ω_X	+20	8.27	-3.80	3.57	-10.18	-2.20	-3.00	-0.53	-2.74	1.23	1.60	-0.61	0.40
	-20	-15.95	4.30	-7.76	11.51	2.37	2.97	0.52	2.81	-1.54	-2.11	0.61	-0.55
Ω_E	+20	12.68	-4.07	7.13	1.31	-2.58	-0.83	-0.48	2.76	-2.58	-2.20	-0.83	0.60
	-20	-23.04	4.47	-13.93	-4.67	2.71	0.61	0.46	-6.39	2.42	1.43	0.95	-0.75
Ω_B	+20	14.93	-4.37	8.69	5.18	4.64	-2.75	0.22	-2.56	1.19	1.5	2.09	-2.12
	-20	-24.86	4.90	-15.51	10.64	-5.22	2.67	-0.24	2.74	-1.46	-1.96	-3.43	2.09
	$\Delta\%$	K_{BU}	$Y_{AA/E}$	$Y_{AB/B}$	A_{MAX}	$\beta_{E/X}$	$\beta_{B/X}$	α'	$Y_{X/CO}$	S_{MAX}	α''	$Y_{CO/E}$	$Y_{CO/B}$
	Unit:	gco/L	gAA/gE	gBA/gB	gacid/L	gE/(gxh)	gB/(gxh)	-	gx/gCO	g _{solv} /L	-	gco/gE	gco/gB
Ω_X	+20	0.32	1.83	0.46	8.04	-0.30	-2.23	-5.59	-3.65	12.41	-9.60	0.43	0.42
	-20	-0.44	-1.89	-0.48	-11.04	0.28	2.28	6.13	2.37	-16.32	9.84	-0.48	-0.44
Ω_E	+20	0.45	-7.46	0.79	6.92	0.42	-2.02	-5.48	-2.62	9.62	-8.95	-0.38	-0.27
	-20	-0.59	6.73	-0.86	-10.72	-0.43	2.02	5.58	-0.23	-15.31	8.16	0.27	0.20
Ω_B	+20	-1.22	1.83	-4.52	7.38	-0.27	8.46	-5.65	-3.46	9.99	-8.80	0.04	0.07
	-20	1.09	-1.87	5.05	-10.79	0.25	-8.83	5.96	1.28	-14.64	8.53	-0.10	-0.12

Effect of operating conditions

The maximum cell concentration and the CO consumption, measured in terms of its concentration in the exhaust gas were assumed as index of the goodness of the fermentation process. The effect of the operating conditions was assessed in terms of variation of these two variables, as reported in Figure 4.4. The Figure 4.4 reports the time-resolved plots of the cell concentration and CO concentration in the exhaust gas stream (eqs. m1 and m5) assessed under a spectrum of operating conditions.

The selection of the variables to characterize the performance of the fermentation was addressed by the potential route to produce solvents: the growth-associated productions, the direct production of alcohols, the former production is associated with the X dynamics, the latter production is highlighted by CO consumption (under constant cell concentration).

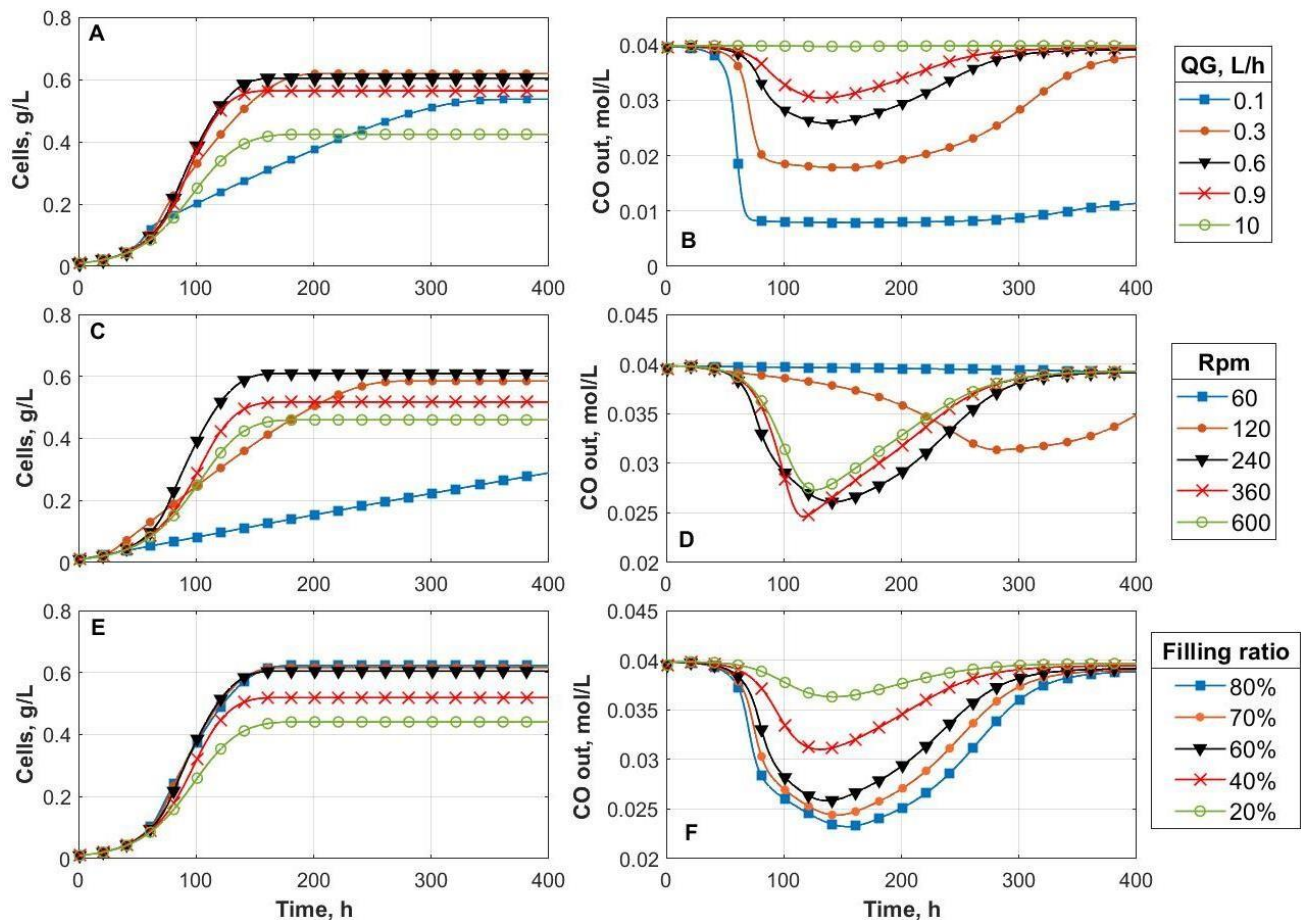


Figure 4.4: Effect of the operating conditions Q_{IN} (A,B), rps (C,D) and V_G (E,F) on cell concentration and CO concentration.

The attention was focused on the following three main operating conditions: the gas fraction of the reactor, the feeding flow rate of CO, and the mixing rate. These operating conditions - expressed by the parameters V_G , Q_G and rps, respectively - affect the gas-liquid mass transport rate. The reactor gas fraction was changed by tuning V_G (or V_L) keeping constant the reactor volume ($V_L + V_G$). Although the effect of

operating conditions as temperature, pH and pressure are of interest, the present study did not include them because of the absence of sufficient dedicated experimental tests to compare with.

The effect of each operating condition was investigated by keeping all the others constant. The tuning interval of each operating conditions was set according to different scenarios. As regards the gas fraction, V_G ranged between from 0 and 2 L (the reactor volume set in the present investigation). As regards the mixing rate and the feeding gas flow rate, agitation rate and Q_G were increased until no further change in the fermentation performance was observed. The latter condition established as the gas-liquid transfer rate was so active that the concentration in the liquid phase of the selected species was maximum. The percentage variation reported in Tables 4.7, 4.8 and 4.9 refers to the values obtained in the standard conditions used for the parametric regression. The lines marked in bold represent the highest value reported without approximation.

A cross search was carried out to assess the optimal conditions characterized by the maxim final cell concentration.

Reactor filling ratio

The amount of liquid in the reactor affects the gas transfer rate, and it turns into substrate availability in the liquid phase. According to eq. 4.1, k_La increases with the power transferred to the unit liquid volume (Pg/V_L). Therefore, increasing ratio between gas and liquid volume V_G/V_L at constant stirring speed leads to much higher power transferred per unit volume of liquid and thus to an increase in k_La . The mass transfer rate affects the CO_L concentration, then the kinetics. The values of k_La calculated tuning V_G are reported in Table 4.7. The value of k_La increased with V_G because the resistance to transport was lower in gas phase than in liquid phase. Keeping other operating conditions constant, the smaller was the reactor liquid fraction the higher was the grade of mixing that may be achieved. The enhancement of the gas-to-liquid mass transfer rate provided a high substrate uptake rate. However, the simulated maximum cell concentration decreased with the increase of the gas headspace volume and k_La . Evidently, the higher concentrations of CO in the medium negatively affected the growth of cells because of the inhibitory effect of the substrate.

Table 4.7. Effect of reactor filling ratio on maximum cell concentration and k_La .

Filling ratio, %	Max cell conc. (g/L)	Variation %	k_La , 1/h
96.8	0.62	3.2%	22.6
96.0	0.62	3.3%	22.7
92.0	0.62	3.2%	23.4
88.0	0.62	3.2%	24.1
84.0	0.62	3.2%	24.9
80.0	0.62	3.0%	25.8
76.0	0.62	2.7%	26.7
72.0	0.61	2.4%	27.7
68.0	0.61	1.8%	28.9
64.0	0.61	1.1%	30.1
60.0	0.60	0.0%	31.5
50.0	0.58	-4.6%	35.8
40.0	0.52	-14.1%	41.9

Agitation speed

The frequency of the blade rotation was tuned between 25 and 600 rpm. The plots in figures 4.4C and 4.4D point out that the agitation speed must be larger of a minimum value to guarantee the sufficient substrate gas-to-liquid mass transfer rate. Under 60 rpm – blue line - the cell concentration did not approach the asymptotic value even after 400. As the agitation rate was larger than 120 rpm the cell concentration approached the constant final value within 240 h. The maximum cell concentration was characterized by a maximum at agitation rate of 182 rpm (Table 4.8). The simulations reported by setting the agitation rate at 600 rpm pointed out asymptotic behaviour with respect to the k_La (Abubackar et al., 2015).

Table 4.8. Effect of the agitation speed on maximum cell concentration and k_La .

Rpm	Max cell conc., g/L	Incr%	k_La , 1/h
25	0.19	-68.1	0.25
50	0.36	-40.8	1.1
75	0.47	-21.7	2.5
100	0.55	-9.3	4.6
125	0.59	-2.0	7.4
150	0.61	1.8	10.8
175	0.62	3.4	14.9
182	0.63	3.5	16.3
200	0.62	3.3	19.7
225	0.62	2.1	25.3
250	0.60	0.0	31.5
600	0.46	-24.0	198.0

Gas feeding flow rate

The gas feeding flow rate of CO to the reactor affected the CO delivered to the cells during the process. The control of gas amount available in the liquid phase is very important because the growth of *C. carboxydivorans* was characterized by substrate inhibition. Setting the CO flow rate higher than the maximum consumption rate provided that the dissolved CO concentration was close to its saturation threshold. This condition is unfavourable for the growth rate and, moreover, the unconverted CO in the exhaust gas stream must be post-treated or recycled. Simulations were carried out by tuning Q_G between 0.1 L/h and 50 L/h. Table 8 reports k_La and final concentration of cells calculated from simulations at several gas feeding flow rates and the corresponding residence time (assessed with respect of the headspace volume V_G). The target was to assess the minimum gas feeding flow-rate to operate the reactor under “differential conditions” with respect to the gas phase: CO consumption negligible with respect to the inlet CO flow-rate. This threshold was fixed at a 5% CO consumption in the gas stream. The minimum value of Q_G to operate the reactor under differential conditions was found to be 3.3 L/h, corresponding to a gas residence time in the headspace of 0.36 h, when the filling ratio and the stirring speed of the bioreactor were set to the reference values.

It is worth to note that high concentration of cells can be achieved at intermediate feeding gas flow rate.

Table 4.9: Effect of the inlet gas flow on maximum cell concentration and k_{La} .

Q_G , L/h	Gas residence time, h	Max cell conc., g/L	Variation %	k_{La} , 1/h
0.10	12.00	0.54	-11.2	22.0
0.18	6.67	0.59	-2.0	24.8
0.24	5.00	0.61	1.2	26.3
0.30	4.00	0.62	2.5	27.5
0.37	3.24	0.62	2.8	28.7
0.50	2.40	0.61	1.8	30.4
0.60	2.00	0.60	0.0	31.5
0.90	1.33	0.56	-6.6	34.2
1.20	1.00	0.53	-12.9	36.2
3.30	0.36	0.46	-23.8	44.2
10.00	0.12	0.44	-27.6	54.7
50.00	0.02	0.42	-29.8	71.2

Multiparametric optimization

The further step was to analyse fermentation tests carried out under a matrix of experimental operating conditions to assess the interference effects among operating conditions. It is worth to note that the analysis of effects of a single operating condition has pointed out that optimal conditions was found at a set of value different with respect to those set during the experimental tests. The target was to find the set of operating conditions associated with the maximum fermentation performances.

The simulations were carried out by tuning simultaneously the operating conditions: a three-dimension matrix of operating conditions was provided. Each set of operating conditions was characterized in terms of fermentation performance expressed in terms of cells and metabolites concentration. The set characterized by the best performances was found. The optimal vector of operating conditions was made of: $V_G = 0.64$ L ($V_L = 1.36$ L), filling ratio 68%; feeding gas flow rate 0.54 L/h, it means dilution rate of the gas phase of 0.84 h^{-1} ; agitation speed of the impellers of 182 rpm. The time-resolved plots of the concentration of substrate and metabolites are reported in Figure 4.5. The Figure 4.5 and Table 4.10 report the simulation carried out by setting the reference operating conditions.

The effect of some operating conditions on the fermentation performance – expressed in terms of cell production and CO consumption - was investigated to address potential design and operation to optimize the fermentation process.

It was pointed out that a slightly improve is possible, but most important is that this is possible even with a low transfer rate of the gas to the medium, leading to a promising scenario where the energy cost of the impellers, or any other diffusion system, is much more sustainable. Moreover, as in most of the cases the consumption of gas is never complete, the same amount can be used for a higher reaction volume, improving the yield and the exploit of the raw materials.

Table 4.10. Multiparametric optimization results.

Parameters	k_{La} (1/h)	Max conc. X(g/L)	Max conc. AA(g/L)	Max conc. BA(g/L)	Max conc. E(g/L)	Max conc. B(g/L)
Reference: $V_g=0.80$ L $Q_G=0.60$ L/h rpm=250	31.5267	0.6041	5.2453	1.0429	7.0317	6.5198
Optimized: $V_g=0.64$ L $Q_G=0.54$ L/h rpm=182	19.3278	0.6258	5.6172	1.1069	7.2847	6.7314

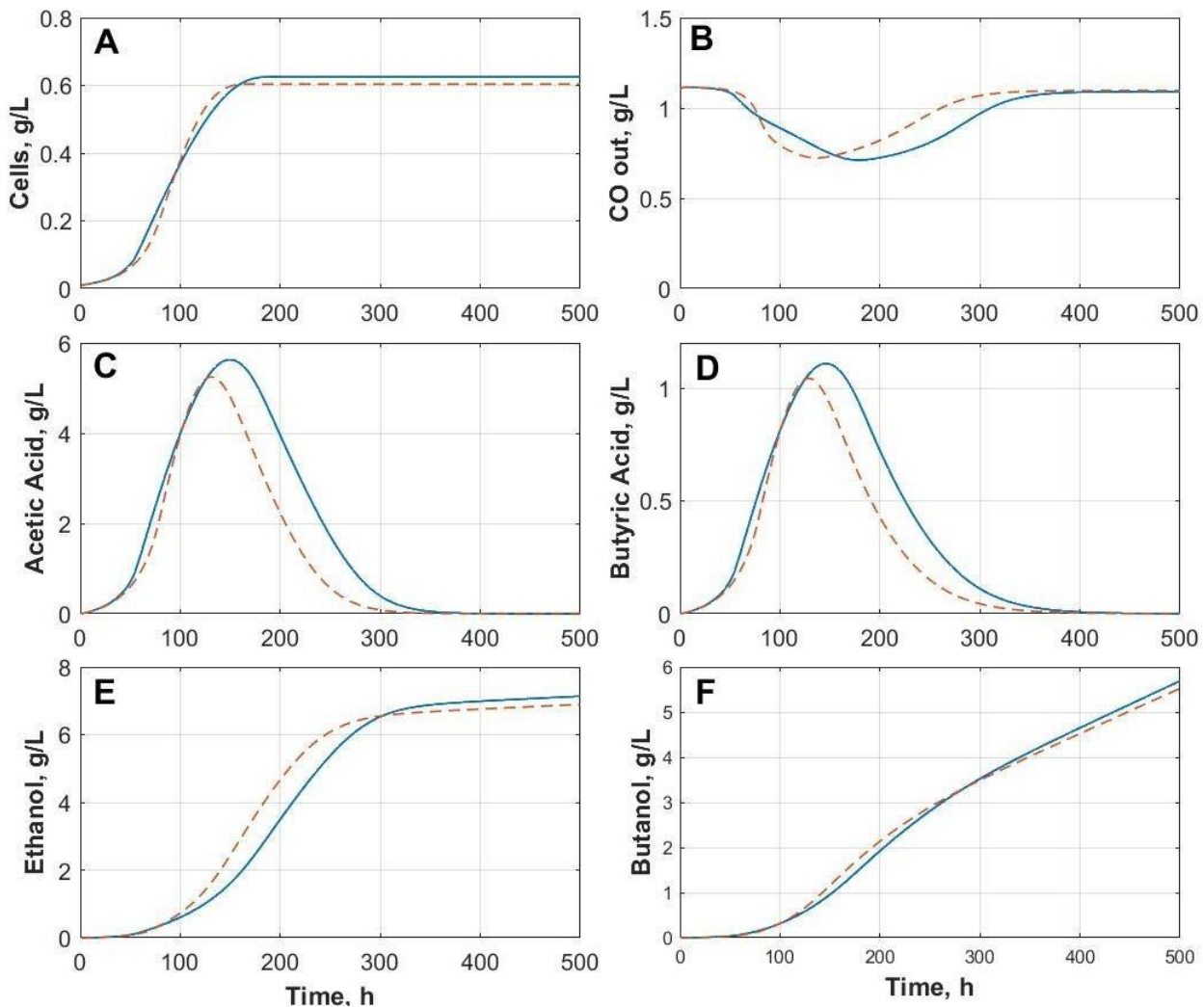


Figure 4.5: Comparison between profiles obtained with optimized parameters (blue) and profiles obtained with the starting set.

Conclusions

A dynamic model of syngas fermentation by *C. carboxidivorans* in a continuously gas-fed STR was developed. The model was used to assess a set of 31 kinetic parameters and product yields based on the regression of literature (Fernández-Naveira et al., 2016a) related to fixed conditions of gas flow rate, stirring rate, gas to liquid volume fraction of the STR.

The model was used to assess the sensitivity of the dynamic prediction against $\pm 20\%$ variation of kinetic parameters and yields. The overall result showed that the model variables (biomass, outlet CO and products concentrations) were affected by variation in kinetic parameters and yields but, except μ_{MAX} , the percentual variation of the “output” was always lower than the percentual variation of the “input”. This result suggests that μ_{MAX} must be estimated with the highest possible grade of accuracy in future experimental investigations to minimize the error in any predictive study aimed at bioreactor design.

The parameters affecting the growth kinetic (eq. k1) were the ones to which the model was most sensitive, with variations around 5 - 15% not negligible. On the other side, the parameters related to direct production of alcohols (eqs. k4 and k5) were the ones with the lowest impact on the system, because the contribute of those mechanisms only affects alcohols production. The contribution to butanol and ethanol to the kinetics lies only in the inhibition terms, and the contribution of those reactions to alcohols production is lower than the other mechanisms, especially in the first phase of the fermentation.

The effect of some relevant operating conditions on the fermentation performance – expressed in terms of cell production and CO consumption - was investigated to depict a first attempt scenario of the practical fermentation process. It was pointed out that a slight improvement in the fermentation performances was possible; in particular, the decrease of the mass transfer rate increased the production of cells and metabolites of interest. This result leads to a promising scenario where the energy cost of the impellers rotation, or any other gas-liquid contact and mixing device, should be properly tuned instead of merely maximized.

The gas flow rate affected not only the mass transfer coefficient, but also the driving force ($CO^* - CO_L$) and the substrate availability, therefore its effect was much more evident even though the optimal mass transfer rate doesn't remarkably change, compared to the other cases: the kLa dropped from 31.5 to 29.6 29 h^{-1} (-9%), in the Q_G analysis, while it dropped to 16 h^{-1} (-48%) in the rpm analysis.

The use of a real or synthetic syngas, instead of pure CO, would reduce the partial pressure of CO, and therefore its inhibitory effect, but it would require the introduction of a different (and more complex) kinetic mechanism that takes into account the presence of more than a single gaseous substrate (CO_2 and H_2 other than CO), further increasing the number of parameters and yields to estimate. A study to assess the effect of the gas composition is one of the most important further steps to exploit the potential of syngas fermentation by *C. carboxidivorans*.

4.2 Biofilm reactor modelling for Syngas fermentation³

G. Ruggiero^a, F. Raganati^a, M.E. Russo^b, M. Brognoli^c, A. Marzocchella^a

^a Department of Chemical, Materials and Production Engineering–University of Naples Federico II,

^b Institute of Science and Technology for Energy and Sustainable Mobility (STEMS) - CNR

^c Solaris Biotechnology, S.r.l.

Abstract

A mathematical model of an anaerobic biofilm reactor for gas fermentation has been proposed. The aim was to investigate the dynamic behavior of the bioreactor as a function of key operating conditions. The ability of some acetogens to form biofilm is a potential development of inestimable importance to increase the productivity of the process and to make it economically attractive.

Suspended cells and biofilm cells were assumed to grow according to a double limiting kinetics with substrate (carbon monoxide) and product (acids and alcohols) inhibition. The model presented is extended to embody key features of the phenomenology of the granular-supported biofilm: biofilm growth and detachment; gas–liquid transport; CO uptake by both suspended and immobilized cells; substrate diffusion into the biofilm.

The system of partial and ordinary differential equations was solved in steady state and transitory condition by mean of a discretization of the biofilm.

Keywords: Biofilm reactor; Modelling; Syngas; *Clostridium carboxidivorans*.

Introduction

Syngas fermentation from C-based feedstock is a hybrid thermal-biological route to produce liquid biofuels and chemicals. It includes: the gasification of biomass and carbonaceous solid wastes to syngas, and the fermentative conversion of C1 gases (CO and CO₂). This innovative and promising strategy has the potential to successfully overcome the main flaws and weaknesses of the traditional conversion processes. Indeed, the exploitation of hard lignocellulosic biomass may be unsustainable from energy, cost and materials point of view, Moreover, the conversion of syngas streams – produced by processing biomasses and/or C-based feedstocks – according to catalytic path may be not advantageous and/or practicable. Major challenges of syngas fermentation include the gas transport rate between gas and liquid phases and the low syngas specific conversion rate.

The gas-transport rate may be expressed in terms of the gas–liquid volumetric transfer coefficients (k_La). Although plenty scientific papers have been proposed to assess k_La for several gas-liquid system/apparatus, just a few studies are available as

³ To be submitted

regards the CO transport. Indeed, the measurement of the dissolved CO concentration at high accuracy, especially in culture medium. (Köpke et al., 2011) is quite difficult.

Biofilm processes may display significant advantages over conventional cell suspension or containment systems. Biofilm reactors are characterized by; high biomass loading; operation at the set dilution rates without any biomass washout; easy cell confinement into the reactor; protection of cells against toxic or inhibitory compounds. Promoting the formation of microbial aggregates/biofilms is an effective strategy for achieving enhanced productivity in bioprocesses. Formation of aggregates makes it possible to establish cultures characterized by cell densities (biomass per unit volume) much larger than those commonly established in liquid broths (Nicolella et al., 2000; Qureshi et al., 2005). Indeed, large cell densities is an attractive feature that can be exploited in a number of fermentation applications to enhance process intensification. Immobilization of cells and membrane reactor technology are the two common strategies to provide high-density confined cell cultures in discontinuous and continuous reactors. Immobilization of cells by adhesion on natural - and typically inexpensive - supports is the first step for the production of biofilm. Proper selection of granular supports, together with careful selection of the microbial strain, are the keys to a successful design of multiphase biofilm reactors. The establishment of solid-supported biomass loading in continuous biofilm reactors results from the competition between cells adhesion/growth on the granular carrier and detachment of biofilm fragments from the granules (Russo et al., 2008).

The number of papers available in the scientific literature to model syngas fermentation is quite small. Only a few authors have focused on the address of kinetic expressions by processing experimental data. Younesi et al. (2005) and Mohammadi et al. (2014) used logistic model to simulate the growth of *C. ljungdahlii* on synthetic syngas by processing experimental data from batch fermentation tests carried out in serum bottles. Mohammadi et al. (2014) carried out the regression of experimental data according to the Gompertz equations. They used data of product concentration and CO concentration to assess kinetic parameters. Chen et al. (2015) used model of Mohammadi et al. (2014) in a dynamic Flux Balance Analysis (FBA) model to simulate the syngas fermentation in a bubble column.

The present paper proposes a dynamic model for gas fermentation of *C. carboxidivorans* to produce ethanol and butanol in a continuous stirred tank reactor (CSTR). A biofilm reactor configuration was assumed and the model aimed to describe the radial profiles of substrate and metabolites concentrations across the biofilm layer as a function of time. The dynamic non-segregated and non-structured model described the evolution of both suspended and immobilized cells of *C. carboxidivorans* in a three-phase reactor, as a function of the operating conditions. The unknown model parameters were estimated according to a multi-response minimization framework by regression of experimental culture data from the literature. The relevance of parameters was assessed by means of statistical analysis.

Model description

Figure 4.6 shows a sketch of the anaerobic bioreactor under investigation. The reactor is assumed to be operated batchwise with respect to the biofilm-carrier phase and continuously with respect to the gas and liquid phases. The dynamic non-

segregated and non-structured model describes the evolution of both suspended and immobilized cells of *C. carboxidivorans* in a three-phase reactor, as a function of the operating conditions. The model is aimed to describe the radial profiles of substrate and metabolites concentrations across the biofilm layer as a function of time. The operative parameters (flow rates, dimension, pH, temperature and so on) used in the various sets of simulations refer to a specific reactor system retrieved in literature, deeply studied (Fernández-Naveira et al., 2016a). The parameters of yields and kinetics are collected in Table 4.1.

The reactor is continuously fed with a liquid stream (volumetric flow rate Q_L) bearing the culture medium. The gaseous stream Q_G fed to the reactor provides the carbon source required for the progress of the process.

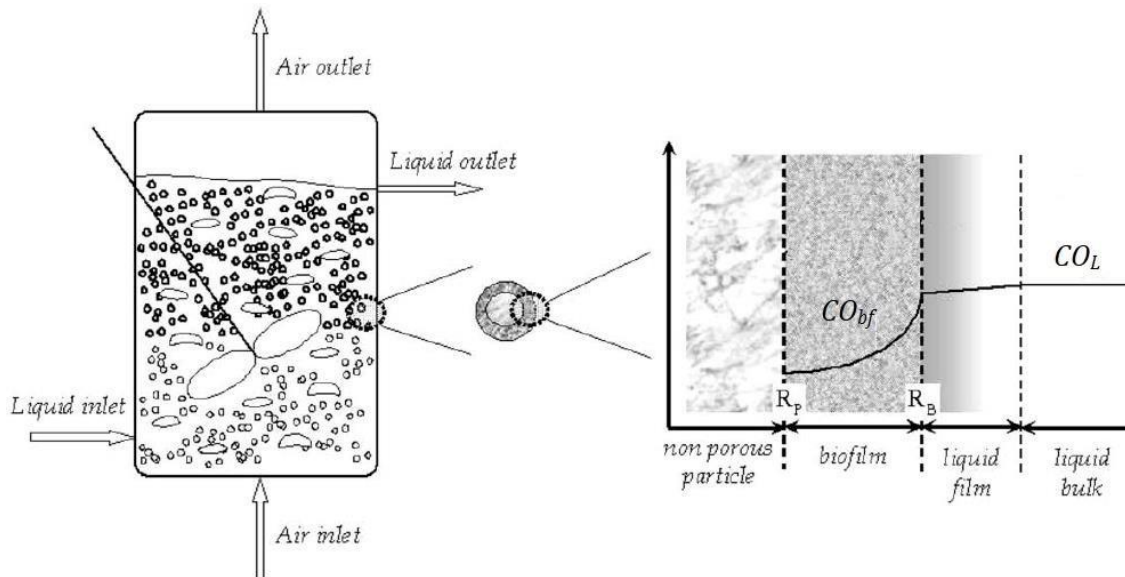


Figure 4.6: Outline of a uniformly mixed three-phase reactor (Olivieri et al., 2011). The qualitative radial profiles of substrate concentration close to and within the bioparticles are represented in the diagram inset (after Olivieri et al., 2011).

The inset of Figure 4.6 highlights the diffusional patterns in the proximity of each biofilm-covered carrier particle: the biofilm uniformly covers a spherical impervious carrier and a thin diffusion limited liquid film establishes around the biofilm. The CO diffuses from the liquid bulk toward and within the biofilm where it is converted. The biofilm thickness and the mass transfer of substrates across the biofilm depend on structure and density. In turn, these features depend on the dynamic equilibrium among cell adhesion, biofilm growth, and detachment (Russo et al., 2008).

To capture the general features of the static/dynamic behavior of the biofilm reactor under investigation, it was assumed that a uniform biofilm is established around each carrier particle. Accordingly, the variability of the biofilm properties with the biofilm's age, its spatial location within the reactor and the conditions prevailing locally (mechanical stresses, substrate availability/depletion, interaction with suspended cells etc.) were not considered.

Assumptions

The main assumptions made to assess the model parameters are reported hereinafter.

The chemical species are: carbon monoxide (CO), carbon dioxide (CO₂), acetic (AA) and butyric acid (BA), ethanol (E), butanol (B) and biomass (X). CO and CO₂ are present in all the phases. The other listed species are present in the biofilm phase and in the liquid phase. The biomass is indicated as: X_L is the concentration in the liquid phase, X_{bf} is the concentration in the biofilm phase (this value was assumed constant), \bar{X} is the concentration of biomass cells in the entire volume of reaction (see eq. 4.13).

The reactor is assumed to have a height/diameter ratio of 2 and an impeller diameter equal to the 40% of the reactor diameter, a standard geometry for most bioreactors.

The system is assumed isothermal (33°C) and at constant pH (5.75).

The liquid phase is well mixed. The gas phase is well mixed. The solid phase is uniformly distributed in the liquid phase.

The liquid phase is the culture medium

Two gaseous species are considered: CO and CO₂. The gas stream feeding to the reactor is pure CO. The gas behaviour is assumed as ideal. In such phase, there are not metabolites or water because their volatilities have been neglected.

The solid phase is the biofilm-carrier particles. A thin layer of aggregated cells uniformly wraps a solid spherical carrier, radius $R_S = 150 \mu\text{m}$ within the range of typical carriers adopted in biofilm reactor. The biofilm is assumed to form a spherical shell of external radius R_{bf} (inset of Figure 4.6) of uniform thickness and cell density (X_{bf}). Typically, this value spans between 20 and 100 g/L, and 50 g/L has been assumed as a representative value (Bishop et al., 1995). The filling rate of the reactor with support carrier (ε) was assumed 0.1.

The biofilm-carrier particles are uniformly distributed in the liquid phase. During the process, the thickness of the biofilm may increase by the cell replication and by the attachment of free cells from the liquid phase. On the contrary, cells can detach from the biomass layer and the layer thickness decrease.

Kinetics and growth models

C. carboxidivorans and other acetogens assimilate CO, H₂ and CO₂ through the Wood-Ljungdahl pathway, to produce acetyl - CoA, which is then transformed into biomass and products (Dürre and Eikmanns, 2015). The complex metabolism, involving gas fixation, cell growth and production of metabolites, has been described by a set of reactions under the hypothesis that carbon monoxide is the only limiting nutrient, and that all other substrates are supplied by the culture medium. A kinetic unstructured/unsegregated model has been applied (Younesi et al., 2005).

Five overall biochemical reactions have been considered: biomass growth associated with metabolite production (s1), carboxylic acid conversion into alcohols (s2, s3) and production of alcohols non-growth associated (s4, s5).

The cells growth has been described by the Haldane kinetic model (Mohammadi et al., 2014). The model takes into account both substrate and product inhibition to

cover a greater generality of the results. Solvent production is also associated to the cell's growth, according to eq. s1 reported in Table 4.1.

The biochemical conversion of CO are reported in Table 4.1. The model of cell growth kinetics and metabolites production have been reported in Table 4.11. The reported kinetic models have been assumed for both suspended and immobilized cells, provided that the local value of concentration of CO and metabolites are considered.

Table 4.11. Kinetic models of the biochemical reactions reported in Table 4.1.

$$\mu = \frac{\mu_M CO_L}{(CO_L + K_M + \frac{CO_L^2}{K_I})} \cdot \left(1 - \frac{A_{TOT}}{A_{MAX}}\right)^{\alpha'} \left(1 - \frac{S_{TOT}}{S_{MAX}}\right)^{\alpha''} \quad (k4.1)$$

$$r_{ET}^{AA} = \frac{r_{MAX}^E \cdot CO_L}{(CO_L + K_{ET})} \cdot \frac{AA}{AA + K_{AA}} \quad (k4.2)$$

$$r_{BU}^{AB} = \frac{r_{MAX}^B \cdot CO_L}{(CO_L + K_{BU})} \cdot \frac{BA}{BA + K_{AB}} \quad (k4.3)$$

$$rd_E = \beta_{E/X} \cdot \left(1 - \frac{E}{E_{MAX}}\right) \quad (k4.4)$$

$$rd_B = \beta_{B/X} \cdot \left(1 - \frac{B}{B_{MAX}}\right) \quad (k4.5)$$

The attachment and detachment rate of free cells to/from the biofilm are described by eq.s 4.9 e 4.10. Both models are assumed linear in free/biofilm cell concentration, where K_A and K_D are the specific rate of adhesion/detachment per unit of liquid volume. (Horn et al., 2003; Gjaltema et al., 1997 a & b). To authors knowledge, no study are available in the literature regarding the dynamic of *C. carboxidivorans* biofilm. The values assigned to K_A and K_D are respectively 0.04 and 0.03 h⁻¹

$$r_{att} = K_A X_L \quad (4.13)$$

$$r_{det} = K_D \frac{\varepsilon V_L}{V_P} X_{bf} \frac{4\pi}{3} (R_{bf}^3 - R_s^3) \quad (4.14)$$

The substrate conversion and product formation throughout the biofilm are not uniform as a consequence of the radial profile of chemical species. The average value over the biofilm depth of the cell growth rate and of the metabolite production rates have been assessed. The integration of the eq.s k4.1 through k4.5 assuming constant value

over a spherical shell domain (Olivieri et al., 2011) provides the biofilm-averaged rates assessed as eq. k4.6 through 4.10.

$$\bar{\mu} = X_{bf} \frac{\varepsilon V_L}{V_P} 4\pi \int_{R_P}^{R_{bf}} \frac{\mu_M CO_L}{(CO_L + K_M + \frac{CO_{bf}^2}{K_I})} \cdot \left(1 - \frac{AA_{BF} + BA_{BF}}{A_{MAX}}\right)^\alpha \left(1 - \frac{E_{BF} + B_{BF}}{S_{MAX}}\right)^{\alpha'} r^2 \cdot dr \quad (k4.6)$$

$$\overline{r_{ET}^{AA}} = X_{bf} \frac{\varepsilon V_L}{V_P} 4\pi \int_{R_S}^{R_{bf}} \frac{r_{MAX}^E \cdot CO_{bf}}{(CO_{bf} + K_{ET})} \cdot \frac{AA_{bf}}{AA_{bf} + K_{AA}} \cdot r^2 dr \quad (k4.7)$$

$$\overline{r_{BU}^{AB}} = X_{bf} \frac{\varepsilon V_L}{V_P} 4\pi \int_{R_S}^{R_{bf}} \frac{r_{MAX}^B \cdot CO_{bf}}{(CO_{bf} + K_{BU})} \cdot \frac{AB_{bf}}{AB_{bf} + K_{AB}} \cdot r^2 dr \quad (k4.8)$$

$$\overline{rd_E} = X_{bf} \frac{\varepsilon V_L}{V_P} 4\pi \int_{R_S}^{R_{bf}} \beta_{E/X} \cdot \left(1 - \frac{E}{E_{MAX}}\right) \cdot r^2 dr \quad (k4.9)$$

$$\overline{rd_B} = X_{bf} \frac{\varepsilon V_L}{V_P} 4\pi \int_{R_S}^{R_{bf}} \beta_{B/X} \cdot \left(1 - \frac{B}{B_{MAX}}\right) \cdot r^2 dr \quad (k4.10)$$

The biofilm-averaged rates are present in the mass balances extended to the liquid phase as terms of mass flux exchange from/to biofilm to/from liquid phase.

The overall CO conversion rate (r_{CO}) and the overall CO₂ production rate (r_{CO_2}) have also been provided as eq.s 4.11 and 4.12.

$$r_{CO} = \left(\frac{\mu}{Y_{X/CO}} + Y_{CO/E} r_{ET}^{AA} + Y_{CO/B} r_{BU}^{AB} \right) \quad (4.15)$$

$$r_{CO_2} = + (Y_{CO_2/X} \mu + Y_{CO_2/E} r_{ET}^{AA} + Y_{CO_2/B} r_{BU}^{AB} + Y'_{CO_2/E} r d_E + Y'_{CO_2/B} r d_B) \quad (4.16)$$

Mass balances

The model is based on mass balances referred to carbon monoxide (CO), carbon dioxide (CO₂), suspended cells (X_L), attached cells (quantified by the biofilm radius R_{bf}), acids - acetic (AA) and butyric (BA) - and solvents - ethanol (E) and butanol (B) - coupled with the constitutive and kinetic equations. Two sets of equations may be identified: the first set regards the mass balance extended to the homogenous liquid (volume V_L) and gas phases; the second set refers to the biofilm phase. The two sub-models are linked each other through the diffusive flux of substrates at the biofilm boundary (Olivieri et al., 2011).

The mass balances reported in Table 4.12 - eq.s (mb1) and (mb2) – are extended to the gas phase and include the accumulation term, the net convective flows in and out, and the mass transfer from the gas-liquid interface.

The mass balances reported in Table 4.13 - eq.s (mb3) - (mb9) – are extended to the liquid phase and include the accumulation term, the net convective flows in and out, the conversion by suspended cells and the flow from/to the biofilm.

The mass balance for suspended cells (mb3) includes the accumulation in the liquid phase, the net convective flows, the detachment of the biofilm debris, the adhesion of suspended cells, and the cell growth term.

Table 4.12. Gas phase mass balances.		
CO	$V_G \frac{dCO_G}{dt} = \frac{Q_{in} \cdot P}{T \cdot R} - Q_{out}CO_G - V_L k_{LCO}(CO^* - CO_L)$	mb1
CO ₂	$V_G \frac{dCO_{2G}}{dt} = -Q_{out}CO_{2G} + k_{LCO_2} V_L (CO_{2L} - CO_2^*)$	mb2

Equation mb8 is the mass balance referred to the CO and takes into account the accumulation in the liquid phase, the net convective flows, the gas–liquid mass transfer, and the conversion by suspended cells and biofilm cells.

The biofilm-cell contribution to CO conversion takes into account the diffusion-reaction feature of the biofilm and embodies the solids volumetric fraction (ε) in the reactor. In agreement with a diffusion-reaction model in spherical coordinates, the mass balances for the investigated species in the biofilm phase are the Eq.s in Table 4.14.a. Each equation refers to a spherical biofilm shell and takes into account the accumulation in the biofilm phase, the diffusion flux, and the conversion by biofilm cells. The system presented for biofilm phase is constituted by partial differential equations (PDE) and it requires an adequate approach to be solved.

To assess the overall concentration of cells in the reactor, and the real contribute of the biofilm, \bar{X}_f has been defined in Eq. 4.13. It is the mass of biofilm in the whole reactor. The comparison between \bar{X}_f and X_L provides the specific contribution of the two cell phases, free and immobilized.

$$X_{bf} = \frac{\left(\frac{4}{3}\pi R_{bf}^3 - \frac{4}{3}\pi R_s^3\right) \cdot \left(\frac{\varepsilon V_L}{V_P}\right) \cdot X_{bf}}{V_L} \quad (4.17)$$

The production of the “i” soluble species has been assessed as the product between the liquid flow and the concentration of “i”:

$$P_i = Q_L \cdot C_i \quad (4.18)$$

The ratio between P_i and the liquid volume yields the specific productivity per unit of time and volume. The productivity of the soluble “i” species is:

$$p_i = \frac{P_i}{V_L} = \frac{Q_L \cdot C_i}{V_L} = C_i \cdot D \quad (4.19)$$

Table 4.13. Liquid phase mass balances.

Biomass	$\frac{dX_L}{dt} = (\mu - K_A) \cdot X_L + K_D \frac{4\pi}{3} (R_{bf}^3 - R_s^3) X_{bf} \frac{\varepsilon}{V_P} - \left(\frac{Q_L}{V_L}\right) X_L$	mb3
Ac. Acid	$\frac{dAA}{dt} = (Y_{AA/X} \cdot \mu - Y_{AA/E} \cdot r_{ET}^{AA}) \cdot X_L + (Y_{BA/X} \cdot \frac{\bar{\mu}}{V_L} - Y_{AA/E} \cdot \frac{r_{ET}^{AA}}{V_L}) - \left(\frac{Q_L}{V_L}\right) AA$	mb4
But. acid	$\frac{dBA}{dt} = (Y_{BA/X} \cdot \mu - Y_{BA/B} \cdot r_{BU}^{AB}) \cdot X_L + (Y_{BA/X} \cdot \frac{\bar{\mu}}{V_L} - Y_{BA/B} \cdot \frac{r_{BU}^{AB}}{V_L}) - \left(\frac{Q_L}{V_L}\right) BA$	mb5
Ethanol	$\frac{dE}{dt} = (Y_{E/X} \cdot \mu + r_{ET}^{AA} + r_{E}^{d}) \cdot X_L + (Y_{E/X} \cdot \mu + r_{ET}^{AA} + r_{E}^{d}) \frac{1}{V_L} - \left(\frac{Q_L}{V_L}\right) E$	mb6
Butanol	$\frac{dB}{dt} = (Y_{B/X} \cdot \mu + r_{BU}^{AB} + r_{B}^{d}) \cdot X_L + (Y_{B/X} \cdot \mu + r_{BU}^{AB} + r_{B}^{d}) \frac{1}{V_L} - \left(\frac{Q_L}{V_L}\right) B$	mb7
CO	$\frac{dCO_L}{dt} = k_{LCO} (CO^* - CO_L) - r_{CO} X_L - \left(\frac{r_{CO}}{V_L}\right) - \left(\frac{Q_L}{V_L}\right) CO_L$	mb8
CO ₂	$\frac{dCO_{2L}}{dt} = -k_{LCO_2} (CO_{2L} - CO_2^*) + r_{CO_2} X_L + \left(\frac{r_{CO_2}}{V_L}\right) - \left(\frac{Q_L}{V_L}\right) CO_{2L}$	mb9

Computational methods

The dynamic fermentation model described by the system of ODEs and PDEs equations (Tables 4.12, 4.13, 4.14), along with the constitutive equations, is a nonlinear algebraic-differential system which demands a specific study to be solved properly. Moreover, the problem can be considered “stiff” because it involves different chemical/physical phenomena that occur on different temporal scale, from the solubilization of the gaseous substrate to the molecular diffusion in the biofilm layer and the cell growth. Therefore, as a first approximation, the system has been solved without the contribute of the biofilm, for a double reason: first, resolving the full system in transitory conditions would be computationally very expensive and it requires first trial values for all the concentrations involved (to be obtained by the integration of the simplified system); second, data obtained in the simplified study have been useful for a comparison to state the impact that a biofilm reactor may have on the syngas fermentation process. The reason why the complete system must be resolved with a numerical method, that requires starting conditions is that biofilm thickness, represented by the variable R_{bf} , is a function of the environmental conditions and it is not known in

advance, but a starting value is strictly required to fix the extremes of integration. Through an iterative calculation procedure, the system under steady state conditions has been studied until a convergence value of the biofilm radius has been obtained. Finally, the dynamic evolution of the fermentation process has been analysed by studying the transitory regime.

Table 4.14.a. Biofilm phase mass balances

Biomass	$\frac{\varepsilon V_L}{V_P} \frac{d}{dt} \left(\frac{4\pi}{3} (R_{bf}^3 - R_s^3) \right) X_{bf} = -K_D X_{bf} \frac{4\pi}{3} (R_{bf}^3 - R_s^3) \frac{\varepsilon V_L}{V_P} + K_A X_L V_L + \bar{\mu}$	b1
CO	$\frac{\partial CO_{bf}}{\partial t} = \frac{1}{r^2} \frac{\partial}{\partial r} \left(\frac{\partial CO_{bf}}{\partial r} \cdot r^2 D_{bf}^{CO} \right) - r_{CO} \cdot X_{bf}$	b2
CO ₂	$\frac{\partial CO_{2bf}}{\partial t} = \frac{1}{r^2} \frac{\partial}{\partial r} \left(\frac{\partial CO_{2bf}}{\partial r} \cdot r^2 D_{bf}^{CO_2} \right) + r_{CO_2} X_{bf}$	b3
Ac. acid	$\frac{\partial AA_{bf}}{\partial t} = \frac{1}{r^2} \frac{\partial}{\partial r} \left(\frac{\partial AA_{bf}}{\partial r} \cdot r^2 D_{bf}^{AA} \right) + (Y_{AA/X} \cdot \mu - Y_{AA/E} \cdot r_{ET}^{AA}) X_{bf}$	b4
But. acid	$\frac{\partial BA_{bf}}{\partial t} = \frac{1}{r^2} \frac{\partial}{\partial r} \left(\frac{\partial BA_{bf}}{\partial r} \cdot r^2 D_{bf}^{BA} \right) + (Y_{BA/X} \cdot \mu - Y_{BA/B} \cdot r_{BU}^{AB}) X_{bf}$	b5
Ethanol	$\frac{\partial E_{bf}}{\partial t} = \frac{1}{r^2} \frac{\partial}{\partial r} \left(\frac{\partial E_{bf}}{\partial r} \cdot r^2 D_{bf}^E \right) + (Y_{ET/X} \cdot \mu + r_{ET}^{AA} + r d_E) X_{bf}$	b6
Butanol	$\frac{\partial B_{bf}}{\partial t} = \frac{1}{r^2} \frac{\partial}{\partial r} \left(\frac{\partial B_{bf}}{\partial r} \cdot r^2 D_{bf}^B \right) + (Y_{ET/X} \cdot \mu + r_{BU}^{AB} + r d_B) X_{bf}$	b7

To solve the PDEs equations in MATLAB environment, the biofilm layer thickness has been discretized in a number of intervals and the equations have been valued at the extremes of these intervals. First and second derivatives have been discretized through the Finite Differences Method (FDM) with a second order centered scheme. Such decision has been taken considering the minor computational times, compared with a finer approximation, and the weak number of elements in the discretization. Ordinary differential equations have been solved with the “ode15s” variable-order method, from MATLAB® library.

The equations b2-b7 need boundary conditions to be solved (table 4.14.b). In particular: i) at the biofilm-liquid interface, equality of concentrations has been set; ii) at the surface of the non-porous biofilm carrier, the boundary condition has been expressed as absence of diffusive flux.

Table 4.14.b. Boundary conditions.

	Biofilm-liquid surface $r = R_{bf}$	Biofilm carrier surface $r = R_s$
CO	$CO_{bf} = CO_L$	$\frac{\partial CO_{bf}}{\partial r} = 0$
CO ₂	$CO_{2bf} = CO_{2L}$	$\frac{\partial CO_{2bf}}{\partial r} = 0$
Ac. Acid	$AA_{bf} = AA_L$	$\frac{\partial AA_{bf}}{\partial r} = 0$
But. Acid	$BA_{bf} = BA_L$	$\frac{\partial BA_{bf}}{\partial r} = 0$
Ethanol	$E_{bf} = E_L$	$\frac{\partial E_{bf}}{\partial r} = 0$
Butanol	$B_{bf} = B_L$	$\frac{\partial B_{bf}}{\partial r} = 0$

Results and discussion

Biofilm-free system

The set of ordinary differential non-linear equations related to gas-liquid phases - eq.s mb1 through mb9 - has been solved to assess the effect of the liquid flow rate Q_L . The kinetic parameters reported in Table 4.4 have been set.

Figure 4.7 reports a series of plots of the microbial concentration as a function of the fermentation time. As expected, each curve approaches a steady state value depending: the time to reach the steady state value and the asymptotic value depend on Q_L . The cyan solid-line in the Figure 4.7 - $D=0.0417$ L/h – points out that the reactor is operated under wash out conditions. The wash-out is a very common issue that needs to be handled in biological reactor systems and it happens when the dilution rate ($D =$ ratio between liquid flow and liquid volume) is larger than the duplication rate of the microorganism. One of the most common strategies to overcome this limitation is to confine the cells inside of the reactor vessel, and a way to achieve this goal is a biofilm reactor. The D assessed as wash-out onset has been **0.0375 h^{-1}** , under the operating conditions assumed. It is worth to note that the assessed D of wash-out is smaller than the specific growth rate assessed in the best growth conditions ($CO_L = CQ_L^{opt}$ and $A_{TOT} = S_{TOT} = 0$) where $\mu = 0.07 \text{ h}^{-1}$. A discussion about this issue is reported in Appendix A.

The undershoot behaviour observed during the fermentation for the Q_L lower than 0.03875 L/h is due to the absence of metabolites (acids and solvents) at the beginning of the test. The gradual increase of the metabolites decreases the cell growth rate and the cell concentration approach the steady state.

Data regarding the productivity of cells and alcohols are reported in Figure 4.8 as a function of the dilution rate. The three reported species are characterized by a maximum. The dilution rate at which the maximum has been found depends on the species: solvent productivity is maximized at $D= 0.02 \text{ h}^{-1}$; cell productivity is maximized at $D = 0.034 \text{ h}^{-1}$. As expected, the maximum of the cell productivity is at D close to the wash-out threshold.

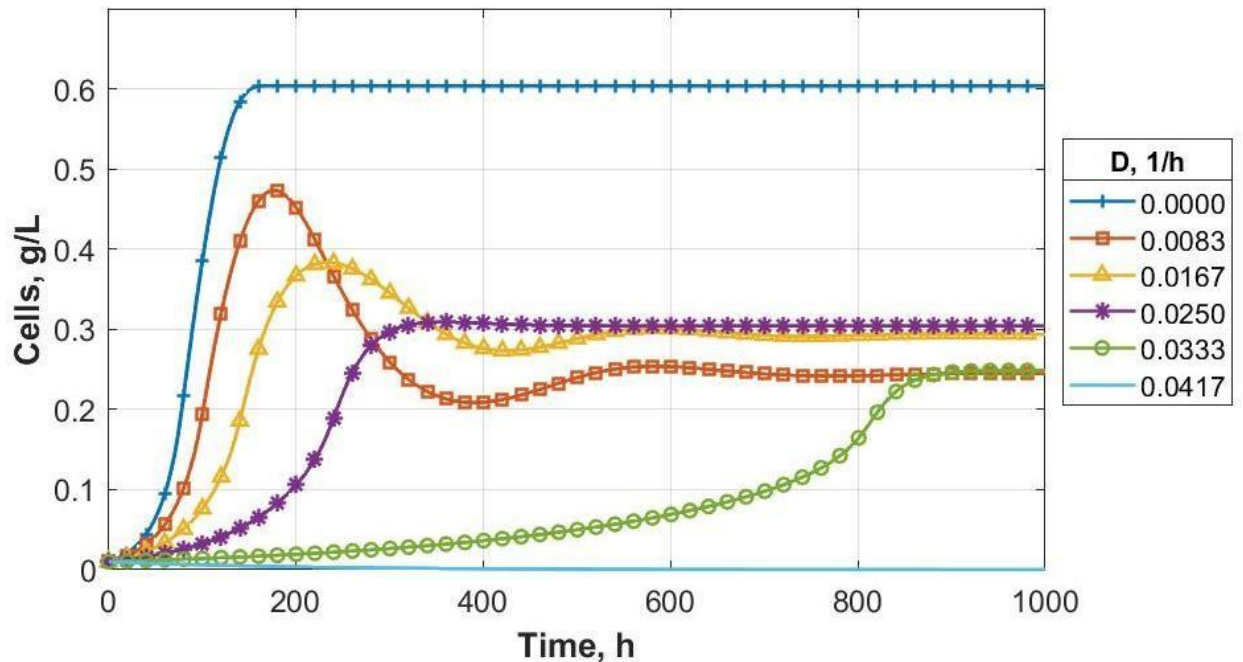


Figure 4.7: Time resolved concentration of cells assessed at different values of Dilution rate (h^{-1}).

Study of the steady state in biofilm layer

The simulation of the biofilm reactor (considering mass balances in gas, liquid and biofilm phase) has been carried out under steady state conditions. Data obtained from the simulation of the free-cell fermenter /see previous section) have been assumed as starting point of the numerical simulation. The carrier radius has been set at $R_s = 150 \mu\text{m}$. The biofilm thickness has been set at $10 \mu\text{m}$, $R_{bf} = 160 \mu\text{m}$ as starting value. As R_{bf} figures both in the condition boundary and in the equations, an iterative calculation was performed, until reaching convergence values. The biofilm cell density X_{bf} has been set at 20 g/L .

The biofilm layer has been discretized in N points. The concentration of each specie has been calculated discretizing the space between R_{bf} and R_s in $N - 1$ regular intervals. The accuracy of the discretization has been checked by comparing the simulations carried out at increasing N from 20 to 70. The minimum discretization path has been set at the N characterized by the relative error - with respect to the results obtained at the lower N - lower than 1%.

The parameter Q_L plays a key role in the dynamic equilibrium, and its effect has been investigated.

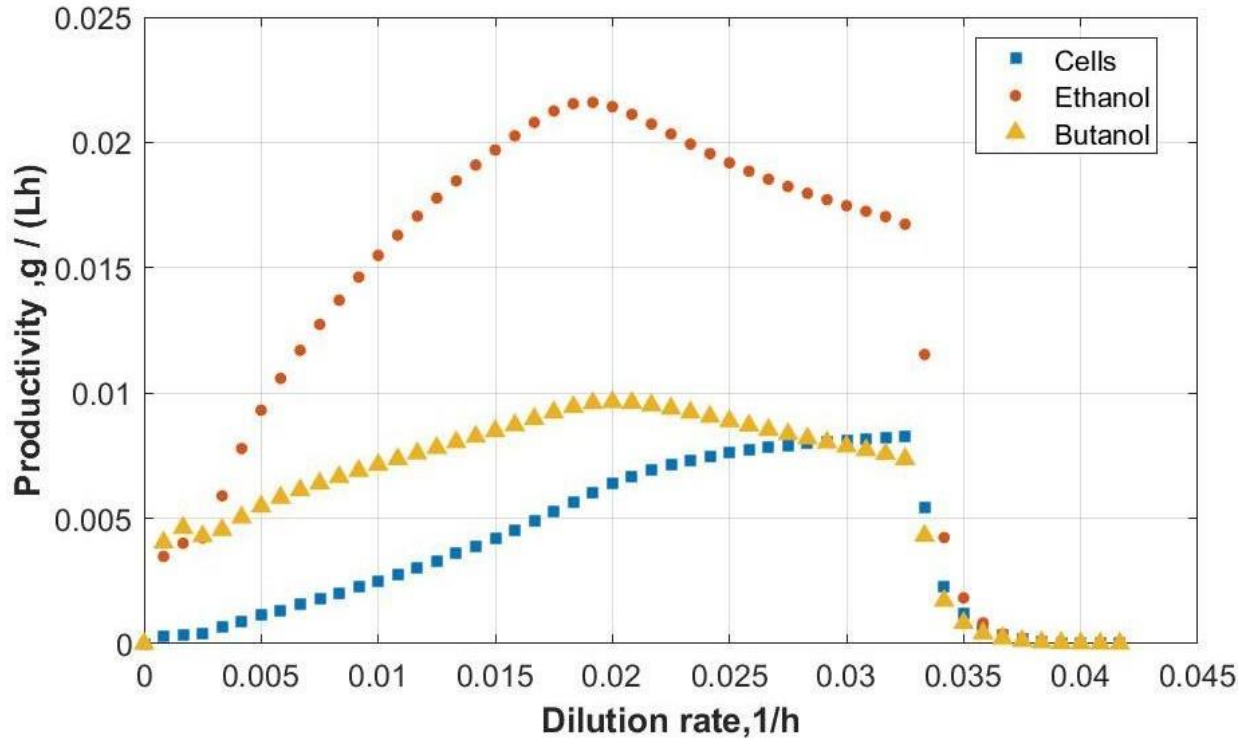


Figure 4.8: Cell and solvents productivity vs. dilution rate

Figure 4.9 reports the concentration profiles of all the species in the biofilm calculated at liquid flow rate set at 0.024 L/h ($D=0.02$ 1/h). The radial coordinate - on the x axis - is reported in dimensionless form: 0 is $r = R_s$ and 1 is $R = R_{bf}$. The profile shape is consistent with the penetration theory and the expectations. The boundary conditions are always respected. The concentration span throughout the biofilm thickness - difference between the concentration at the carrier surface and the bulk value - is quite small, as can be observed by the scale of the y axis. The largest span is in the CO concentration: from 0.00225 to 0.0024 g/L. Although the CO concentration span is about 10% of the concentration at the biofilm surface, it is worth to note that the CO concentration at the biofilm surface is already very low – 10% - with respect to the CO saturation concentration under the investigated conditions (0.023 g/L).

The steady state thickness of the biofilm layer was about 14 μm of thickness, the biofilm external radius $R_{bf}= 164 \mu\text{m}$.

Table 4.15 reports a comparison of the steady state fermentation picture under the same operating conditions with and without biofilm. Data reported for the condition without biofilm refer to steady state values approached after long time, typically 1000 hours. The last column of the table reports the increment of the concentration with respect to the no-biofilm condition. As expected, data point out that the presence of the biofilm leads to: i) a decrement of CO concentration (larger conversion); ii) an increment of the products of the fermentation (cell and metabolites). The butanol concentration quite doubles with respect to that assessed during the free cell fermentation. The cell concentration increase is probably due to the production by the biofilm.

Transient regime

The study of the transient regime of the system has been carried out under a key approximation: the concentration profile inside the biofilm has been assumed constant and equal to that at the biofilm interface with the liquid. This approximation has provided a very strong reduction of the computational burden, and it has been required to solve the mathematical model with MATLAB® library. Without the proposed approximation an *ad-hoc* code would be required. The initial conditions set for the transient simulation are: absence of CO in liquid phase; no biofilm (biofilm radius equals to the carrier radius); inoculum $X_L = 0.05$ g/L.

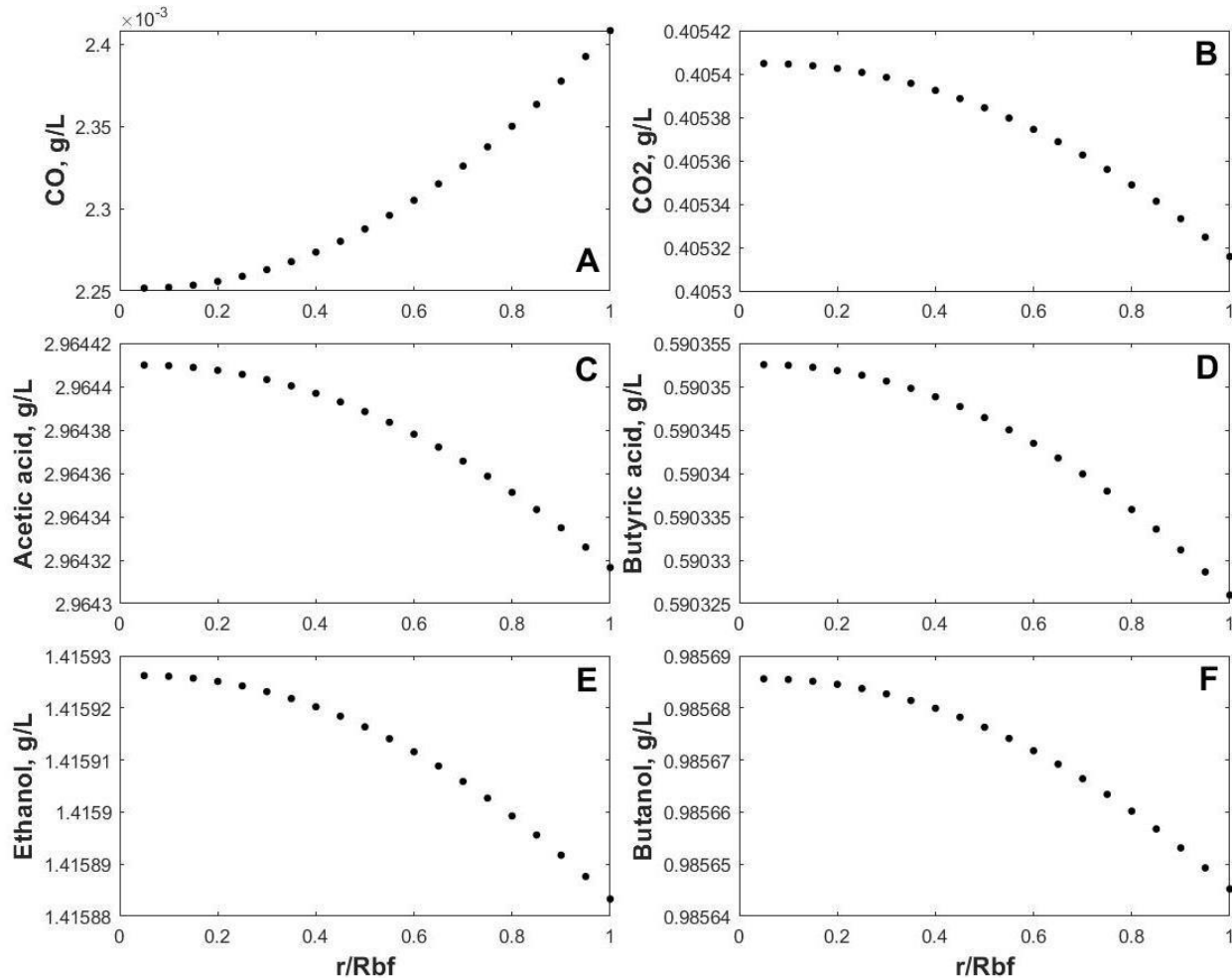


Figure 4.9. Simulated radial profiles of CO (A), CO₂ (B), acetic acid (C), butyric acid (D), ethanol (E) and butanol (F) in of the biofilm layer. Carrier radius= 150 μm ; $D = 0.02$ h⁻¹. The biofilm thickness was = 14 μm .

Figure 4.10 reports the plots of the transitory simulations expressed in terms of concentration of dissolved CO, free cells, metabolites, and biofilm thickness. The dissolved CO concentration (4.10A) approaches steady state conditions in about 50 hours after an underdamped behaviour. It should be noted that a time zoom has been set for Figure 4.10A to highlight the start-up dynamics. The time-resolved profile of the

CO concentration points out a fast increase due to the mass transfer from the gas phase, then a progressive decline as the bioconversion starts to be significant. The CO concentration reduces fast as the biofilm builds-up and approaches the steady state condition, less than 0.005 g/L of CO dissolved, about the 22% of the saturation level. Biofilm and free cells growth are characterized by a time-sigmoid profile as a mirror of the CO-dissolved time-resolved profile. The time-resolved concentration profiles of the metabolites are as expected too. Acetic and butyric acids are massively produced during the first 100 h, then a slight reduction is observed as a result of the conversion path (s2, s3), whose kinetics are function of the acid concentrations.

Table 4.15. Steady state concentration approached by the species for fermentation carried out with and without biofilm. Data are expressed in g/L.

Variable	Without Biofilm	With Biofilm	Difference, %
CO _G	0.0319	0.0257	-19.4357
CO _{2G}	0.0079	0.0141	78.48101
CO _L	0.0094	0.0024	-74.4681
CO _{2L}	0.2274	0.4053	78.23219
X _L	0.3010	0.3491	15.98007
Acetic acid	2.463	2.9643	20.35323
Butyric acid	0.5074	0.5903	16.33819
Ethanol	1.2485	1.4159	13.40809
Butanol	0.5321	0.9856	85.22834

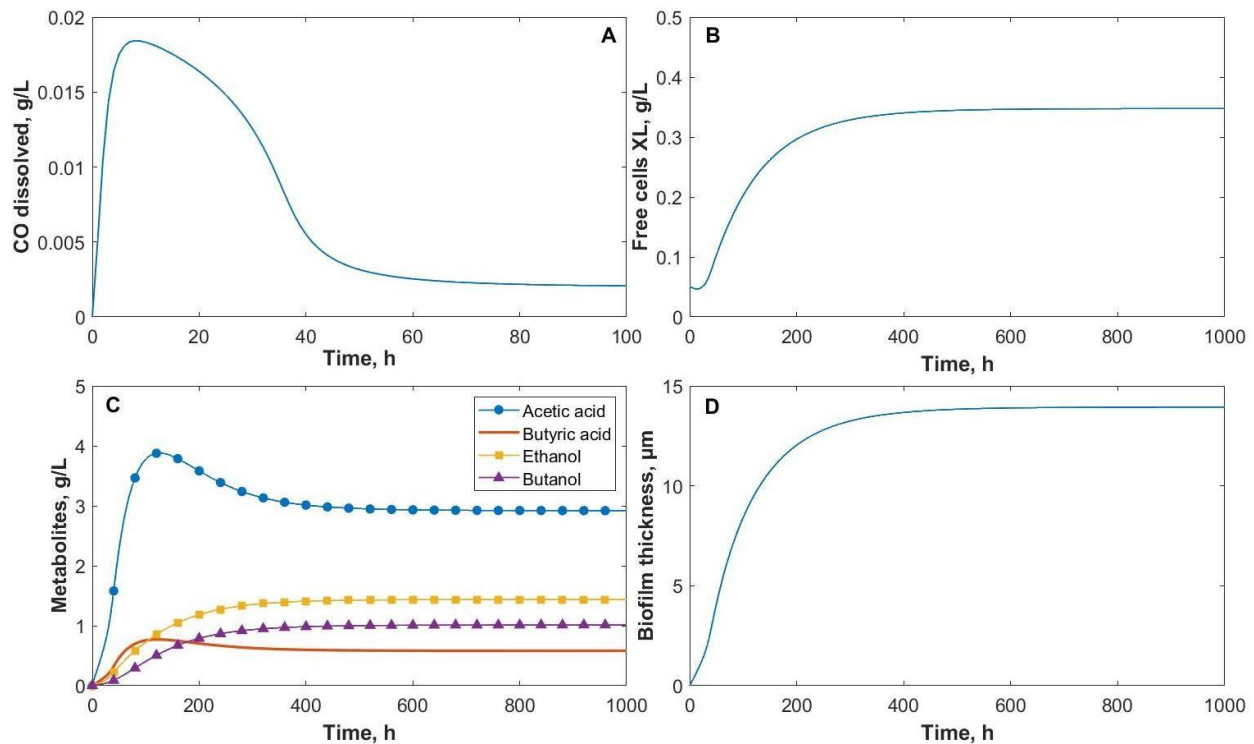


Figure 4.10: Results of the transient simulation of the concentration of dissolved CO (A), free cells (B), metabolites (C) and biofilm thickness (D). Operating conditions reported in Figure 4.9, except biofilm thickness (0 μm). Temporary scale on A was zoomed to highlight the dynamic evolution.

The soundness of the simplified hypothesis reported at the beginning of this section has been proved by comparing the steady state fermentation performances - expressed in terms of substrate and metabolites concentration as well as biofilm thickness – of simulations carried out under initial pre-set of biofilm and initial absence of biofilm. The effect of such approximation has been reported in Table 4.16. The last column of the table reports the increment of the concentration when concentration in the biofilm has been constant for all the species. The analysis of data report in the table points out that:

- the effect of the pre-established biofilm is negligible under operating conditions simulated and for kinetic parameters set;
- CO is the specie most affected by the assumption. In agreement with the radial profiles reported in the previous section, the substrate is the specie characterized by a steeper change in the biofilm;
- Butanol is the metabolite mainly affected by the assumption even though the variation is negligible. A slight increment of the concentration (about 3%) is assessed under iso-concentration biofilm conditions;
- Effect on ethanol concentration is still more negligible (about 1.5%) than butanol;
- The biofilm thickness does not remarkably change as a consequence of the different initial conditions. This result support the soundness of the model with respect to the biofilm dynamic. It is worth to note the biofilm forms a quite thin layer (about 14 μm). It may be the result of the parameters set for the attachment/detachment cell rate. The role of this parameters has been further investigated and results are reported in the “Effect of detachment rate” section.

Table 4.16. Asymptotic concentration of the substrate and metabolites. Data refer to initial conditions with initial absence of biofilm (developed under iso-concentration conditions) and pre-established initial biofilm. Concentration data are expressed in g/L.

Variable	No initial biofilm	Pre-established biofilm	Difference, %
CO _G	0.0255	0.0257	-0.56
CO _{2G}	0.0143	0.0141	1.41
CO _L	0.0023	0.0024	-3.31
CO _{2L}	0.4102	0.4053	1.21
X _L	0.3474	0.3491	-0.48
Acetic acid	2.920	2.9643	-1.50
Butyric acid	0.5821	0.5903	-1.39
Ethanol	1.4375	1.4159	1.52
Butanol	1.0123	0.9856	2.71
R _{bf} (μm)	164.0	163.9	0.03

Effect of the liquid flow rate

The presence of the biofilm has already pointed out the enhancement of the fermentation performance: increase of the concentration of metabolites and of the microbial concentration. The many advantage, as expected, has been the possibility to operate the fermenter at high liquid flow to increase the productivity. A set of simulations has been carried out to investigate the assess the fermentation performance at liquid

flow rate larger than the washout threshold. The washout flow rate threshold has been assessed to be about 0.05 L/h for the liquid reaction volume of 1.2 L, dilution rate 0.417 h⁻¹.

The effect of the liquid flow rate, Q_L , has been assessed in terms of final concentration and productivity of ethanol and butanol, and in terms of concentration of free and immobilized cells. Simulations have been carried out under the assumption reported in the previous section to reduce the computational time.

Figure 4.11 reports the plots of the time-resolved concentration of the soluble gases – substrate CO and metabolite CO₂ - both gas and liquid phases at different liquid flow rates. The plots are consisting with the theoretical background. They point out: i) how fast the mass transfer between liquid and gas phases acts; ii) gas-liquid phases are always under equilibrium conditions. The maximum value of dissolved CO established in very short time of the fermentation, when the microbial population was still under exponential growth phase. As expected, the final value of equilibrium is a function of the dilution rate. Indeed, the increase of Q_L : i) decreases product concentrations; ii) CO profile, its trend is opposite, as it gets consumed, and the limit value of 0.0395 mol/L represents the concentration of the gas inlet, in accordance with the equation of state of ideal gases.

It is worth to note that CO₂ does not play a key role in the proposed model because it cannot be assimilated without an electron source (like H₂). The fate of the CO₂ is relevant to assess the environmental impact of the process. This assessment requires a more global study of the process, the renewable material exploitation included.

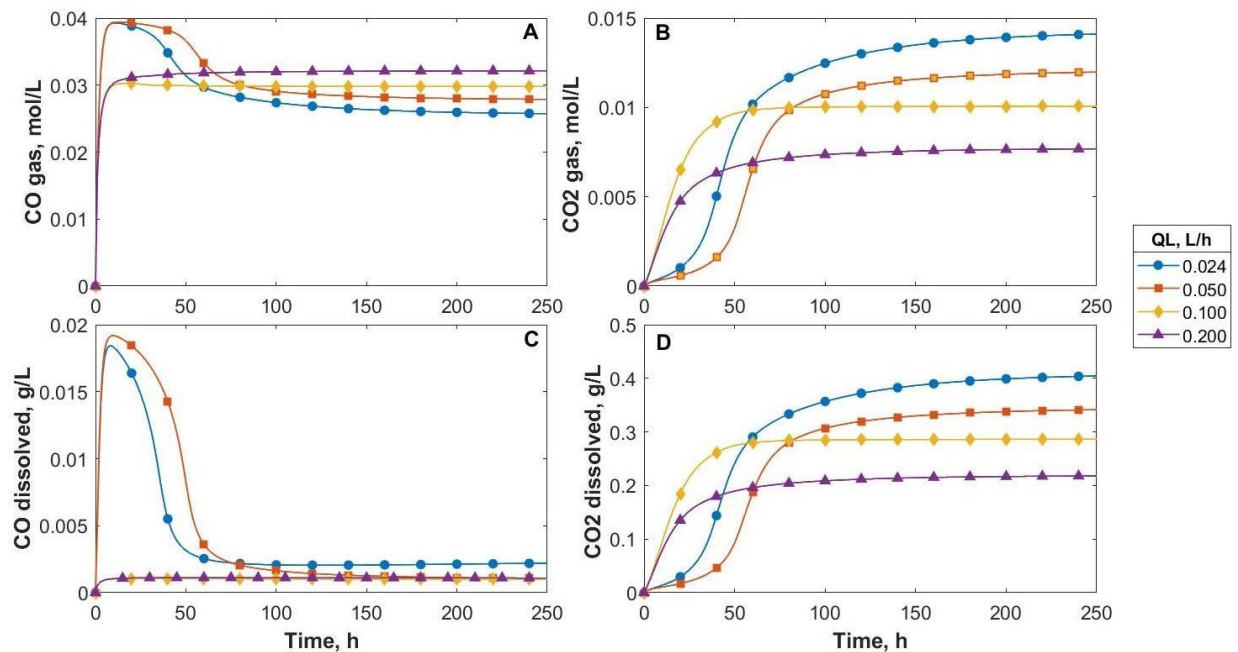


Figure 4.11: Time-resolved concentration CO and CO₂ at different Q_L .

The effect of Q_L on the final asymptotic concentration of the liquid soluble metabolites reproduces the dynamic of CO₂. The increase of the dilution rate –

decreases of the residence time - has a negative effect on the final metabolite concentrations. It is worth to note that the time-resolved concentration of acetic and butyric acids has been characterized by a slight peak at dilution rate smaller than the wash-out threshold. The production rate of the acids has been faster than convective flow out couple with re-assimilation rate to produce solvents and accumulation of acids occurred.

The productivity of ethanol and butanol has been calculated according to eq. (4.15) and reported in Figure 4.13 as a function of the liquid flow rate, Q_L , at different value of the gas flow rate. The analysis of the Figure points out that:

- the productivity of ethanol is always larger than that of butanol;
- the productivity of a solvent vs. the liquid flow rate is characterized by maximum and approach a constant value as Q_L increases;
- the productivity of a solvent increases with the Q_G . The maximum of the productivity vs. Q_L increases and moves at high Q_L as the Q_G increases.

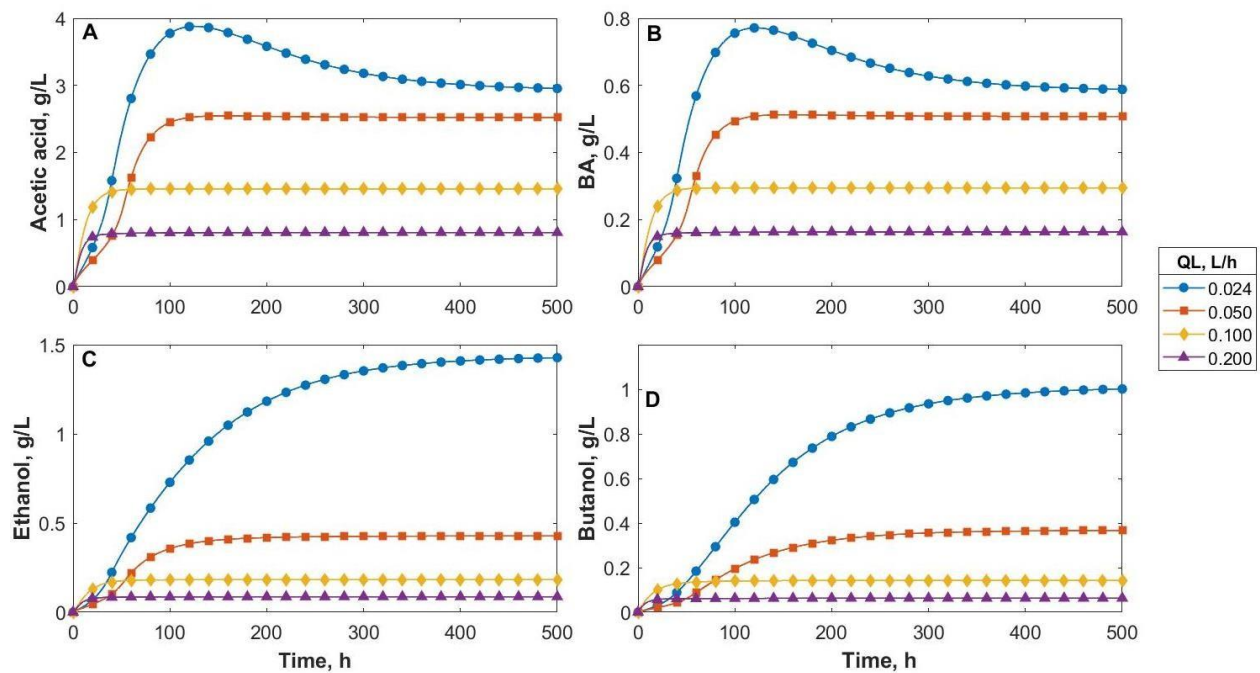


Figure 4.12.: Time-resolved concentration acids and solvents at different Q_L .

The asymptotic productivity assessed at high liquid flow rate may be due to a substrate limitation issues. When the fermenter is operated at high dilution rate, the CO concentration in the liquid phase is very low and the substrate supply to the cells is the real bottleneck. A proof of this bottleneck may be the effect of the gas flow rate of the stream fed to the fermenter keeping in mind that differential assumption has been made. The analysis of the productivity vs. Q_L plots as Q_G increases points out that the limit productivity increases with Q_G . The increase is due to the larger availability of CO . However, the increase of the solvent productivity at high dilution rate is less than proportional to the increase of the Q_G . Therefore, the exploitation of the CO streams asks for strategies (e.g. recycle) to exploit all the substrate and to keep cost as low as possible. As regards the economic point of view, it should be stressed that the increase

of the productivity with Q_G at fixed Q_L means the increase of the solvent concentration. The latter condition is an advantageous condition to reduce the cost of recovery and concentration of the solvent.

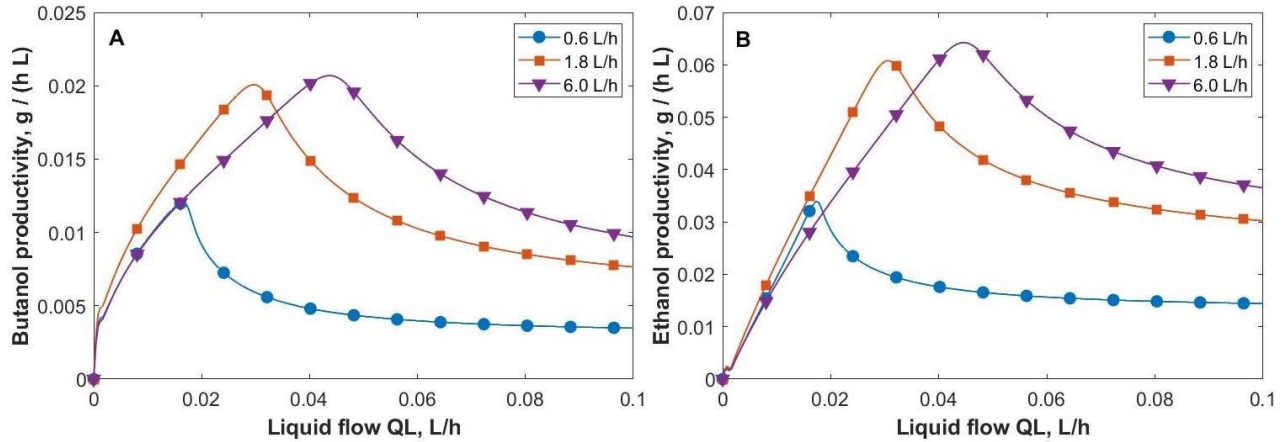


Figure 4.13: Productivity of alcohols vs. liquid flow rate at different values of Q_G .

Free cells vs. biofilm fermentation

The comparison of the fermentation performance assessed in the fermenter operated with biofilm is on order: the aim has been to assess the contribute of biofilm and how the ratio between the two contributions is affected by the operating conditions. The two indicators are strictly connected each other by means of the attachment and detachment terms. X_L - the population of cells in liquid phase - is strongly affected by the convective flow out (Q_L) of the fermenter (e.g. washed out phenomena). The detrimental effects on biofilm – the negative term of the biofilm cell balance - is just the detachment term that it is a function of R_{bf} . Therefore, the amount of cells in the biofilm layer is less sensible to the environmental conditions.

Figure 4.14 reports data of the simulations. As expected, the contribution of biofilm to the total cells increases with the liquid flow rate (Figure 4.14B). Indeed, the liquid flow has no direct effects on the biofilm. Obviously, as the free cells concentration drops down, the attachment term becomes negligible over time.

The contribute of the biofilm varies from 57%, when no liquid is fed, to 78% when the feeding is 0.1 L/h. Data stop at this value because for higher flows the trend is quite monotone. Moreover it was observed that optimum values are around 0.02. For higher flows, the amount of free cells tends to zero, but even before, probably, most of the contribute comes from the biofilm that grows and release into the liquid phase. As the time of residence of those cells is very low, probably they don't have the time to replicate and get washed away.

Effect of the detachment rate

A key phenomenon of the investigated fermentation is the biofilm-cell detachment mechanism. The main characteristic parameter is the detachment constant, K_D . Its role is to assess the importance of such a fundamental mechanism in a biofilm reactor system. The attachment and detachment of cells is a physical phenomenon due

to several factors: shear thinning, mechanical breakages and so on. These factors are in turn influenced by the fluid dynamics. Therefore, it is legitimate to think that those value may depend on the operating conditions. To the author knowledge, no data is available in the literature regarding the biofilm dynamic: attachment and detachment phenomena, K_D and K_A parameters. Therefore, the simulations have been carried out by setting the K_D and K_A parameters from a study on *C. acetobutylicum* (Piscitelli, 2018).

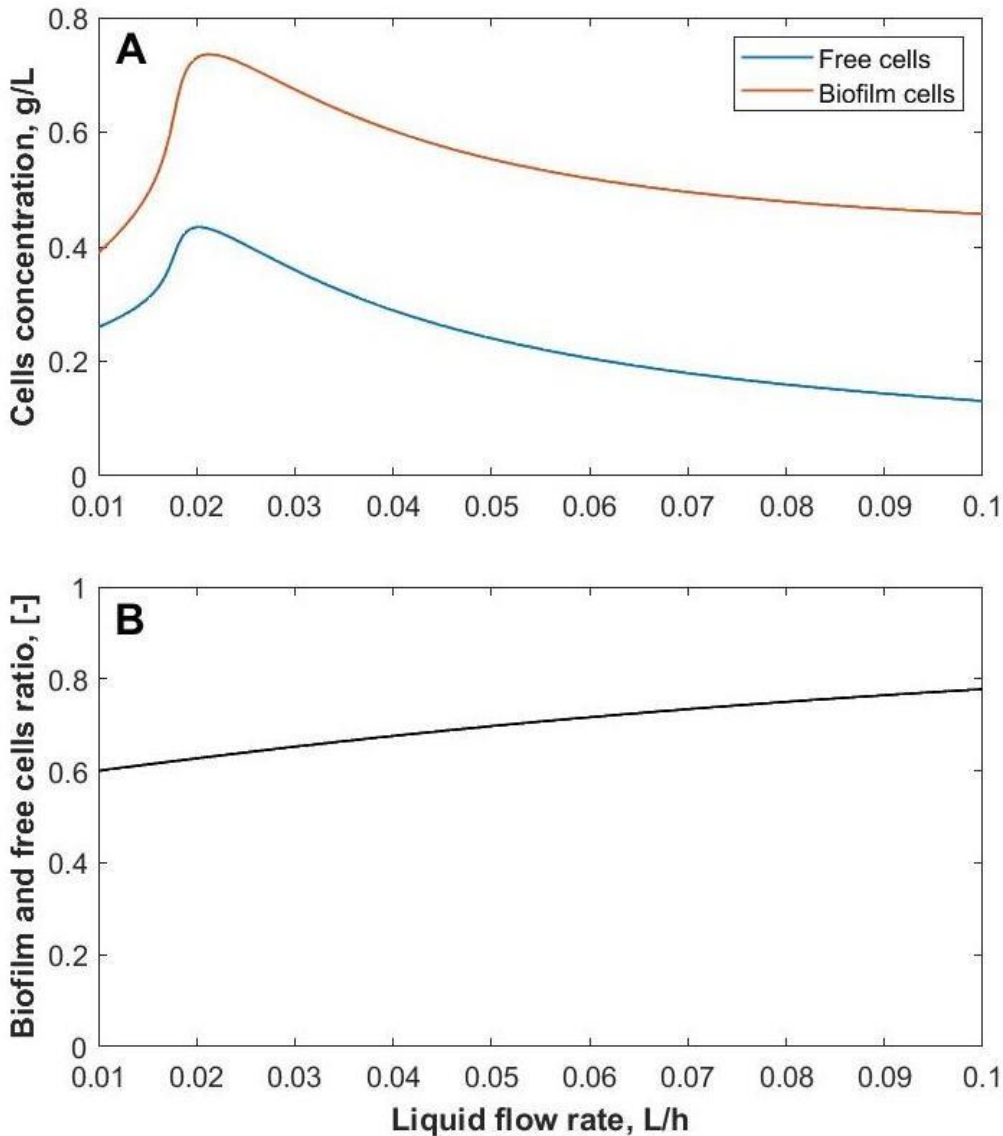


Figure 4.14: Comparison between free cells and immobilized cells vs. liquid flow rate. Steady-state cell concentration (A) and fraction of biofilm cells on the total (B).

The effect of a significative variation of the detachment constant has been assessed. The different thickness of the biofilm has been assessed as a function of the K_D . The time required to get steady state conditions and the final concentration of butanol have also been assessed. Simulation results are reported in Table 4.17. The

bold line reports the data assessed as reference simulation. The transient time is the time required to reach a biofilm dimension equal to the final value $\pm 5\%$. The analysis of the table points out that the change of K_D over four order of magnitudes changes the biofilm thickness of less than a factor 80 and the transient time of one order of magnitude. The biofilm thickness decreases with K_D . The transient time is characterized by a minimum at $K_D=0.03 \text{ h}^{-1}$. The quite high sensitivity of the reported data points out that the dynamics of the biofilm growth plays a key role on the fermentation performances. Indeed, the final butanol concentration ranges on a factor 6. As pointed out in the previous section the increase of the final butanol concentration plays a key role in the economics of the solvent production.

Table 4.17. Relevant data from the simulations carried out at several K_D value.

$K_D, \text{ h}^{-1}$	Biofilm thickness, μm	transient time, h	Butanol final conc., g/L
0.0003	79.56	1246	3.145
0.003	55.05	956	2.398
0.006	41.24	628	1.957
0.01	31.63	421	1.632
0.02	19.77	251	1.215
0.03	13.94	142	1.012
0.30	1.188	221	0.544

Conclusions

A theoretical study regarding the performance of a biofilm reactor for syngas fermentation was carried out. The study aimed to assess the potential of a biofilm reactor, as an innovative strategy for the production of biofuels by syngas fermentation plant. A set of simulations was carried out, focusing on the equilibrium conditions of a dynamic system, with gas and liquid continuous feeding and dynamic evolution of the system to reach such conditions.

The use of biofilm on support particles increased the production of alcohols, reaching a concentration of butanol 85% higher. Other significative benefits are the reduction of intermediates concentrations and the increase of substrate utilization.

The amount of the immobilized cells was, in the best conditions, almost the double of the free cells, as reported in Figure 4.14A. As a consequence, the system benefited and improved its performance. It was observed that a layer of $10 \mu\text{m}$ forms around the carrier, and because of its reduced dimensions, the mass transfer between the two phases (liquid and biofilm) has characteristic time negligible.

Biofilm's potential lies in the possibility to confine the cells into the reactor and avoid the washout. However, it was observed that increasing the flow rate of liquid or gases too much doesn't have any positive effect.

The detachment plays a key role on the system dynamic: compared with the residence time, it affects the wash out conditions. As already written, in addition to the analysis of its variation consequences, its experimental determination is needful.

The present work aims to offer a guideline in the development of a biofilm reactor and the optimization of the operating conditions. However, an experimental study should be carried out to find suitable carriers to promote the biofilm formation, and verify the results obtained.

Acknowledgement

Pasquale Izzo and Sabato Piccolo are gratefully acknowledged for the help provided during the development of the scripts in MATLAB® environment, utilized to gather all the data reported in this chapter.

5. DISCUSSION

The requirement of the modern society to overcome the dependence on fossil fuels is addressing the scientific community on the research of alternative routes to obtain energy, chemicals, and commodities from renewable sources. The petrochemical route to produce fuels is still the most competitive alternative, but the awareness of the long-term scenario, with the depletion of fossil sources and the global warming, requires efficient solutions in the shortest time possible. For what concerns the biofuels and chemicals, several processes have been studied and developed, by converting different kinds of biomass to a wide spectrum of products according to the biorefinery approach. The huge availability of raw biomass and its low cost are one of the strongest advantages of biorefinery. The selection of the feedstock is an important issue in most of the processes. Indeed, the composition of biomass affects the upstream processes, and the fraction of lignin, cellulose and hemicellulose affects the yield itself. Moreover, the ethic concerning the edible biomasses has forbidden the use of these resources as biofuel process feedstocks because the competition with the food industry.

The pre-treatment step is one of the main bottlenecks of the fermentative route to produce biofuels by sugar conversion. An alternative solution that is gaining increased attention in the last years is the gas fermentation, a hybrid thermochemical and biological process that allows to exploit the whole carbon content of the biomass by mean of the gasification process. Gasification is an established technology to produce syngas, a gaseous mixture at high energy content. Syngas is the feedstock for many different industrial processes, for example synthesis of ammonia or methanol, or liquid fuels with the Fischer-Tropsch process.

To make syngas fermentation an economically competitive technology, further improvements are required as regards the biological step. So far, the main limitations emerged are that related to the low concentrations achieved and the growth kinetics, low in comparison to Acetone-Butanol-Ethanol fermentation. Another important bottleneck is the gas transfer to the liquid phase, that involves multiple issues: the low solubility of CO in the liquid phase, the energy required for the agitation (strongly affected by the size of the reactor) and the substrate inhibition, whose effect was investigated in this Ph. D. thesis.

5.1 Batch fermentation

The fermentation tests carried out under batch conditions have been aimed to assess the potentiality of *Clostridium carboxidivorans* as a biocatalyst to produce biofuels. Its peculiarity is to produce not only ethanol, but also long-chain alcohols, including butanol. The selected strain has been characterized in terms of growth rate and metabolites production. The dependence of the growth rate on the CO concentration has also been investigated. The main advantage of this strategy lies in its simplicity of set-up and handling, and the reduced consumption of resources, e.g. medium components and gas. Moreover, the reproducibility has been guaranteed: once the serum bottle is sealed and sterilized, the possibility of contaminations or the interaction with external agents is remote. As evidence, samples of the culture were

periodically examined with an optical microscope, to check for any contamination that would invalidate the results.

During the batch experiments, it has been observed a fast duplication of cells during the first 48 h, usually without any lag phase, and then a sudden settlement close an asymptotic value. The effect of the investigated parameters, P_{CO} and V_L/V_G ratio, has showed that high concentrations of dissolved CO have an inhibitory effect on the strain. After the exponential growth, a stationary phase has been observed, and then a progressive decrease of the cell concentration due to cells death/lysis. The reason why this interruption occurred are not completely clear because in most of the experiments the CO has not been depleted, moreover the inhibition effect should have been decreased as well, during the fermentation. A possible explanation to this behavior may be in the depletion of some other fundamental nutrients of the culture medium. The pH value varied according to the cell concentration, and it confirms that acids are products of the primary metabolism of *C. carboxidivorans*. An acidogenesis-solventogenesis mechanism has been expected, as it happens during the ABE fermentation. However, the detection of ethanol since the beginning of the fermentation suggests that both phases take place at the same time, even though the production of alcohols is not completely clear. According to the Wood-Ljungdahl pathway, the formation of alcohols may occur according to two different path: directly from acetyl-CoA or by the reduction of acetate/butyrate to the corresponding aldehyde and then alcohol. The latter reaction is affected by the pH of the culture medium, as the bacteria tends to keep pH close to the best value for its health. Nevertheless the pH during the batch experiments reached low values, the reassimilation of acids has not been observed. A possible explanation is the depletion of the energy source, which led to the inexorable decrease of the microbial population, not only due to the lack of a key nutrient, but also because the low pH may be a stressful condition for the cells. Alcohols inhibition has not been considered during this study because the concentration of ethanol and butanol has been quite low.

The study carried out allowed to assess the effect of the initial amount of CO with respect to the cells. The attention has been paid to the gas pressure and the gas fraction of the reactor volume: P_{CO} and V_L/V_G . An optimal value of initial pressure P_{CO} has been of about 1.7 bar, where the highest alcohols concentration has been achieved. It has been pointed out that the bacteria have benefited of the high amount of gas available in the case of $V_L/V_G = 0.28$. It is worth to point that in both cases, with the same pressure, to saturate the liquid phase, a smaller amount of gas is required, and therefore, the CO supply lasted longer.

One of the main limitation of the batch fermentation is the impossibility to measure the specific growth rate under constant concentration of substrate.

5.2 Effect of the continuous gas feeding

The tests carried out in the continuously fed bioreactor have been aimed to overcome the main limitations that affected the batch bottles. First of all, the different agitation has allowed to increase the $k_L a$ significantly, from 4 - 5 h^{-1} to 25 - 30 h^{-1} . The possibility to control some variables over time, such as temperature and pH, has offered a wide spectrum of solutions to investigate, in order to find what conditions grant the best results. With respect to the batch case, working with a continuous-open system turned out to be more challenging, and obtaining reliable data regarding a single set of

operating conditions required several attempts. In every experiment, the gas flow was set to operate the reactor under differential conditions for the substrate. Under these conditions it has been possible to assume the dissolved CO constant during the whole test.

The attention has been focused on the effect of the pH of the culture medium. The simplest strategy has been to set the level of pH at a constant value and observe how this value has affected the production. To have a fair comparison, tests without any pH control have also been carried out to observe the natural acidification of the culture medium. Due to the poor reproducibility of the tests carried out without pH control, the data have not been reported in the present thesis. A simple observation regarding these tests is: the pH initially dropped, according to the microbial growth, than increased sometimes to values even higher than the starting point. This behavior could not be explained with the available data, nor reported in any published study so far, to the author knowledge. Therefore, it has been decided a different strategy for the pH control. The fermentation strategy 2 has included:

- a first period during which cells have growth without any pH control. The cells concentration has reached a significative value, typically at pH around 5;
- the second period during which the pH has been kept constant at the pre-set value;

In both fermentation strategy, the continuous supply of the gaseous substrate enhanced the production of alcohols remarkably. The fermentation carried out at constant pH, the high pH favoured the accumulation of a major concentration of acids, in particular acetic acid. Acids have been converted during the solventogenic phase, started between 24 and 48 hours of fermentation. Acetic, butyric and hexanoic acid have been produced and consumed during the same time interval. In the solventogenic phase, the production rate of ethanol and butanol has increased, thanks to the contribution of the acid conversion reaction, which is added to the straight production from acetyl-CoA.

When the pH was left free to drop, the production of acids has not been favoured. In particular, acetic acid peak concentration has been more than double in the experiment carried out at pH set at 5.75. The lower acid accumulation achieved in the strategy 2 experiment may be the reason why the growth did not stop within the first days of fermentation, but went over for a longer time, reaching the highest value reported so far, of 0.81 g/L. This operating condition has also improved the production of hexanol, which could be an added value, apart from the production of molecules suitable as biofuels.

5.3 Kinetic characterization

The acquisition of data regarding the growth rate and yields is a fundamental step to provide a predictive model suitable to describe the fermentation process and predict the dynamic evolution of such a complex system. The proposed model - characterized by three different biological reactions, and their mathematical expression - has been formulated taking into account the results collected during the experimental campaign and the dedicated literature. As a results, a vector of 31 parameters has been identified, made by various kinetic and yield parameters, taking into account the main species involved in the process. The effect of hexanoic acid and hexanol has not been considered because data regarding these species are scarce and, when reported, the

concentrations are lower than the other metabolites. Moreover, the number of parameters is already quite high, therefore weighing the model down further has been deemed not necessary. The sensitivity analysis has pointed out that only a few parameters affect the production remarkably. In particular, the parameters involved in the expression of the specific growth rate must be estimated with extreme care.

The growth kinetic is the main model that describes *C. carboxidivorans* behavior, as with this reaction all the metabolites are produced. The acid conversion reactions take place, obviously, after the beginning of the fermentation, when the concentration of acetic and butyric acid reaches significant values.

The existence of a third pathway to produce alcohols has been hinted mainly by the observed increase of their concentration, even when the growth has been stopped and the concentration of acids was quite low. Moreover, the balance between converted acids and produced alcohols has not been even. This mechanism has been very helpful to improve the fidelity of the model itself with respect to the experimental data. The proposed model describes very well the production of metabolites, as reported by the R^2 calculated in Table 4.5 and is in general quite faithful.

5.4 Effect of the operating conditions

One of the main topics of this Ph.D. thesis has been related to the investigation of the best operating conditions to be carried out syngas fermentation. This research involved both experimental and simulation activity. For what concerns the experimental activities, the effect of pH and CO partial pressure have been assessed and discussed in the previous section. In general, it has been observed that the uptake rate of CO for the cells is a key issue.

Several parameters affect the amount of CO in the liquid phase: the agitation, the gas flow rate, the gas/liquid fraction in the reactor (studied in detail in the simulation framework). The temperature also plays a key role, as it affects the CO solubility other than the microorganism kinetics.

Experimental and theoretical evidence suggest that to increase the mass transfer rate is not the most effective strategy to enhance the performances of CO fermentation, as it has been expected. In fact, the inhibitory effect of the substrate plays a key role in the dynamics of the reactor, and the uptake should be modulated to let the concentration of CO always near the optimum value. An effective strategy to achieve this goal may be to feed a gaseous stream at a low CO fraction. This strategy should, on one side, give better results in terms of CO consumption and biofuels production. On the other side, this strategy helps to control the issue related to the effective and safe operation of the plant.

5.5 Biofilm bioreactor potential

The potential of a biofilm bioreactor has been investigated by exploiting the mathematical model proposed for a gas-fed reactor system. The proposed model has been extended to the biofilm phase and has included the presence of a continuous liquid stream fed and withdraw at constant flow rate. The operation under continuous conditions with respect to the liquid phase has increased the complexity of the model. In particular, the problems related to the washout. The washout occurs when the dilution rate - the ratio between liquid flow and the reaction volume - exceeds the specific

growth rate, causing a progressive decrease of the cells inside of the reactor. The washout threshold conditions - related to a gas and liquid-fed reactor – have been presented in the Appendix A. The peculiarity of the function of the specific growth rate as regards the CO concentration and the continuous CO pumping into the medium provided the washout conditions at a dilution rate lower than that corresponding at the maximum of the specific growth rate. Indeed, the CO concentration that establishes in the medium as equilibrium with the pure CO was in the range where inhibition is active. As a consequence, the feeding of a gas stream at CO concentration with inert may enhance the fermentation performances.

One of the main advantages of biofilm reactor is the possibility to retain the cells, keeping high their concentration in the system, and avoiding problems related to the washout. The study has been carried out developing and solving the extended model with MATLAB®. It has been possible to process a large amount of data and estimate the contribute of the biofilm to the process, assessed in terms of final concentration and productivity of ethanol and butanol.

The increase of the overall number of cells in the reactor has allowed to increase the concentration of butanol (+85%) and ethanol (+13%). The improvement observed in butanol formation is particularly encouraging. This result should promote further studies regarding the realization of an innovative biofilm reactor suitable for syngas fermentation.

The dynamic evolution of the biofilm - measured in terms of thickness of the biofilm layer - has been investigated. The biofilm grew with an exponential trend approaching thickness between 10 and 15 μm . The thickness was not very high, confirming the difficulty of *C. carboxidivorans* to reach particularly high biofilm thickness. The reason why the concentration profiles of metabolites in the biofilm layer are almost constant, is probably that the latter is extremely thin.

Nevertheless, the biofilm cells contribution has been estimated to be between 60% and 80% of the total cells, depending to the liquid flow rate.

Another important task regarding the biofilm impact is the effect of attachment and detachment of cells during the process. Studies about this topic are extremely scarce. Therefore, a range of rate has been investigated. In particular, the attention has been focused on the detachment rate. Its effect on biofilm formation and production of butanol is strongly not linear, as can be seen from table 4.17, but it is consistent with the theoretical background.

This study points out once again how the control of every single parameter is fundamental to optimize the process of syngas fermentation.

6. CONCLUSIONS AND FUTURE PERSPECTIVES

The present Ph.D. project has been aimed at the optimization of the production process of biofuels - in particular biobutanol - by syngas fermentation by the acetogenic strain, *Clostridium carboxidivorans*. The activities have focused on the biological step of the gas fermentation process and have involved the set-up of the reactor system, fermentation experiments under a wide interval of operating conditions, and the development of a mathematical model to describe the complex process of the gas fermentation. The research activity have been carried out at Dipartimento di Ingegneria Chimica, dei Materiali e della Produzione Industriale of the Università degli Studi di Napoli 'Federico II'.

The fermentation of *C. carboxidivorans* has been successfully carried out under batch and gas-fed conditions. The maximum cell concentration achieved has been respectively 0.68 and 0.8 g_{DM}/L. The results are in a satisfactory agreement with data reported in literature. The metabolites production has been modest, during the batch experiments, but increased almost twice in the mechanical agitated apparatus fed continuously with a gas stream. Therefore, the continuous feeding is a consistent improvement of the overall performances.

The batch experiments allowed to investigate the CO inhibition on the cell growth. During the batch experiments no reconversion of acids has been observed, no production of alcohols independent from growth has been observed. It may be concluded that the only conversion mechanism active has been the growth associated production of metabolites.

The experiments in the gas-continuous fed bioreactor has pointed out the fermentation sensibility to the pH. The continuous gas feeding has allowed the strain to grow remarkably, to produce metabolite at high concentration – with respect to batch tests - and to show clearly the reassimilation of acids. The concentration of acids is strongly affected by the pH, and subsequently all the kinetics. It has been observed how the natural acidification of the culture medium limited the accumulation of acids and allowed the bacteria to achieve a high cell concentration.

The autotrophic growth of *C. carboxidivorans* has been modelled by five main reactions for the CO fermentation. The proposed model has successfully described the bacterial growth, CO uptake, and acid/solvent production. The accuracy and the soundness of the model have been assessed.

The proposed model has been used to assess the effects of some operating conditions. The dynamic behaviour of a biofilm reactor has also been addressed. It has been pointed out how the optimization of the operating conditions may easily lead to a saving of the substrate and a high production of metabolites of interest.

The study carried out on the biofilm reactor has confirmed the high potential of this configuration. The proposed model has reported high concentration of ethanol and butanol, a good CO exploitation and the possibility to work at high flows of gas and liquid.

The results reported in the present Ph.D. thesis put the basis for future investigations. Investigations should regard the effect of a gaseous substrate close the real syngas. The possibility of CO₂ fixation would represent a huge contribution to the reduction of GHG. Furthermore, other syngas main compounds (H₂) or impurities (NO_x)

may have an inhibitory effect, similar to CO. This effect should be investigated, to evaluate the weight of these impurities and the need to remove them upstream or not.

The experimental configuration of the bioreactor system requires further study in particular it is necessary to understand more the microbiological phenomena and the mechanisms that regulate the growth of *C. carboxidivorans*. The possibility to switch to engineered strains may represent a turning point in the syngas fermentation scale-up.

The proposed mathematical model is open to update and to improvement whenever more data are available: the aim is to get a high correlation factor, and to extend simulations to a wide spectrum of possible operating conditions. The biofilm reactor is only one of the possible solutions that can be investigated by a computational approach, saving time, resources and addressing the research to the most favorable solutions.

In conclusion, syngas fermentation is a promising biotechnological application to produce biofuels and chemicals from renewable sources. It is a potential solution to overwhelming problems of modern society, such as the control of the emissions and the depletion of fossil sources, promoting the circular economy and the reuse of many different C-based waste materials.

NOMENCLATURE

AA	Acetic acid (g/L, mg/L)
BA	Butyric acid (g/L, mg/L)
HA	Hexanoic acid (g/L, mg/L)
E	Ethanol (g/L, mg/L)
B	Butanol (g/L, mg/L)
CO _G , CO _{2G}	Carbon monoxide and dioxide in gas phase (mol/L)
CO _L , CO _{2L}	Carbon monoxide and dioxide in liquid phase (g/L, mg/L)
CO*, CO ₂ *	Carbon monoxide and dioxide equilibrium concentration (g/L)
X, X _L	Cell concentration in liquid phase (g/L)
X _{bf}	Cell concentration in biofilm phase (g/L)
R _s	Radius of support particles (μm)
R _{bf}	Radius of biofilm particles (μm)
Y _{i/j}	j-to-i yield coefficient (g _i /g _j)
b, c	van't Riet equation parameters (adim)
D _{fj}	Diffusivity of the j specie in water (m ² /s)
P _g	Gassed power (W)
u _g	Gas velocity (m/s)
r ^{AA} _{ET} , r ^{AB} _{BU}	Specific acids to alcohols rate
rd _E , rd _B	Direct production of alcohols rate
V _L , V _G	Liquid and gas phase volume in the reactor (L)
Q _L , Q _G	Inlet liquid and gas flow rate (L/h)
Q _{OUT}	Out gas flow rate (L/h)
n _{CO}	Moles of CO (mol)
N _{Gout}	Molar flux of gas in the out stream (mol/h)
t	time (h)
D	Dilution rate (1/h)
R	Universal gas constant (L *bar/K/mol)
T	Temperature (°C)
P	Pressure (bar)
H _i	Solubility in water of the specie "i" (g/L/bar)
k _{La}	Mass transfer rate (1/h)
μ	Specific cell growth rate (1/h)
α', α''	Kinetic parameters
ξ _{CO}	Conversion degree of carbon monoxide
ε	Solid/liquid volume ratio (L/L, adim)
Ω _i	Sensitivity function of "i"

APPENDIX A

The specific growth rate kinetics assessed in section 4.1 is analysed in this appendix. The kinetics is reported as eq. A1 and the assessed parameters are reported in Table A1.

$$\mu = \frac{\mu_M CO_L}{(CO_L + K_{CO} + \frac{CO_L^2}{K_I})} \cdot \left(1 - \frac{A_{TOT}}{A_{MAX}}\right)^{\alpha'} \left(1 - \frac{S_{TOT}}{S_{MAX}}\right)^{\alpha''} \quad \text{A.1}$$

Table A.1. Estimated values of kinetic parameters.

Parameter	Value	Unit
μ_{max}	0.373	1/h
K_{CO}	0.011	g _{CO} /L
K_I	0.003	g _{CO} /L
α'	0.759	-
α''	2.544	-
A_{MAX}	9.192	g _{Acid} /L
S_{MAX}	5.184	g _{Solvent} /L

Assuming a continuous stirred tank reactor for the fermenter, the balanced feeding is characterized by the dilution rate equals to the specific growth rate. Therefore, wash-out condition is expected at the maximum specific growth rate. Equation A.1 under the hypothesis of metabolites absent ($A_{TOT} = S_{TOT} = 0$) provides that the specific growth rate is maximum at CO concentration CO_L^{opt} .

$$CO_L^{opt} = \sqrt{K_{CO} \cdot K_I} = \sqrt{0.011 \cdot 0.003} = 0.0057 \quad \text{A.2}$$

and the maximum specific growth rate is:

$$\mu(CO_L^{opt}) = \frac{0.373 \cdot 0.0057}{\left(0.0057 + 0.011 + \frac{0.0057^2}{0.003}\right)} = 0.07 \text{ h}^{-1} \quad \text{A.3}$$

The values obtained for the affinity and inhibition constant have the peculiarity that $K_{CO} > K_I$. This condition, not common in general, strongly affects the trend of the specific growth rate μ from CO, as shown in Figure A.1. The maximum value is reached for a value around the 20% of the saturation level, after that the growth sharply decrease.

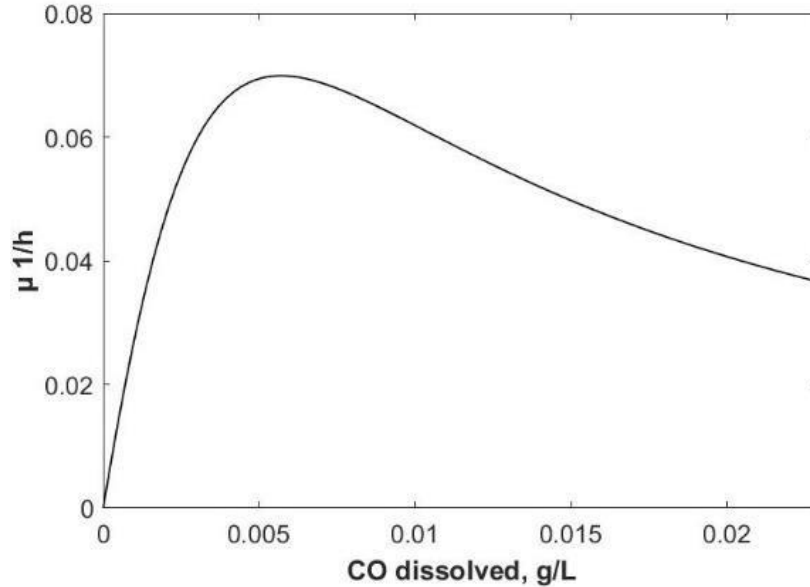


Figure A.1: Specific growth rate vs. CO dissolved concentration, without the metabolites effects.

The comparison of the $\mu(CO_L^{opt})$ with the wash-out dilution rate assessed in section 4.1 ($D_{w.o.} = 0.0375$ 1/h) points out that the wash-out occurs at CO_L different from CO_L^{opt} . It is expected that the continuous feeding of the substrate provides CO_L concentration equals at the saturation concentration under equilibrium with the CO gas stream. Therefore, under wash-out conditions the CO_L is expected to be 0.023 /L. Under these conditions assuming that the metabolites concentrations are equal to 0, eq. (A.1) yields:

$$\mu = \frac{0.373 \cdot 0.023}{(0.023 + 0.011 + \frac{0.023}{0.003})} \cdot \left(1 - \frac{0}{9.192}\right)^{0.759} \left(1 - \frac{0}{5.184}\right)^{2.544} = 0.0365 h^{-1} \quad A.4$$

The threshold value obtained for the washout conditions in the simulation test was $0.0375 h^{-1}$, very close to the μ calculated in absence of reaction. As the simulations were performed for a finite number of values of D , most likely, increasing the number of experiments near $D = 0.0365$ 1/h the margin of error will tend to decrease.

Additional data regarding the dissolved concentration of CO over time and the corresponding value of the specific growth rate μ are shown in Figs. A.2 and A.3.

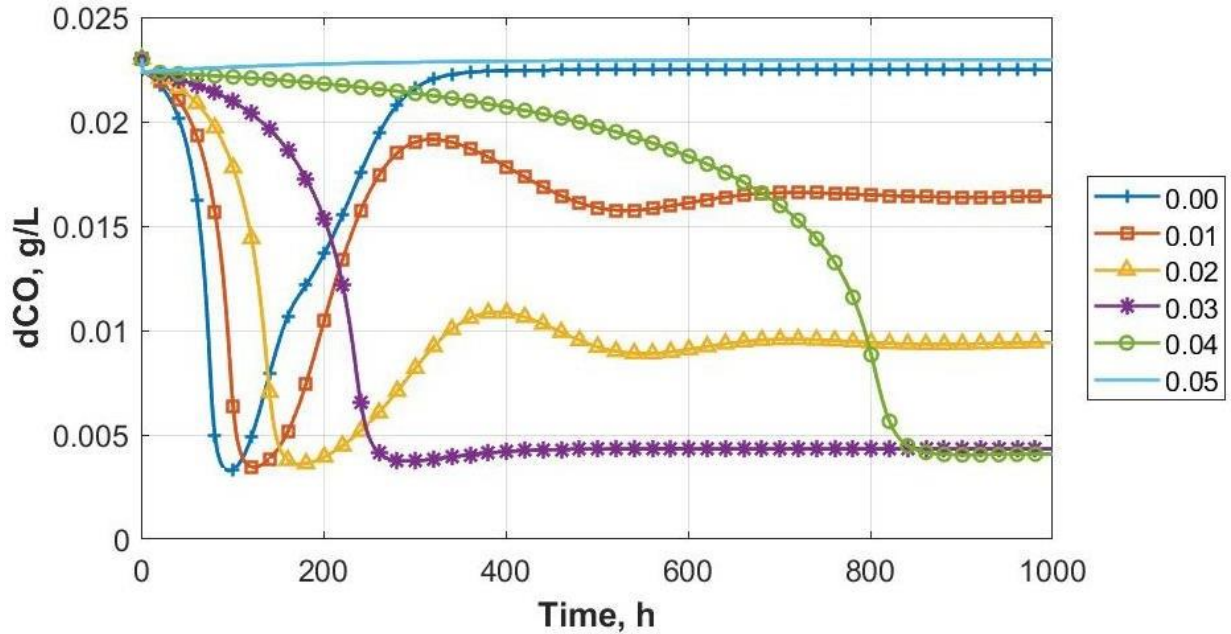


Figure A.2: Time-resolved dissolved CO concentration at different values of Q_L . Values in the legend are expressed in L/h.

The peaks reported in Figure A.3 are in proximity of the calculated value of CO_L^{opt} . The progressive raise of the dissolved CO concentration is explained by the production of inhibitors that reduce μ . It's worth to observe that, together with the cells, part of the inhibitors are washed away, allowing the system to find a dynamic equilibrium, in which the production of cells and metabolites is continuous. Obviously, such conditions cannot take place for $Q_L = 0$ (blue cross line).

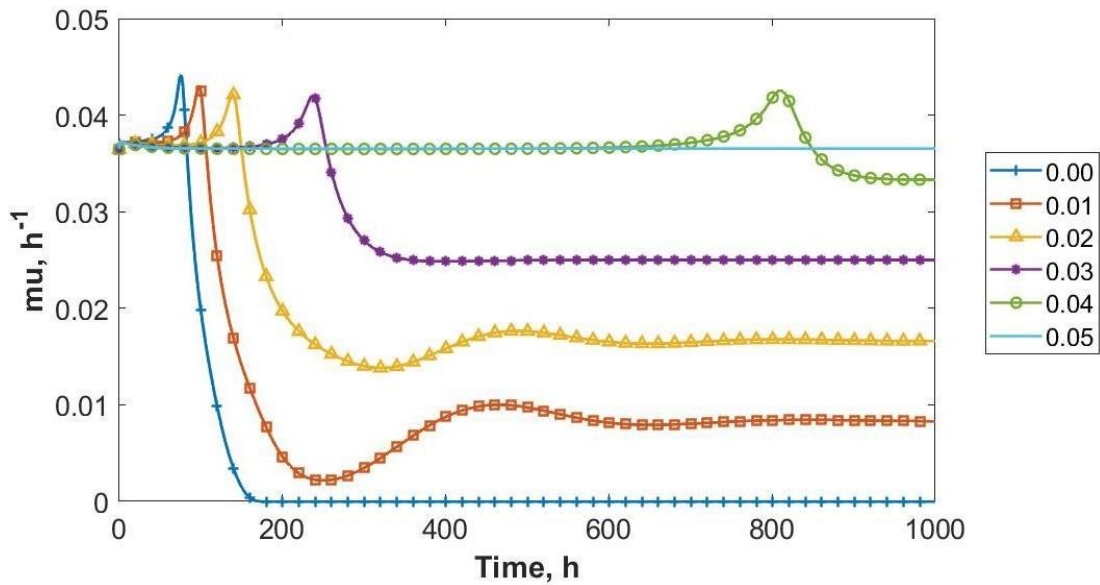


Figure A.3: Time-resolved μ at different values of liquid flow rate Q_L . Values in the legend are expressed in L/h.

Finally, Table A.2 reports the values of D and μ for long times, confirming what explained previously.

Table A.2. Asymptotic values of μ compared with the dilution rate.

Q_L, L/h	D, 1/h	Asymptotic μ, 1/h
0.00	0	0
0.01	0.0083	0.0083
0.02	0.0167	0.0167
0.03	0.0250	0.0250
0.04	0.0333	0.0333
0.05	0.0417	0.0365

REFERENCES

- Abubackar HN, Veiga MC, Kennes C. Biological conversion of carbon monoxide: rich syngas or waste gases to bioethanol. *Biofuels Bioprod Biorefin* (2011); 5:93–114
- Ahmed A and Lewis RS, Fermentation of biomass-generated synthesis gas: effects of nitric oxide. *Biotechnol Bioeng* 97:1080–1086 (2007).
- Babu, B.K., Atiyeh, H., Wilkins, M., Huhnke, R. Effect of the reducing agent dithiothreitol on ethanol and acetic acid production by *Clostridium* strain P11 using simulated biomass-based syngas. *Biol. Eng. Trans.* 3, 19–35 (2010).
- Bai, F., Anderson, W., Moo-Young, M., 2008. Ethanol fermentation technologies from sugar and starch feedstocks. *Biotechnol. Adv.* 26(1), 89- 105.
- Birgen Cansu (2019). Experimental and Modeling Studies of Fermentative Butanol Production from Lignocellulosic Sugars. PhD thesis.
- Burk MJ, Schilling CH, Burgard AP, Trawick JD. Methods and organisms for utilizing synthesis gas or other gaseous carbon sources and methanol, US Patent No. 7,803,589; 2010.
- Chen, X., & Ni, B. J. (2016). Anaerobic conversion of hydrogen and carbon dioxide to fatty acids production in a membrane biofilm reactor: A modeling approach. *Chemical Engineering Journal*, 306, 1092–1098.
- Cherubini, F. (2010). The biorefinery concept: Using biomass instead of oil for producing energy and chemicals. *Energy Conversion and Management*, 51(7), 1412–1421.
- Ciliberti, C., Biundo, A., Albergo, R., Agrimi, G., Braccio, G., de Bari, I., Pisano, I., 2020, Syngas derived from lignocellulosic biomass gasification as an alternative resource for innovative bioprocess. *Processes* 2020, 8, 1567.
- Daniell, J., Köpke, M., Simpson, S., 2012. Commercial biomass syngas fermentation. *Energies* 5 (12), 5372–5417.
- de Medeiros, E. M., Posada, J. A., Noorman, H., Filho R., 2019. Dynamic modeling of syngas fermentation in a continuous stirred-tank reactor: Multi-response parameter estimation and process optimization. *Biotechnology and Bioengineering*; 116:2473–2487.
- Devarapalli M., Atiyeh H.K. A review of conversion processes for bioethanol production with a focus on syngas fermentation. *Biofuel Research Journal* 7 (2015) 268-280.
- Diender M, Stams AJM and Sousa DZ, Production of medium-chain fatty acids and higher alcohols by a synthetic co-culture grown on carbon monoxide or syngas. *Biotechnol Biofuels* 9:82 (2016).
- Doll, K., Rückel, A., Kämpf, P., Wende, M., & Weuster-Botz, D. (2018). Two stirred-tank bioreactors in series enable continuous production of alcohols from carbon monoxide with *Clostridium carboxidivorans*. *Bioprocess and Biosystems Engineering*, 41(10), 1–14.
- Dry, M.E., 2002. The Fischer–Tropsch process: 1950–2000. *Catal. Today* 71, 227–241.
- Drzyzga, O., Revelles, O., Durante-Rodríguez, G., Díaz, E., García, J. L., & Prieto, A. (2015). New challenges for syngas fermentation: Towards production of biopolymers. *Journal of Chemical Technology and Biotechnology*, 90(10), 1735–1751.
- Dudynski M, Kwiatkowski K, Bajer K. From feathers to syngas - Technologies and devices. *Waste Management*. 2012 Apr;32(4):685–91.

- Dürre P, Biobutanol: an attractive biofuel. *Biotechnol J* 2:1525–1534 (2007).
- Dürre, P., Eikmanns, B.J., 2015. C1-carbon sources for chemical and fuel production by microbial gas fermentation. *Curr. Opin. Biotechnol.* 35, 63–72.
- EC. Towards a European knowledge-based bioeconomy – workshop conclusions on the use of plant biotechnology for the production of industrial biobased products. EUR 21459. European Commission, Directorate-General for Research. Brussels, Belgium.; 2004.
- Fernández-Naveira, A., Abubackar, H.N., Veiga, M.C., Kennes, C., 2016a. Efficient butanol-ethanol (B-E) production from carbon monoxide fermentation by *Clostridium carboxidivorans*. *Appl. Microbiol. Biotechnol.* 100, 3361–3370.
- Fernández-Naveira, A.; Abubackar, H.N.; Veiga, M.C.; Kennes, C. Carbon monoxide bioconversion to butanol-ethanol by *Clostridium carboxidivorans*: Kinetics and toxicity of alcohols. *Appl. Microbiol. Biotechnol.* 2016b, 100, 4231–4240.
- Fernández-Naveira, Á., Haris, N., Abubackar, N., & Veiga, M. C. (2017a). Production of chemicals from C1 gases (CO, CO₂) by *Clostridium carboxidivorans*. *World Journal of Microbiology and Biotechnology*, (0), 33–43.
- Fernández-Naveira, Á., Veiga, M. C., & Kennes, C. (2017b). H-B-E (Hexanol-Butanol-Ethanol) fermentation for the production of higher alcohols from syngas/waste gas. *Journal of Chemical Technology & Biotechnology*, (February), 712–731.
- Fernández-Naveira, Á., Veiga, M. C., & Kennes, C. (2017c). Effect of pH control on the anaerobic H-B-E fermentation of syngas in bioreactors. *Journal of Chemical Technology & Biotechnology*, (February).
- Frankman, A. W., (2016). Redox, pressure and mass transfer effects on syngas fermentation. MSc thesis.
- Gaddy, J.L., Arora, D.K., Ko, C.-W., Phillips, J.R., Basu, R., Wikstrom, C.V., Clausen, E.C., 2007. Methods for Increasing the Production of Ethanol from Microbial Fermentation. US Patent 7285402.
- Garcia-Ochoa, F. Gomez, E. (2009). Bioreactor scale-up and oxygen transfer rate in microbial processes: An overview. *Biotechnology Advances*, 27(2):153–176.
- Gasol CM, Gabarrell X, Anton A, Rigola M, Carrasco J, Ciria P, Life Cycle Assessment of a Brassica carinata bioenergy cropping system in southern Europe. *Biomass Bioenergy* 2007;31(8):543–55.
- Gòdia, F, Solà, C. Fluidized-bed bioreactors. *Biotechnol Progr.*1995;11:479–497.
- González-Figueroa C, Flores-Estrella RA and. Rojas-Rejón OA (November 21st 2018). Fermentation: Metabolism, Kinetic Models, and Bioprocessing, Current Topics in Biochemical Engineering, Naofumi Shiomi, IntechOpen.
- Gowen C.M. and Fong S.S., Applications of systems biology towards microbial fuel production. *Trends Microbiol* 10:516–524 (2011).
- Gunes B., A critical review on biofilm-based reactor systems for enhanced syngas fermentation processes, *Renew. Sustain. Energy Rev.* 143 (2021)
- Halkos, G.E.; Gkampoura, E.C. Reviewing usage, potentials, and limitations of renewable energy sources. *Energies* 2020, 13, 2906.
- Henstra, A.M., Sipma, J., Rinzema, A., Stams, A.J., 2007. Microbiology of synthesis gas fermentation for biofuel production. *Curr. Opin. Biotechnol.* 18, 200–206.

- Hoops, S., Gauges, R., Lee, C., Pahle, J., Simus, N., Singhal, M., Xu, L., Mendes, P., Kummer, U. COPASI - a COmplex PATHway SImulator, *Bioinformatics* 22 (2006) 3067–3074.
- Hurst, K.M.; Lewis, R.S. Carbon monoxide partial pressure effects on the metabolic process of syngas fermentation. *Biochem. Eng. J.* 2010, 48, 159–165.
- IEA BioEnergy Agreement Task 33: Thermal Gasification of Biomass. Available online: <http://task33.ieabioenergy.com/> (accessed on 1 November 2020).
- IEA, Key World Energy Statistics 2019
- Jones D.T., Woods D.R., Acetone-butanol fermentation revisited. *Microbiol Rev.* 1986;50(4):484–524.
- Kennes C and Veiga MC, Air pollution prevention and control: bioreactors and bioenergy. J Wiley & Sons; Chichester, United Kingdom, 549 (2013).
- Kim S, Dale BE. Life Cycle Assessment of various cropping systems utilized for producing biofuels: bioethanol and biodiesel. *Biomass Bioenergy* 2005; 29:426–39.
- Köpke M., Mihalcea C., Bromley J.C., Simpson S.D (2011) Fermentative production of ethanol from carbon monoxide, *Current Opinion in Biotechnology* 2011, 22:320–325
- Kundiyana, D. K., Huhnke, R. L., and Wilkins, M. R. (2010). Syngas fermentation in a 100-L pilot scale fermentor: Design and process considerations. *Journal of Bioscience and Bioengineering*, 109(5):492–498.
- Lange JP. Lignocellulose conversion: an introduction to chemistry, process and economics. *Biofuels Bioprod Bioref* 2007; 1:39–48.
- Latif, H., Zeidan, A. a., Nielsen, A. T., and Zengler, K. (2014). Trash to treasure: Production of biofuels and commodity chemicals via syngas fermenting microorganisms. *Current Opinion in Biotechnology*, 27:79–87.
- Lee SY, Park JH, Jang SH, Nielsen LK, Kim J and Jung KS, Fermentative butanol production by clostridia. *Biotechnol Bioeng* 101:209–228 (2008).
- Lee, R. A., Lavoie, J.-M. (2013). From first- to third-generation biofuels: Challenges of producing a commodity from a biomass of increasing complexity. *Animal Frontiers*, 3(2), 6–11.
- Li Y, Liao S and Liu G, Thermo-economic multi-objective optimization for a solar-dish Brayton system using NSGA-II and decision making. *Int J Electr Power Energy Syst* 64: 167–175 (2015).
- Liakakou E.T., Infantes A., Neumann A., Vreugdenhil B.J., Connecting gasification with syngas fermentation: Comparison of the performance of lignin and beech wood, *Fuel*. 290 (2021)
- Liew, F.M., Köpke, M., Simpson, S.D., 2013. Gas fermentation for commercial biofuels production. In: Fang, Z. (Ed.), *Liquid, Gaseous and Solid Biofuels - Conversion Techniques*. InTech, Rijeka, pp. 125–173.
- Liou, J.S., Balkwill, D.L., Drake, G.R., Tanner, R.S., 2005. *Clostridium carboxidivorans* sp. nov., a solvent-producing *clostridium* isolated from an agricultural settling lagoon, and reclassification of the acetogen *Clostridium scatologenes* strain SL1 as *Clostridium drakei* sp. nov. *Int. J. Syst. Evol. Microbiol.* 55, 2085–2091.

- Liu T, Jiaqiang E, Yang J W, Hui A and Cai H, Development of a skeletal mechanism for biodiesel blend surrogates with varying fatty acid methyl esters proportion. *Appl Energy* 162:278–288 (2016).
- M.E. Russo, P.L. Maffettone, A. Marzocchella, P. Salatino, 2008. Bifurcational and dynamical analysis of a continuous biofilm reactor. *Journal of Biotechnology* 135 (2008) 295–303.
- Maddipati, P., Atiyeh, H. K., Bellmer, D. D., and Huhnke, R. L. (2011). Ethanol production from syngas by *Clostridium* strain P11 using corn steep liquor as a nutrient replacement to yeast extract. *Bioresource Technology*, 102(11):6494–6501.
- Marris E. Sugar cane and ethanol: drink the best and drive the rest. *Nature* 2006; 444:670–2.
- Mayank, R., Ranjan, A., & Moholkar, V. S. (2013). Mathematical models of ABE fermentation: review and analysis. *Critical Reviews in Biotechnology*, 33(4), 419–447.
- Mohammadi, M., Mohamed, A. R., Najafpour, G. D., Younesi, H., & Uzir, M. H. (2014). Kinetic studies on fermentative production of biofuel from synthesis gas using *Clostridium ljungdahlii*. *The Scientific World Journal*, 2014(January).
- Mohammadi, M., Najafpour, G. D., Younesi, H., Lahijani, P., Uzir, M. H., & Mohamed, A. R. (2011). Bioconversion of synthesis gas to second generation biofuels: A review. *Renewable and Sustainable Energy Reviews*, 15(9), 4255–4273.
- Munasinghe, P.C., Khanal, S.K., 2010a. Biomass-derived syngas fermentation into biofuels: opportunities and challenges. *Bioresour. Technol.* 101, 5013–5022.
- Naik, S., Goud, V.V., Rout, P.K., Dalai, A.K., 2010. Production of first and second generation biofuels: A comprehensive review. *Renew. Sustainable Energy Rev.* 14(2), 578-597.
- Nicolella, C., van Loosdrecht, M.C.M., Heijnen, J.J., 2000. Wastewater treatment with particulate biofilm reactors. *Journal of Biotechnology* 80, 1–33.
- Oelgeschläger E and Rother M, Carbon monoxide-dependent energy metabolism in anaerobic bacteria and archaea. *Archiv Microbiol* 190:257–269 (2008).
- Pendyala, V.R.R., Jacobs, G., Bertaux, C., Khalid, S., Davis, B.H., 2016. Fischer-Tropsch synthesis: effect of ammonia on supported cobalt catalysts. *J. Catal.* 337, 80–90.
- Piscitelli, R., (2018) Models for continuous bioreactor systems for butanol production, MSc thesis.
- Phillips, J.R., Atiyeh, H.K., Tanner, R.S., Torres, J.R., Saxena, J., Wilkins, M.R., 2015. Butanol and hexanol production in *Clostridium carboxidivorans* syngas fermentation: medium development and culture techniques. *Bioresour. Technol.* 190, 114–121.
- Procentese A., Raganati F., Olivieri G., Russo M., Salatino P., Marzocchella A., (2015) Continuous lactose fermentation by *Clostridium acetobutylicum* –Assessment of solventogenic kinetics; *Bioresource Technology*, 180, 330–337;
- Qureshi, N., Annous, B.A., Ezeji, T.C., Karcher, P., Maddox, I.S., 2005. Biofilm reactors for industrial bioconversion processes: employing potential of enhanced reaction rates. *Microbial Cell Factory* 4. (24)

- Raganati, F., Procentese, A., Olivieri, G., Russo, M.E., Salatino, P., Marzocchella, A., Biobutanol Production from Hexose and Pentose Sugars, *Chem. Eng. Trans.* 38 (2014) 193–198.
- Raganati F., Procentese A., Olivieri G., Russo M.E., Gotz P., Salatino P., Marzocchella A. (2016), Butanol production by *Clostridium acetobutylicum* in a series of packed bed biofilm reactors, *Chemical Engineering Science*, 152, 678;
- Ragauskas, A.J., Williams, C.K., Davison, B.H., et al. 2006. The Path Forward for Biofuels and Biomaterials. *Science* 311:484–489.
- Ragsdale, S. W., & Pierce, E. (2008). Acetogenesis and the Wood-Ljungdahl pathway of CO₂ fixation. *Biochimica et biophysica acta*, 1784(12), 1873–1898.
- Ramachandriya, K.D.; Kundiyana, D.K.; Sharma, A.M.; Kumar, A.; Atiyeh, H.K.; Huhnke, R.L.; Wilkins, M.R. Critical factors affecting the integration of biomass gasification and syngas fermentation technology. *AIMS Bioeng.* 2016, 3, 188–210.
- Redl S., Dienderb M., Jensena T.O., Sousab D.Z., Toftgaard Nielsena A., (2017) Exploiting the potential of gas fermentation, *Industrial Crops and Products* 106 21–30
- Ruane J, Sonnino A, Agostini A. Bioenergy and the potential contribution of agricultural biotechnologies in developing countries. *Biomass Bioenergy* 2010; 34:1427–39
- Safarian S., Unnthorsson R., Richter C., Simulation and Performance Analysis of Integrated Gasification-Syngas Fermentation Plant for Lignocellulosic Ethanol Production, *Fermentation.* 6 (2020).
- Schuchmann, K. and Müller, V. (2014). Autotrophy at the thermodynamic limit of life: a model for energy conservation in acetogenic bacteria. *Nature reviews. Microbiology*, 12(12):809–821.
- Schügerl K. Three-phase-biofluidization—application of threephase fluidization in the biotechnology—a review. *Chem Eng Sci.* 1997;52:3661–3668.
- Shaw AJ, Podkaminer KK, Desai SG, Bardsley JS, Rogers SR, Thorne PG, Metabolic engineering of a thermophilic bacterium to produce ethanol at high yield. *Proc Nat Acad Sci USA* 105:13769–13774 (2008).
- Shen, S., Wang, G., Zhang, M., Tang, Y., Gu, Y., Jiang, W., Wang, Y., Zhuang, Y.; Effect of temperature and surfactant on biomass growth and higher-alcohol production during syngas fermentation by *Clostridium carboxidivorans* P7. *Bioprocess.* (2020) 7:56.
- Shen, Y., Jarboe, L., Brown, R., Wen, Z., 2015. A thermochemical-biochemical hybrid processing of lignocellulosic biomass for producing fuels and chemicals. *Biotechnol. Adv.* 33 (8), 1799–1813.
- Shen, Y.; Brown, R.; Wen, Z. Enhancing mass transfer and ethanol production in syngas fermentation of *Clostridium carboxidivorans* P7 through a monolithic biofilm reactor. *Appl. Energy* 2014, 136, 68–76.
- Sims, R.E. H., Mabee, W., Saddler, J.N., Taylor, M. An overview of second generation biofuel technologies. *Bioresour Technol* 2010; 101:1570–80.
- Sims, R., Taylor, M., Saddler, J., Mabee, W., 2008. From 1st-to 2nd-generation biofuel technologies: An overview of current industry and RD&D activities, International Energy Agency. Paris, France, pp. 120.

- Suna, X., Atiyeha, H. K., Huhnkea R. L., Tannerb R. S.; 2019. Syngas fermentation process development for production of biofuels and chemicals: A review. *Bioresource Technology Reports* 7 (2019) 100279.
- Talbot, P., Gortares, M. P., Lencki, R. W., de la Noue, J. (1991). Absorption of CO₂ in algal mass culture systems: A differen characterization approach. *Biotechnology and Bioengineering*, 37, 834–842.
- U.S. Energy Information Administration | Short-Term Energy Outlook October 2019
- Van Groenestijn JW, Abubackar HN, Veiga MC and Kennes C, Bioethanol (Chapter 18), in *Air Pollution Prevention and Control: Bioreactors and Bioenergy*, ed by Kennes C and Veiga MC. J. Wiley & Sons, Chichester, UK, pp. 431–463 (2013).
- Vandecasteele, J. (2016). Experimental and modelling study of pure-culture syngas fermentation for biofuels production. MSc thesis.
- Wagner, T., Gonçalves dos Santos, R. (2017). Review on the characteristics of butanol, its production and use as fuel in internal combustion engines. *Renewable and Sustainable Energy Reviews*. 69. 642-651.
- Wallner T, Miers SA and McConnell S, A comparison of ethanol and butanol as oxygenates using a direct-injection, spark-ignition engine. *J Eng Gas Turbines Power* 131:032802 (2009).
- Younesi, H., Najafpour, G., and Mohamed, A. R. (2005). Ethanol and acetate production from synthesis gas via fermentation processes using anaerobic bacterium, *Clostridium ljungdahlii*. *Biochemical Engineering Journal*, 27(2):110–119.

SCIENTIFIC COMMUNICATION

PAPERS

Lanzillo F., **Ruggiero G.**, Raganati F., Russo M.E., Marzocchella A. "Batch Syngas fermentation by *Clostridium carboxidivorans* for production of acids and alcohols". 2020, Processes, Vol. 8: 1075. <https://doi.org/10.3390/pr8091075>

Ruggiero G., Raganati F., Russo M.E., Marzocchella A. "Bioreactor modelling for syngas fermentation: Kinetic characterization", submitted.

Ruggiero G., Raganati F., Russo M.E., Marzocchella A. "Biofilm reactor modelling for Syngas fermentation", submitted.

CONFERENCE PRESENTATIONS

"Bio-fuel production by syngas fermentation" presented to: "Waste2Fuel: Towards bio-butanol as fuel: biorefinery, processes and technologies".

"Syngas fermentation: A modelling Approach" presented to: ICEEM10, 10th International Conference on Environmental Engineering and Management.

COLLABORATION WITH FOREIGN RESEARCH INSTITUTION

July 2019 – December 2019: Research activity at the Department of Chemical and Biochemical Engineering, University of Western Ontario (UWO), London (Ontario, Canada) on the issue: "**Effect of gas composition to syngas fermentation of *Clostridium carboxidivorans***". Supervisor: Prof. Lars Rehm.

COURSES AND SEMINARS

Attended courses

1. Biotecnologie microbiche, E. Parrilli, V. Faraco
2. Extremophiles and Extremozymes: perspectives for industrial biotechnology, G. Fiorentino, 15/5-5/6/2018
3. Bioactive molecules from natural sources: purification and applications, D. Monti, 26-28/6/2018
4. Introduction to data analysis, R. Velotta, 10-14/2018.
5. Enzymatic and microbial applications in biotransformations and nanotechnology, R. Istatico, 10-11/10/2018.

6. First steps in writing and publishing a scientific manuscript, Viola Calabrò, Daria Maria Monti 9-13/9/2019.
7. Versatile nano display-platform based on bacteria - Prof. Rachele Isticato, 4/6/2020.
8. Microscopic methodologies for Life and Materials Sciences - Prof. Angela Arciello, Prof. Rocco di Girolamo, 2-3/7/2020
9. Discovery of carbohydrate active enzymes from hyperthermophiles: genomic and metagenomic approaches - Dr. Andrea Strazzulli. 11/11/2020.
10. Advanced mass spectrometry, Prof. Piero Pucci, 14-18/9/2020.

Seminars

1. Dynamic control: Mathematical challenges and applications, Enrique Zuazua, 17/1/2018;
2. The collapse of complex societies, Prof. Giuseppe Zollo and Prof. Luca Landoli 06/06/2018;
3. Smart cities in a smart world, Dr. Gabriella Ferruzzi, 08/06/2018;
4. Energy efficient operations: best practice for improving organizational processes, Dr. Giuseppe Bruno, 18/06/2018;
5. En route to synthetic biology: discussion from several examples, Thierry Tron, 22/6/2018;
6. Sustainability challenges in wastewater treatment, Carmen Teodosiu, 27/06/2018;
7. Environmental impact: conventional vs integrated approach, Mihaela Sluser Brindusa, 27/06/2018;
8. Design and characterization of an edible film based on starch and chitosan, Carlos Regalado Gonzales 29/6/2018;
9. Study of the formation and control of biofilm on stainless steel, Blanca Garcia Almendarez, 29/6/2018
10. Transient techniques in the investigation of three-phase processes, Tapio Salmi, 12/11/2018
11. Multicomponent Polymer Film Nanotechnologies, Alamgir Karim, 18/03/2019
12. L'orchestra della scienza, Ferdinando Boero, 2/4/2019
13. Valorisation of agricultural lignocellulosics in the context of circular economy, Dan Gravilescu, 16/05/2019
14. Phyto and microbial remediation – Potential application, Maria Gravilescu, 16/05/2019
15. Extremophiles: untapped source of Biological and metabolic diversity, Donato Giovannelli, 27/06/2019
16. Development of catalysts and catalytic processes for biomass to biofuel, Ying Zheng, 01/10/2019
17. "From basic research to industrial processes – what constitutes an ideal pathway for commercialization", Jesse Zhu, 29/10/2019
18. Empower Low Carbon Future via Catalytic Process Intensification, Ying Zheng, 19/11/2019

19. Il processo di innovazione nell'industria alimentare/1. Modello e strategia, A. Budelli, 9/5/2019
20. Il processo di innovazione nell'industria alimentare/2. Le fasi, A. Budelli, 23/5/2019
21. Il brief di prodotto, A. Budelli, 27/5/2019

University activities

Teaching experiences

- Ideal reactor exercises for students of the course “Introduzione agli impianti biotecnologici” (Prof. Antonio Marzocchella).
- Exercises on product recovery techniques (filtration, sedimentation, centrifugation, extraction) for students of the course “Introduzione agli impianti biotecnologici” (Prof. Antonio Marzocchella).
- Mass balance exercises for students of the course “Tecnologia degli impianti dell'industria farmaceutica” (Prof. Antonio Marzocchella).
- Exercises on product recovery techniques (filtration, sedimentation, centrifugation, extraction) for students of the course “Tecnologia degli impianti dell'industria farmaceutica” (Prof. Antonio Marzocchella).
- Ideal reactor exercises for students of the course “Ingegneria delle reazioni biotecnologiche” (Prof. Antonio Marzocchella).
- Contribute to lesson “Produzione di biofuels da fermentazione di syngas” for students of the course “Microbiologia Generale e Applicata” (Prof. Rachele Isticato), 15/12/2020

Other activities

- Participation to the “Open Day” of Department of Chemical Sciences for the orientation of high school students – Complesso universitario Monte Sant'Angelo, via Cinthia, Napoli, 13/02/2019.
- Participation to the “Open Day” of Department of Chemical Sciences for the orientation of high school students – Complesso universitario Monte Sant'Angelo, via Cinthia, Napoli, 14/02/2020.

La borsa di dottorato è stata cofinanziata con risorse del
Programma Operativo Nazionale Ricerca e Innovazione 2014-2020 (CCI 2014IT16M2OP005),
Fondo Sociale Europeo, Azione I.1 “Dottorati Innovativi con caratterizzazione Industriale”



UNIONE EUROPEA
Fondo Sociale Europeo



PON
RICERCA
E INNOVAZIONE
2014 - 2020